SEQUENTIAL CLICK REACTIONS TO SYNTHESIZE AND FUNCTIONALIZE HYDROGEL BIOMATERIALS

A Dissertation

by

FARAZ JIVAN

Submitted to the Office of Graduate and Professional Studies of
Texas A&M University
in partial fulfillment of the requirements for the degree of

DOCTOR OF PHILOSOPHY

Chair of Committee, Daniel L. Alge
Committee Members, Akhilesh K. Gaharwar
Roland R. Kaunas
Ken Muneoka
Head of Department, Michael K. McShane

December 2019

Major Subject: Biomedical Engineering

ABSTRACT

Click chemistry reactions have become an important synthetic tool for fabrication of user-defined hydrogels consisting of poly(ethylene glycol) (PEG) and bioactive peptides/proteins for tissue engineering. In this work, novel approaches were developed for the creation of next-generation, bio-instructive PEG-based hydrogels using various sequential click reactions. The sequential click paradigm utilizes stoichiometric control of complimentary reactions, each leveraged for their own individual advantages, towards the goal of creating bio-instructive hydrogel platforms for stem cell and therapeutic protein delivery.

Firstly, thiol-ene and tetrazine click reactions were explored. PEG microparticles were prepared off-stoichiometry using a photo-initiated thiol-ene click reaction resulting in microparticles with free norbornene groups. Subsequently, bioactive proteins alkaline phosphatase and glucose oxidase were functionalized with tetrazine groups for bio-orthogonal conjugation to norbornene-bearing microparticles. This sequential click strategy allowed for scalable microparticle fabrication along with facile and dose-dependent protein conjugation without compromising bioactivity

Next, microporous annealed particle (MAP) hydrogels, a new class of hydrogels fabricated from crosslinking hydrogel microparticles together, was investigated. Here, the sequential click platform was leveraged by assembling protein-functionalized microparticles into MAP hydrogels using a secondary tetrazine click reaction with a PEG-di-tetrazine crosslinker. This novel MAP hydrogel for tissue engineering was

mechanically characterized, assessed for cellular compatibility, and demonstrated to be highly versatile by creating user-defined patterns with bioactive protein-functionalized microparticles.

Next, protein modification strategies, specifically stochastic amine functionalization and site-selective functionalization, were compared to improve bioactivity of tethered growth factor bone morphogenetic protein-2 (BMP2). A bis-sulfone reagent, tetrazine-PEG-bis-sulfone, was successfully used to modify recombinant BMP2 with tetrazine groups selectively at C-terminal histidine-tags, which was further conjugated to MAP hydrogels. The bis-sulfone modification strategy resulted in tetrazine-BMP2 functionalized MAP hydrogels that were more osteoinductive compared to all other MAP hydrogel counterparts and negative controls. This approach is promising for the delivery of sensitive, therapeutic proteins and can be extended to other biomaterial platforms.

Lastly, the versatility of the sequential click approach was extended to other click reactions in order to overcome synthetic challenges associated with macromer-based hydrogel formation. Briefly, a thiol-maleimide Michael addition reaction was used to make PEG-peptide block co-polymers from short, linear components and subsequently assembled into hydrogels using a thiol-ene click reaction. This highly customizable platform was also coupled with a complimentary tetrazine click reaction for protein patterning. By leveraging the reactivity of norbornene, the utility of a tri-click system was demonstrated, thus opening the door to explore other unique combinations for creating user-defined hydrogel platforms.

ACKNOWLEDGEMENTS

First and foremost, I would like to thank my family: my Mom, Dad, and sister Sabrina. I am truly blessed to have all of you in my life. Your constant encouragement and unwavering support during my academic journey have meant everything to me.

Next, I would like to thank my graduate advisor and committee chair, Dr. Daniel L. Alge. Danny, I can't even begin to describe how much I admire and respect you, both as a scientist and friend. I will always be grateful to you for taking a chance on me as your first Ph.D. student and giving me the opportunity to start a laboratory with you. Your mentorship over the years has helped me develop my skills as a researcher and grow as an individual.

Next, to my committee members, Dr. Akhilesh K. Gaharwar, Dr. Roland R. Kaunas, and Dr. Ken Muneoka. Thank you all for your guidance, input, and support throughout the course of my graduate research.

Finally, thanks to all of my friends and colleagues for making my time at Texas A&M University a great experience.

CONTRIBUTORS AND FUNDING SOURCES

Contributors

This work was supervised by a dissertation committee consisting of Professors Daniel L. Alge, Akhilesh K. Gaharwar, and Roland R. Kaunas of the Department of Biomedical Engineering and Professor Ken Muneoka of the Department of Veterinary Physiology and Pharmacology.

The data presented in Chapter II was conducted in part by Ram Yegappan, Hannah Pearce, and James K. Carrow under the direction of Professors Akhilesh K. Gaharwar and Michael J. McShane.

The data presented in Chapter III was conducted in part by Alisa Isaacs and Shangjing Xin under the direction of Professor Daniel L. Alge.

The data presented in Chapter V was conducted in part by Natalia Fabella and Zachary Davis under the direction of Professor Daniel L. Alge.

All other work conducted for the dissertation was completed by the student independently.

Funding Sources

Chapter II of this work was made possible in part by the NIH Director's Transformative Research Award under Grant Number 1R01EB016414. Its contents are solely the responsibility of the authors and do not necessarily represent the official views of the NIH.

Chapter III, IV, and V of this work were made possible by the National Institute of Arthritis and Musculoskeletal and Skin Diseases of the National Institutes of Health under Grant number R21 AR071625. Its contents are solely the responsibility of the authors and do not necessarily represent the official views of the NIH.

TABLE OF CONTENTS

Page

LIST OF FIGURES

Page

LIST OF TABLES

Page

CHAPTER I

INTRODUCTION

1.1 Overview

Hydrogels are defined as crosslinked, hydrophilic polymeric networks with the ability to swell extensively and retain large amounts of water within their three-dimensional structure.[1] In addition to their hydrophilic properties, which are similar to highly hydrated soft tissues, they exhibit desirable biocompatibility, thus making them attractive materials for biomedical and tissue engineering applications such as contact lenses, drug delivery devices, wound dressings, and artificial tissues.[2-4] The overarching goal of tissue engineering centers on delivery of cells and growth factors encapsulated within a tissue-like material to a defect site in order to enhance tissue growth and regeneration of new functional tissue. Thus, in order to develop suitable hydrogel biomaterials for biomedical and tissue engineering applications, a number of important design criteria must be considered, and are more elaborately stated below (**Figure I-1**).[5, 6] First, hydrogels should be non-immunogenic and any hydrogel byproducts should be non-toxic within the body. Accordingly, hydrogels should provide a cytocompatible and biocompatible environment for encapsulated cells and proteins in order to carry out their function. Second, mechanical integrity of the hydrogel is important for withstanding forces during handling and after implantation to remain secure at the site of injury, but should ideally be able to degrade over time, if desired. Additionally, the mechanical properties of the hydrogel, and indirectly the hydrogel mesh size, are important for nutrient

diffusion and directly influencing cell behavior and/or growth factor release. Lastly, the ability to easily control and manipulate hydrogel properties can not only reduce batch-to-batch variability, but also allow researchers to tune biochemical and physical properties towards specific tissues and applications. These hydrogel design criteria can be addressed by the choice of polymer, hydrogel crosslinking chemistry, hydrogel form factor, and method of incorporating bioactive cues. The following literature review will serve as background and progress through these topics to motivate the focus of this dissertation: leveraging synthetic chemistries to develop next-generation hydrogels for bioactive growth factor delivery.

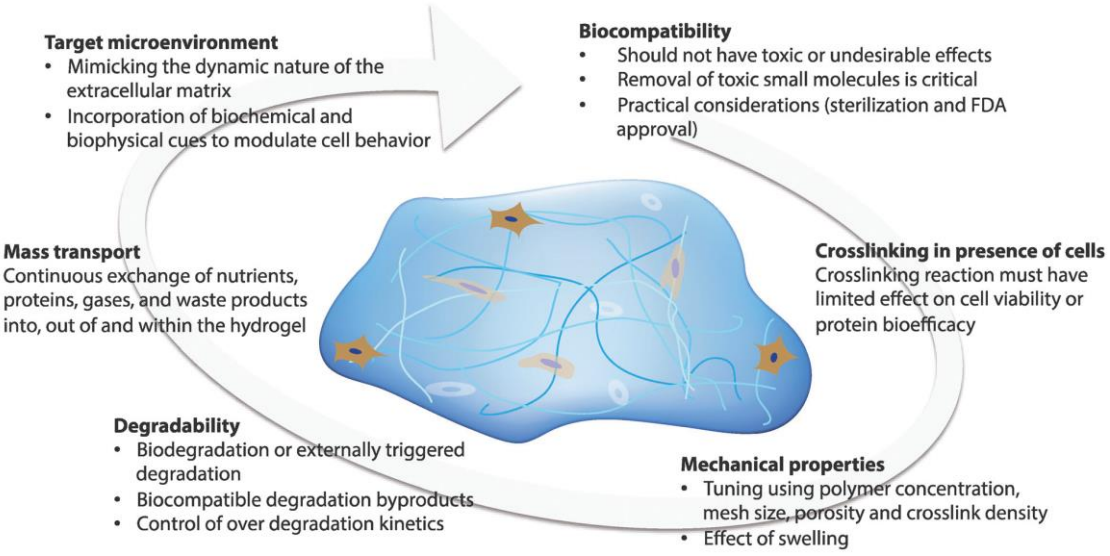

Figure I-1. Design considerations of hydrogels for tissue engineering. Reprinted with permission from P. M. Kharkar, K. L. Kiick and A. M. Kloxin, *Chem. Soc. Rev*., 2013, 42, 7335-72 – Published by The Royal Society of Chemistry.[6]

1.2 Literature Review

1.2.1 Polymers for Hydrogel Synthesis

Hydrogels are designed from polymer precursors which can be either naturally- or synthetically-derived. These two general classes of polymers lend to the production of a wide range of hydrogels for biomedical applications. This review will only focus on a handful of natural and synthetic polymers relevant to recent tissue engineering endeavors, seen in **Figure I-2**.

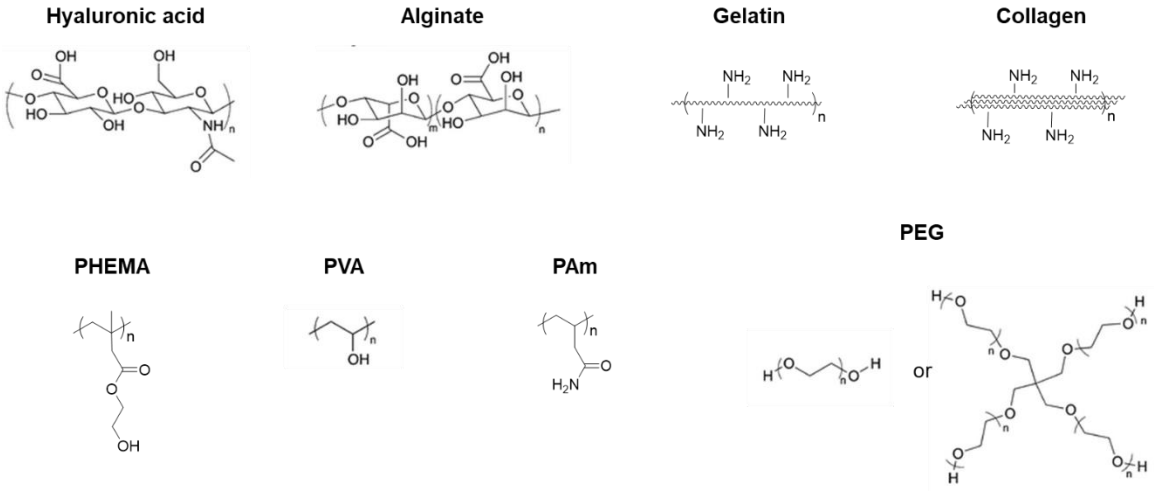

Figure I-2. Natural and synthetic polymers for hydrogel design

1.2.1.1 Natural Hydrogels

Natural hydrogels are comprised of polysaccharides (*e.g.* hyaluronic acid and alginate) and proteins (*e.g.* collagen and gelatin). In general, natural hydrogels are inherently biocompatible and often biodegradable. Additionally, protein-derived sources contain recognizable domains for cells to spread and remodel, while polysaccharide-

derived sources, rely on chemical modification with cell-adhesive peptides, such as the fibronectin-derived arginine-glycine-aspartic acid (RGD) motif.[7] Despite their biomimetic characteristics, they typically have poor mechanical stability. Additionally, because of batch-to-batch variability from naturally derived sources, it is difficult to control for heterogeneous mechanical properties and presentation of endogenous biochemical signals. Lastly, derivation of materials from biological sources has the potential to illicit adverse immune responses. Nonetheless, natural hydrogels meet many of the biological design parameters necessary for tissue engineering constructs and have found applications in the biomedical field.

Hyaluronic acid is a non-sulfated glycosaminoglycan commonly seen in the ECM of connective and epithelial tissues and found in the synovial fluid and within scaffolding of cartilage. Hyaluronic acid is biocompatible, non-immunogenic, and biodegradable *via* hyaluronidase, however proper purification and processing when obtained from bacterial fermentation and rooster combs is necessary to remove impurities and endotoxins that may elicit an immune response.[3, 8] Typically, hyaluronic acid based hydrogels have weak mechanical properties or rapidly degrade *in vivo*, but modification of the carboxylic acids or alcohol groups along the backbone have allowed for chemical crosslinking.[9-13]

Alginate is an anionic polymer derived from brown seaweed. Its biocompatibility, low toxicity, low cost, and mild crosslinking conditions have led to applications such as wound healing, and delivery of cells and therapeutic agents.[14, 15] Alginate can be crosslinked into hydrogels through non-covalent means with divalent cations, however depending on the cationic agent, rapidly lose mechanical properties due to outflux of the

crosslinking ion.[16] Alternatively, chemical crosslinking methods using bifunctional crosslinkers impart more robust and controllable mechanical properties.[17]

Collagen is a key structural protein secreted by fibroblasts and found in mammalian ECM. In humans, collagen is prevalent in many tissue systems throughout the body such as bone, skin, and tendons, and makes up a quarter of total body protein. A total of 29 different collagen sub-types exist, including collagen types I, II, III, V, and XI, however collagen type-I is predominately used in the tissue engineering field.[18] Collagen can be readily isolated from tissues while preserving its natural triple-helical organization and processed into crosslinked hydrogels that are generally non-toxic, biocompatible, and biodegradable. The collagen polypeptide fibers can self-aggregate to form stable fibers or be mechanically enhanced with the introduction of a chemical crosslinker such as glutaraldehyde. Advantageously, collagen already contains many recognizable amino acid sequences allowing for cell attachment and cell-mediated enzymatic degradation (*i.e.* collagenase). Collagen matrices have been used to study cellular mechanotransduction effects[19, 20] and serve as a bio-ink for 3D printing.[21]

Gelatin is a derivative of collagen, produced from denaturation of collagen, specifically type-I collagen. Collagen sources used for gelatin production generally come from bovine and porcine sources, thus similar to collagen, can be weakly antigenic. Similar to collagen, gelatin also contains the same cell recognizable domains for attachment. Due to its shear thinning material properties and reversible thermal gelation, gelatin has been used in tissue engineering,[22] drug delivery,[23] and 3D printing applications.[21, 24] However, the weak mechanical integrity of physically crosslinked

gelatin has prompted backbone functionalization to allow for further stability through chemical crosslinking.[25-28]

1.2.1.2 Synthetic Hydrogels

Synthetic hydrogels are composed of man-made, chemically synthesized polymers including poly(hydroxyethyl methacrylate (PHEMA), poly(vinyl alcohol (PVA), poly(acrylamide) (PAAm), poly(*N*-isopropyl acrylamide) (PNIPAm)), poly(ethylene glycol) (PEG).[29] With the advantage of being chemically synthesized, synthetic polymers can produce highly consistent hydrogels with exquisite control over material properties. Inherently, these polymers are not biologically functional, however strategies have been developed to integrate biological domains within these materials. While not all synthetic hydrogels are typically degradable, reverse gelation can be achieved through hydrolysis or incorporation of a degradable monomer or crosslinker, however, consideration of the degradation byproducts should be taken as they can potentially be toxic. Nonetheless, the aforementioned synthetic hydrogels have found widespread use in the healthcare field as drug delivery depots, incorporated in tissue-contacting devices, and employed for tissue replacement (**Figure I-3**).

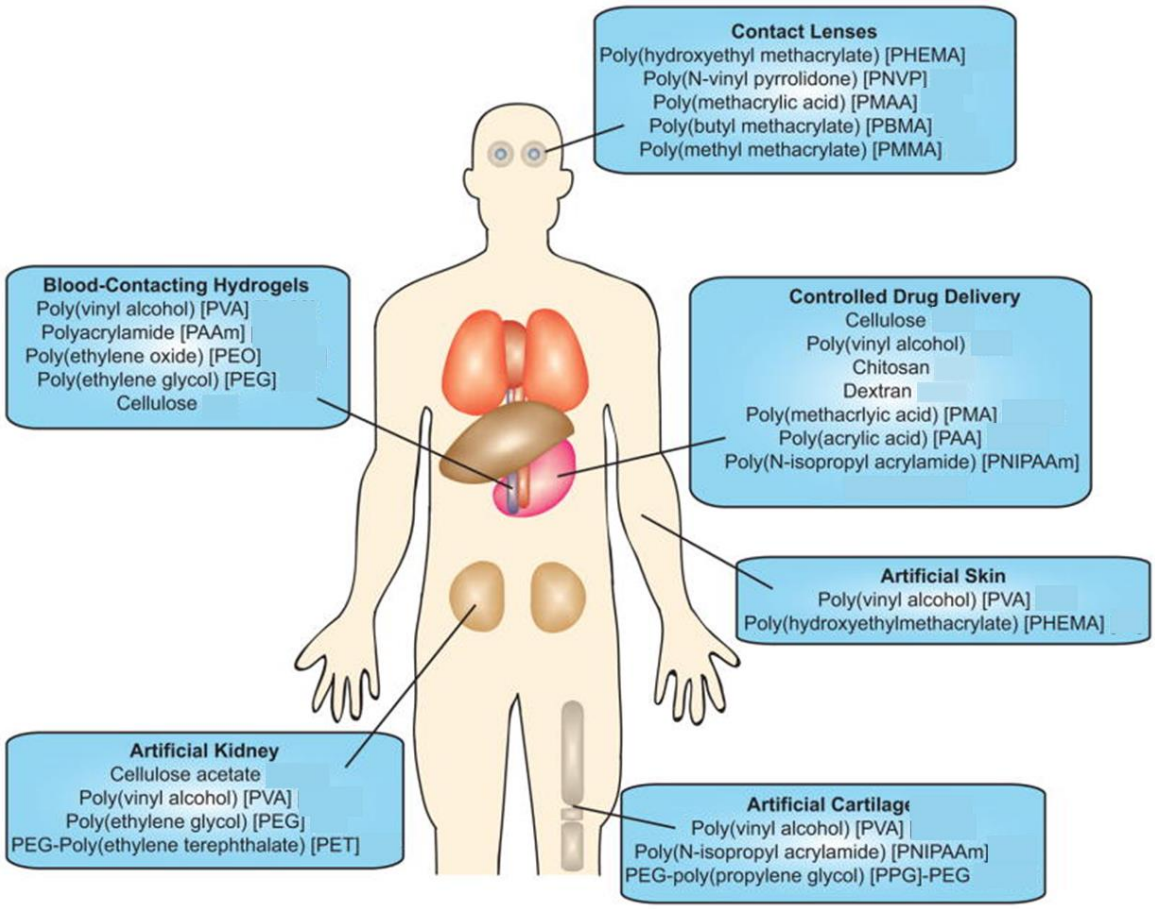

Figure I-3. Hydrogel applications in biomedical and healthcare field. Reprinted from "Hydrogels in healthcare: from static to dynamic material microenvironments" C. M. Kirschner and K. S. Anseth, *Acta Materialia*, 2013, 61, 931-44. with permission by Elsevier. [2]

PHEMA was one of the first synthetic hydrogels designed specifically for biomedical application. In 1960, Wichterle and Lim developed PHEMA from co-polymerization of 2-hydroxyethyl methacrylate (HEMA) and crosslinker ethylene dimethacrylate (EDMA) in aqueous solution.[30] The resulting hydrated material was flexible and nutrient permeable, making it immediately useful as a soft contact lens to replace the rigid plastic lenses of that time. Since then, improvements have been made

through copolymerization with other monomers leading to higher water uptake and oxygen permeability.[31]

PVA was also an early popular synthetic choice for hydrogels because of its hydrophilic properties, clarity, and wear resistance. PVA hydrogels can be crosslinked using chemical crosslinking agents, high energy irradiation, or freeze/thawing.[32] When crosslinking with chemicals such as glutaraldehyde or other monoaldehydes, residual crosslinker within the hydrogels can remain, requiring extraction before use in biomedical/pharmaceutical applications in order to avoid toxicity or negative effects on encapsulated bioactive agents. Electron beam or gamma irradiation allowed for chemical crosslinking without toxic eluting agents, however undesired bubble formation within the hydrogel could impair mechanical properties. To circumvent these issues with chemical crosslinking strategies, repeated freezing and thawing cycles of aqueous PVA, which resulted in crystallite formation, could be used to physically crosslink PVA hydrogels with enhanced mechanical strength.[33] By adjusting the polymer molecular weight, polymer weight percentage, and freeze-drying parameters, the gel properties could be controlled. These favorable properties have led to PVA hydrogels being used as drug delivery vehicles.[34, 35] Additionally, since PVA is inherently non-degradable and bio-inert, it has been used for applications requiring permanent scaffolds such as for articular cartilage repair[36] or soft contact lenses.[37]

PAm has been used most notably in the field of biology for the study of nucleic acids and proteins for gel electrophoresis due to their non-adherent nature. PAm hydrogels can be crosslinked by free radical polymerization with a crosslinker such as bis-

acrylamide, initiated by ammonium persulfate, and accelerated by tetramethylethylenediamine. In 1978, PAm hydrogels were used for surface immobilization of sugars, with cells grown on their non-adherent surfaces.[38] Nearly two decades later, strategies for protein functionalization and improved tunability of PAm hydrogel stiffness allowed for these hydrogels to emerge as an important elastic substrate for two-dimensional studies of cellular mechanics and probing interactions at the cell-substrate interface.[39-43] Unfortunately, limited strategies existed for efficient protein incorporation with PAm hydrogels (*e.g.* physical encapsulation or chemical modification with sulfo-SANPAH,[43] EDC/NHS,[44] or hydrazine hydrate[45]), yet they have found some use in enzyme immobilization and drug delivery applications.[46] Additionally, early on, the mechanical deformation and cellular traction forces on PAm hydrogels was difficult to measure and not easy to analyze,[47] however the tracking of embedded fluorescent microbeads with improvement in microscopy techniques aided in these processes.[48, 49] Finally, due to concerns of acrylamide toxicity,[50, 51] PAm hydrogels were found to be unsuitable for three-dimensional cell culture, although methods to try to mimic tissue-like conditions were employed.[52]

PNIPAm, a thermoresponsive polymer, is attractive for tissue engineering applications because it exhibits a phase transition above its lower critical solution temperature (LCST). Often co-polymerized with other hydrophilic or hydrophobic monomers/polymers, PNIPAm's LCST can be tuned, and may even coincide with body temperature to aid in injectability and act as a stimulus for crosslinking *in situ*.[53-56] Additionally, temperature changes for crosslinked PNIPAm above and below the volume

phase transition temperature (VPTT) result in deswelling/reswelling have been used to trigger drug release,[57] cell detachment,[58, 59] and demonstrated for implantable biosensor cleaning *via* temperature stimulus.[60]

PEG has received considerable attention for its use in hydrogels, as it is a hydrophilic polymer known for its high water content/swelling, and most importantly, its non-fouling nature. Combined with its chemical simplicity and easily tunable mechanical properties, PEG is an ideal choice for creating tissue-mimetic hydrogel constructs. PEG hydrogels are considered "blank slate" materials that can be easily engineered into well-defined extracellular matrix (ECM) mimics through the incorporation of relevant synthetic peptides and proteins to allow for cell binding sites and cell-mediated enzymatic degradation within the three-dimensional (3D) environment. [61-66] From a modification standpoint, PEG macromers can be end-functionalized (*e.g.* PEG-diacrylate or methacrylate), or can be developed into a multi-arm, end-functionalized macromers connected to a pentaerythritol core (*i.e*. star polymers). Initial preparation of PEG hydrogels for biomedical applications was achieved through gamma and electron beam radiation,[67-69] followed by alcohol crosslinking with isocyanates,[70, 71] and free radical polymerization through acrylate groups,[72-75] and more recently step growth reactions.[76-78] Regardless, both macromer forms of PEG allow for rapid chemical crosslinking and have been used to synthesize PEG hydrogels for applications in drug delivery[79-81] and tissue engineering.[61, 82]

A summary and direct head-to-head comparison of natural versus synthetic polymer attributes is shown below in **Table I.1**.

Table I.1. Summary of advantages/disadvantages of natural and synthetic polymers for hydrogel synthesis. Adapted and reprinted with permission from P. M. Kharkar, K. L. Kiick and A. M. Kloxin, *Chem. Soc. Rev*., 2013, 42, 7335-72 – Published by The Royal Society of Chemistry.[6]

Feature/function	Natural polymers	Synthetic polymers
Biocompatibility	Polymer dependent	Polymer dependent
Bioactivity	Possible	Limited
Inherent biodegradability	✓✓	✓
Tunability of degradation	✓	✓✓
Degradation byproducts	Biocompatible	Potentially harmful
Flexibility for chemical modification	✓	✓✓
Commercial availability	✓	✓✓
Batch to batch variation	Likely	Controlled

1.2.2 Hydrogel Crosslinking Chemistries

Hydrogel polymerization strategies fall into two main categories: physical and chemical crosslinking. Chemical crosslinking can be further subdivided based on the reaction used, either chain growth or step growth polymerization. The method and degree of crosslinking can influence many of the network properties such as swelling and modulus.

1.2.2.1 Physical Crosslinking

Physical crosslinking involves non-covalent interactions between chemical groups resulting in reversible gel net points. These reversible netpoints can be achieved through polymer chain entanglements, interaction between cationic/anionic agents/functional groups, hydrogen bonding with electronegative atoms, or hydrophobic interactions.

Ionic gelation in particular involves the Coulombic attraction between cationic and anionic functional groups or ionic agents such as charged ions.[83] For example, hydrogels such as alginate can be physically crosslinked with cationic agents such as silver (Ag^{2+}) or calcium (Ca^{2+}) which intercalate between carboxylic acid side chains along the polymer backbone and act as physical net points to crosslink the gel. These cationic agents are transient and can easily be washed out, resulting in dissolution of the gel. Anionic polymers can also be gelled with cationic polymers such as alginate and polylysine. Physically gelling systems can be useful for rapidly degrading hydrogel systems and aiding in shear thinning bioinks[84, 85]

Aside from association between charged moieties, hydrogen bonding with electronegative atoms has also been shown for hydrogel crosslinking. For example, poly(acrylic acid) (PAA) can form complexes with PEG from hydrogen bonding between the oxygen of PEG and carboxylic acid group of PAA.[86] Additionally, hydrogen bonding can be used in high density[87] or as sacrificial bonds[88] and paired with other chemical bonding strategies to create mechanically strong yet elastic hydrogels.

Crystallization is another method achieved by freeze-thawing processes that creates elastic gels by formation of crystallites that act as netpoints to redistribute stresses across the hydrogel.[32] This method was used with PVA to make elastic gels with improved mechanical properties.[89] Additionally, employing directional freeze drying can also be used to introduce aligned porosity within hydrogel constructs.[90]

Hydrophobic interactions can be used with block co-polymers containing hydrophilic and hydrophobic domains. The aggregation of such hydrophobic regions is

thermodynamically favorable and results in physical net points. The amphiphilic block co-polymer Pluronic F-127, which consists of a triblock of synthetic polymers (poly(ethylene oxide)-poly(propylene oxide)-poly(ethylene oxide)) relies on such interactions for self-assembly into micelles in aqueous solution.[91]

1.2.2.2 Chemical Crosslinking

Chemical crosslinking involves formation of covalent bonds between chemical groups. Chemical crosslinking can be further categorized as either chain growth or step growth polymerization. Traditionally radical mediated chain growth reactions are used with acrylate-containing polymers for chemical crosslinking and polymerization. While their simplicity and widespread use cannot be understated, chain growth reactions lack sufficient control over crosslinking kinetics and efficiency, making them ideal as a "one-pot" approach for hydrogel synthesis, but ineffective for fine-tuned control over hydrogel design and the development of predictable homogeneous polymer networks. Alternative chemical approaches such as step-growth click chemistry reactions have allowed for greater synthetic control, amenability with biologics and an extension to a plethora of chemical moieties within the click chemistry toolkit. Additionally, many of the reactions involve similar chemical functional groups, which can allow for simultaneous or sequential reactions within the same system.

1.2.2.2.1 Chain Growth Polymerization

In hydrogels, polymerization occurs through pendant functional groups along the polymer backbone or through end-functionalized macromers. Chain growth reactions, also known as vinyl polymerization, can be divided into three main steps: initiation, propagation, and termination. Initiation, the formation of an initial radical source, occurs with a chemical initiator and/or energy input (*i.e.* light or heat). During propagation, acrylate end-groups undergo homolytic cleavage of their carbon-carbon double bond in the presence of the initiator and rapidly polymerize with another acrylate end group to generate a propagating radical center. Lastly, the reaction is terminated upon quenching of the radical center through radical combination. An important side reaction that can divert chain growth polymerization is chain transfer, which results in transfer of the propagating radical to a chemical species aside from the polymer (*i.e*. solvent, other monomer/polymer, or a designated chain transfer agent). While chain transfer agents have been used in polymeric synthesis to control molecular weight, chain transfer is undesirable in the context of creating tissue engineering hydrogels, as radical transfer to functional groups found on incorporated biologics such as cells and proteins can result in detrimental viability and bioactivity, respectively.[78, 92-94] Additionally, ambient or dissolved oxygen also acts as a radical scavenger and can severely inhibit acrylate polymerization under typical biological conditions,[95] although strategies to mitigate these effects exist.[96] In general, chain growth reactions proceed rapidly, with the kinetic rate constants for each step dictating the overall hydrogel synthesis and propensity for chain transfer events.

1.2.2.2.2 Step Growth Polymerization

Step growth reactions on the other hand are reactions between two different complementary functional groups, while these can also include acrylate groups, they can also involve other chemical groups as well such as carboxylic acids, amines, or thiols. In contrast to chain growth reactions, step growth reactions create positively or negatively charged reactive centers as opposed to radical centers, and because these are one-to-one reactions between end groups, the extent of reaction can be more simply and predictably controlled through relative end-group concentrations. Step growth reactions yield more homogeneous network structures and strength compared to chain growth networks with similar crosslink density. An idealized hydrogel network of chain growth and step growth polymerized gels is shown in **Figure I-4** along with mechanical characterization.[76]

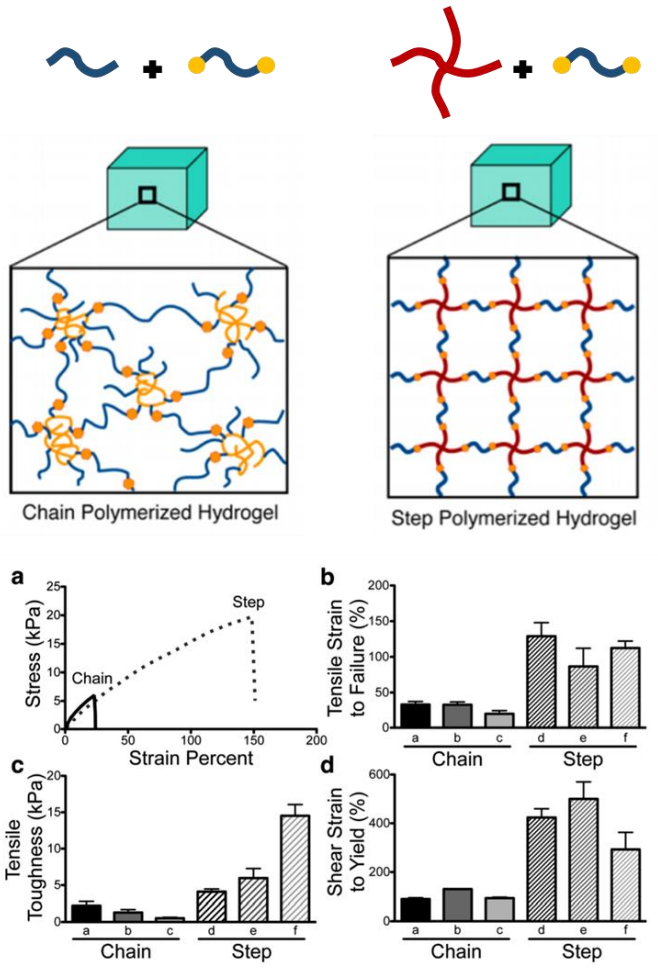

Figure I-4. Fabrication and mechanical characterization of chain growth and step growth polymerized hydrogels. Adapted and reprinted from "Mechanical Properties and Degradation of Chain and Step-Polymerized Photodegradable Hydrogels" by M. W. Tibbitt, A. M. Kloxin, L. A. Sawicki, K.S. Anseth. *Macromolecules*, 2013, 46, 2785-92. with permission by the American Chemical Society. [76]

1.2.2.3 Click Chemistry

A subset of step-growth reactions meet the criteria for consideration as a "click chemistry" reaction, a term coined by Sharpless *et al*. in 2001.[97] Click reactions must be modular, stereospecific, give very high yields under simple reaction conditions, and produce inoffensive byproducts. The unique characteristics of click chemistry were

expected to drive the discovery of synthetic targets such as drugs, biological probes, and new materials. Since the identification of the first quintessential click reaction, copper-catalyzed azide-alkyne cycloaddition (CuAAC), many reactions have been added to the click chemistry toolbox (**Figure I-5**).

As these click reactions have grown in number, so too have their adoption and utility in hydrogel engineering. For example, base-catalyzed, thiol-Michael addition reactions with electron-deficient alkenes was an easy extension from chain growth reactions, as these acrylates and methacrylate groups were already traditionally used for homopolymerization. The click reaction with thiols allowed for facile incorporation of thiol-containing peptides and proteins in hydrogels under mild conditions for tissue engineering constructs.[98] Notably, Hubbell and Lutolf,[99-102] Garcia,[77] and Anseth have all demonstrated a range of vinyl functional groups (methacrylates, maleimides, vinyl sulfones, acrylamides, etc.) for hydrogel crosslinking and incorporation of cysteine-containing peptides.

Thiol-norbornene (thiol-ene) photopolymerizations, reactions with electron-rich alkenes, have also been significantly used for rapid formation of user-defined, bio-instructive hydrogels under cytocompatible conditions. In contrast with Michael addition reactions, thiol-ene click does not require alkaline conditions thus reducing potential disulfide formation, and due to the photoinitiation capability can be spatially and temporally controlled.[63] Thiol-ene gels have been used for drug delivery, presentation of biochemical cues, cell encapsulation, tissue engineering.[63, 65, 78, 94, 103]

Other click reactions that do not require an external initiator or catalyst entirely and proceed under physiological conditions have also been explored for hydrogel synthesis. These bio-orthogonal click reactions, as the name suggests, do not inherently interact with biological functionalities and can be performed in the presence of biologics without detrimental effect. For example, strain promoted azide alkyne cycloaddition (SPAAC) utilizes cyclic alkyne strain rather than copper as a catalyst, as high concentrations of copper could be toxic to cells. SPAAC hydrogels have been used for creating cell-laden hydrogels. Tetrazine-norbornene click (i.e. tetrazine ligation) is an inverse electron demand Diels-Alder reaction between tetrazines and electron-rich dienophiles. Tetrazine ligation offers much of the same benefits as SPACC in regards to polymerization, however tetrazines are more synthetically tractable and commercially available thus improving their accessibility to the biomaterials field. Tetrazine click reactions have been used for direct cell labeling with fluorophores[104, 105] and creation of *in situ* forming hydrogels for cell delivery and 3D culture.[106]

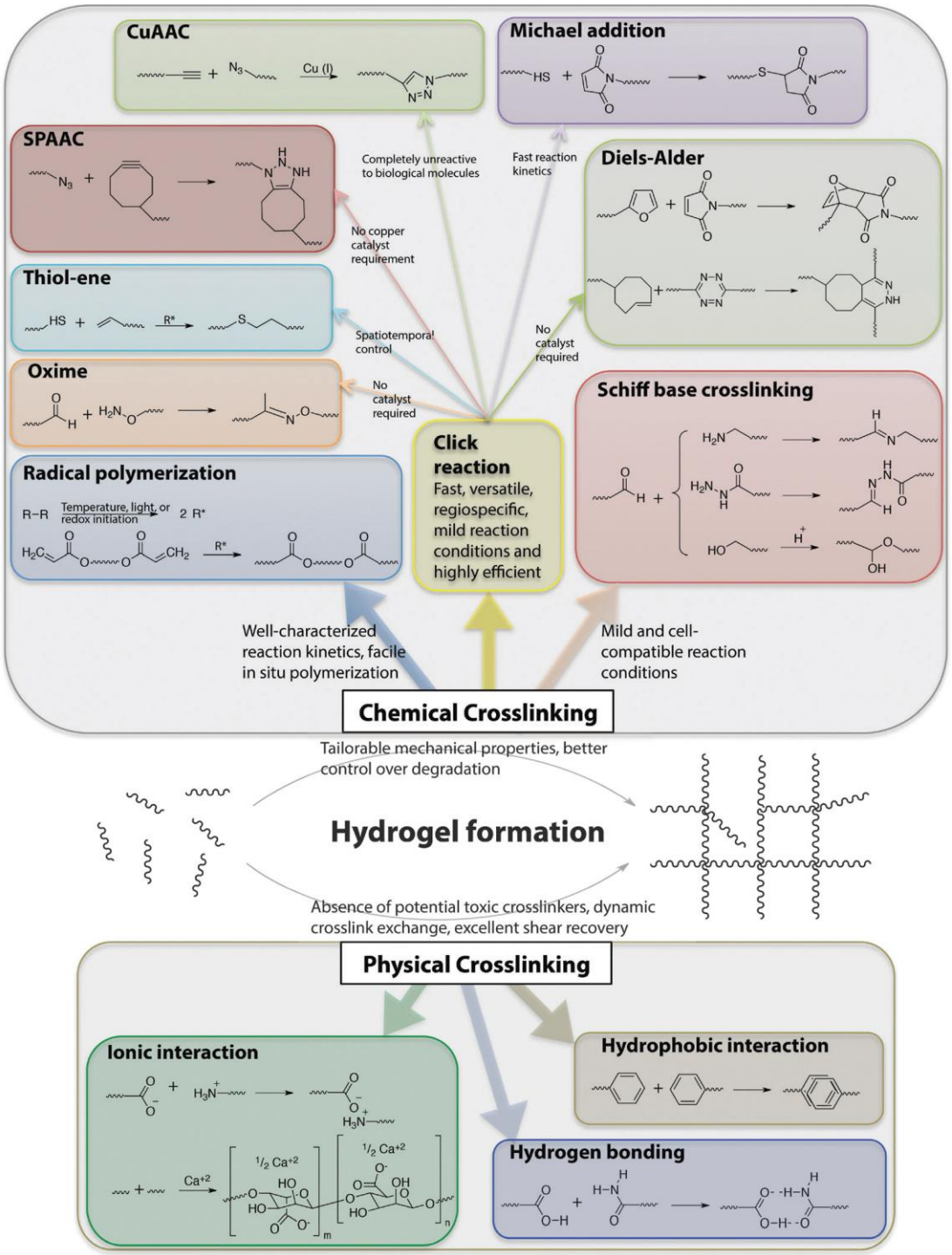

Figure I-5. Chemical functional groups for the diversity of hydrogel crosslinking strategies. Reprinted with permission from P. M. Kharkar, K. L. Kiick and A. M. Kloxin, *Chem. Soc. Rev.*, 2013, 42, 7335 - 72 – Published by The Royal Society of Chemistry.[6]

1.2.2.3.1 Sequential Click Chemistry

As the field of click chemistry has evolved, so too have the unique strategies for using them. The combination of multiple orthogonal click reactions has led to the ability to create tunable biomaterials by leveraging the advantages of individual reactions without compromising simplicity or efficiency.

The first approach in utilizing multiple reactions relies on performing two separate and independent reactions in a sequential manner. For example, Mabry *et al.* created PEG hydrogels with the ability to dynamically stiffen cell microenvironments by performing two separate thiol-ene photopolymerization reactions at different times.[107] After the initial PEG hydrogel had formed and cells had spread/degraded the material, the hydrogel was immersed in PEG-norbornene and PEG-thiol solution and a second photopolymerization was performed resulting in a secondary network embedded within the first.

The second approach utilizes stoichiometric control to perform sequential reactions that interact with each other. Burdick and co-workers leveraged dual reactivity of acrylate-functionalized hyaluronic acid to probe mechanical effects on cell-spreading in 3D. A stoichiometrically-controlled thiol-acrylate Michael addition reaction was initially used for hydrogel fabrication and cell encapsulation followed by spatiotemporally stiffening using a radical-mediated acrylate polymerization to increase crosslinking density and selectively prevent cell spreading.[108]

DeForest *et al*. combined SPAAC and thiol-ene photopolymerization for direct cell encapsulation and spatiotemporal patterning of biological functionalities, respectively.[109] By incorporating a photoreactive electron-rich allyl ester within bis(cyclooctyne)-

functionalized peptide crosslinkers, a secondary thiol-ene reaction was used to pattern and incorporate functional collagenase-sensitive peptides. Alge *et al.* combined bio-orthogonal tetrazine and thiol-ene click reactions to demonstrate the potential for biochemical patterning.[106] By reacting norbornene-functionalized, thiol-containing peptides with a PEG-tetrazine macromer, free pendant thiol groups were installed within the hydrogel which were subsequently used to pattern norbornene-functionalized proteins *via* thiol-ene photopolymerization.

The idea of a sequential click paradigm can be used to overcome the constraints and limitations of certain click reactions (*e.g.* use of potentially toxic catalysts or excess photoinitiators, etc.) or combine new orthogonal reactions to allow for facile temporal control over polymerization strategies.

1.2.3 Constructing Hydrogels from Solutions versus Microparticle Building Blocks

Hydrogels are formed from crosslinking of aqueous polymer precursors. The pre-polymer solution can be added to a desired mold and crosslinked to take that shape. More recently, pre-polymer solutions have been used as bio-inks with 3D printing to create more intricate and complex structures with high precision.[85, 110-115] Regardless, formation of mechanically robust hydrogels in this manner results in a high internal crosslinking density and nanoporous mesh size. When used for tissue engineering, nanoporous hydrogels require degradability for host cells to spread and/or encapsulated proteins to be released, resulting in progressively weaker hydrogels. Additionally, nutrient and mass transport of soluble factors and gasses through bulk of the hydrogel are important for cell survival.

Ideally, material degradation would precisely match the rate of tissue formation in order to prevent mechanical mismatch with surrounding tissue and ensure enough scaffolding is present for cells, however tuning these parameters is difficult to achieve as cellular infiltration and mechanical stability are inextricably linked. Some top-down strategies for introducing pores within hydrogels include using dissolvable poragens, foaming gasses, and freeze-drying, however these processes require multiple processing steps and are often not suitable in the presence of cells and biologics.

Polymer precursors have also been used in the production of hydrogel microparticles on the order of tens to hundreds of microns. One common method of microparticle formation is driven by an emulsion of the pre-polymer solution with an immiscible solution (either another polymer or oil) and crosslinked. Microparticles found initial use in drug delivery, as their small size, large surface area, and injectable form factor made them ideal as carriers for therapeutics. With regards to porous hydrogels, another recently emerging bottom-up approach is the development of microporous annealed particle (MAP) hydrogels which use hydrogel microparticles to fabricate 3D porous scaffolds. Crosslinked microparticles are packed into a mold and subsequently annealed together to form a cohesive network. Due to the assembly of microparticles in this manner, natural interconnected porosity on the order of hundreds of microns is formed between particles allowing for cells to grow on the surfaces of microparticles and spread easily through the void space within the hydrogel. Griffin *et al.* demonstrated MAP hydrogels facilitated enhanced cell spreading over nanoporous bulk hydrogels *in vitro*, and found MAP hydrogels promoted cell infiltration and accelerated vascular wound healing and

network formation *in vivo*.[116] Additionally, MAP scaffolds fundamentally allow for spatial control by tuning the mechanical and biochemical properties of microparticle building blocks independent of bulk properties. Caldwell *et al.* demonstrated differences in cell spreading and morphology when assembling MAP hydrogels using discretely sized microparticles.[117] Also, Xin *et al.* recapitulated cell spreading markers YAP/TAZ, traditionally seen in two-dimensional culture, within MAP hydrogels that could be mechanically tuned with a crosslinker independent of individual microparticle stiffness.[118] Lastly, spatial arrangement of microparticle building blocks can also be controlled to create complex structures as well as potentially engineer user-desired mechanical or biochemical gradients. Xin *et al.* also recently showed how microparticles could be used as a 3D-printable bio-ink for the creation of tissue-like structures.[119]

Taken together, the method of hydrogel formation, either from solution or pre-made hydrogel particles, can play an important role in overall mechanical properties, mass transport, and user-control which have the potential to affect cellular behaviors.

1.2.4 Incorporating Bioactive Cues

As previously discussed, the artificial incorporation of biological motifs, namely peptides and proteins, within both natural and synthetic hydrogels has permitted degradability, cell adhesion,[61] and delivery of therapeutic agents.

Peptides are synthetic, linear analogs of whole proteins that are derived from functional domains within the protein. Peptides, unlike proteins, are simple to use since they exhibit a primary structure void of function-dependent conformation and are more

stable and less susceptible to degradation. The incorporation of peptides within hydrogels has relied on conjugation through chemical functional groups inherently found on the peptide (*e.g.* amines and thiols) or synthetically incorporated. Hern and Hubbell grafted bioactive adhesion ligand RGD to PEGDA hydrogels by modifying the N-terminal amine end of the peptide using an acryl-PEG-N-hydroxy succinimidyl ester.[61] The peptide acrylate allowed for co-photopolymerization with PEGDA using radical mediated crosslinking. West and co-workers used carbodiimide chemistry to functionalize aminated photoactive PVA with RGD peptide along the polymer backbone.[120] Mooney and co-workers also used carbodiimide chemistry for peptide functionalization of alginate hydrogels.[7]

While peptide incorporation holds a major milestone in the development of bioactive hydrogels, incorporation of whole proteins is the ultimate goal. Moving beyond peptides brings the field closer to creating more representative biomimetic tissues, as proteins are more biologically active than peptides. Protein incorporation can occur in a few ways: physical encapsulation (*i.e.* entrapped within the hydrogel matrix until degradation of mesh for release), the use of affinity ligands that non-covalently interact with growth factors to control loading/release, or covalent binding to the polymer network.[121] Conjugating proteins within hydrogel scaffolds is thought to improve long-term therapeutic efficacy by allowing for sustained protein presentation with less concentration than soluble delivery. Additionally, protein tethering allows for more spatial availability of localized growth factors in the direct vicinity of encapsulated cells or tissue defect without concern for leaching into surrounding tissues. However, the additional

complexity and sensitivity of proteins requires more biologically compatible conjugation methods. The use of more cytocompatible chemistries like thiol Michael additions and thiol-ene photopolymerizations greatly improved bio-functionalization by allowing for facile incorporation of cysteine-containing peptides and proteins with alkene-containing polymers.[77, 82, 100, 122, 123] Proteins such as epidermal growth factor (EGF)[124] and transforming growth factor-beta (TGFβ)[125] were grafted using non-click reactions. McCall *et al.* used thiol-acrylate photopolymerization for covalently tethering thiolated-TGFβ to PEG hydrogels towards mesenchymal stem cell chondrogenesis.[82] While protein bioactivity under these reaction conditions were shown to be compatible, they are not ideal. In some cases, proteins required amine modification strategies to provide a functional handle for conjugation such as Traut's reagent to introduce thiols or acroloyl-PEG-NHS for acrylate groups. These modifications are non-specific and bind ubiquitously across the protein resulting in a mixture of modified protein with uncontrolled protein orientation post-conjugation. Additionally, photopolymerized strategies result in the production of free-radicals which can negatively affect proteins through unwanted chain transfer events.

Development of engineered proteins can circumvent the challenges of functional handle presentation by engineering pre-determined, site-specific locations within the protein. Seliktar *et al.* used an engineered thiol-containing vascular endothelial growth factor (VEGF) and conjugated it to PEG hydrogels *via* Michael addition along with physically entrapped TGFβ.[126] Cambria *et al.*[127] and Shadish *et al.*[128] both engineered proteins with LPXTG-motifs and used sortase enzymatic-mediated ligation of proteins to

scaffolds. Additionally, engineered chimera proteins can enhance kinetics and thermodynamics of cell receptor binding compared to native protein, allowing them to be more potent and therapeutically active.[129] However, tailoring engineered proteins for desired conjugation strategies, while site-specific, is not greatly accessible to biomaterial scientists nor allows for easily interchangeable proteins in a "plug-and-play" fashion, thus potentially hindering its adoption in the field.

Recently, the use of sulfone reagents have been shown as a facile, reagent-based method of specifically modifying proteins at disulfide bonds.[130] Subsequent work has also shown the use of PEG-bis-sulfone for PEGylation of proteins at poly-histidines, which are commonly included at the terminal ends of recombinant proteins.[131, 132] This approach could be promising when applied to the biomaterials field for site-specific installation of functional handles without compromising protein bioactivity.

1.3 Innovation and Approach

Conjugation of bioactive therapeutic proteins to hydrogel biomaterials remains a major challenge for the development of effective bio-instructive tissue engineering platforms. Chemical strategies used for hydrogel fabrication are often incompatible with biologics, thus synthetic approaches that take into account both factors without compromise can be appreciated. Here, click reactions are key, because individual reactions have distinct advantages towards one factor or the other, however the ability of functional groups to participate in multiple click reactions under different conditions can be leveraged for sequential reactions in a temporal manner. Here, the dual reactivity of

norbornene for both thiol-ene photopolymerization and tetrazine-norbornene ligation are used initially for rapid hydrogel fabrication and protein functionalization, respectively. In later studies, the lack of norbornene reactivity as an electron-rich alkene under basic conditions is capitalized upon in order to perform an orthogonal Michael addition reaction in the presence of norbornene which can then subsequently be leveraged for hydrogel crosslinking *via* thiol-ene photopolymerization and protein patterning *via* tetrazine ligation.

From a materials standpoint, MAP hydrogels are still an emerging class of hydrogel biomaterials with many properties yet to be explored and exploited. The focus on hydrogel microparticles and MAP hydrogels in this work will add to the growing scientific body of work on engineering hydrogel porosity for tissue engineering and decoupling local mechanics from bulk properties.

Additionally, to date, there have been only a handful of studies using the bio-orthogonal tetrazine click reaction in the biomaterials field despite its amenability for biological applications. The innovation demonstrated in this work hopes to expand the application of tetrazine click chemistry to bioactive whole protein delivery in a manner that can be applied to the more prolific Michael addition and thiol-ene click reactions.

Importantly, the approach used for site-specific protein modification of tetrazine groups is the first application of its kind extended for bioconjugation to hydrogel scaffolds. Here, the application towards bioactive bone morphogenetic protein conjugation and mesenchymal stem cell osteogenesis is also an important achievement in bio-instructive hydrogels. The simplicity of the modification strategy and the potential for functionalizing

any recombinant protein-of-interest, are important factors for broad utility that may help with widespread adoption of this technology in the biomaterials field.

CHAPTER II

SEQUENTIAL THIOL-ENE AND TETRAZINE CLICK REACTIONS FOR POLYMERIZATION AND FUNCTIONALIZATION OF PEG HYDROGEL MICROPARTICLES[*]

2.1 Overview

Click chemistry is a versatile tool for the synthesis and functionalization of polymeric biomaterials. Here, we describe a versatile new strategy for producing bioactive, protein-functionalized poly (ethylene glycol) (PEG) hydrogel microparticles that is based on sequential thiol-ene and tetrazine click reactions. Briefly, tetra-functional PEG-norbornene macromer and dithiothreitol (SH) crosslinker were combined at a 0.75:1 [SH]:[norbornene] ratio, emulsified in a continuous Dextran phase, and then photopolymerized to form PEG hydrogel microparticles that varied from 8 to 30 μm in diameter, depending on the PEG concentration used. Subsequently, tetrazine-functionalized protein was conjugated to unreacted norbornene groups in the PEG microparticles. Tetrazine-mediated protein tethering to the microparticles was first demonstrated using fluorescein-labelled ovalbumin as a model protein. Subsequently, bioactive protein tethering was demonstrated using alkaline phosphatase (ALP) and glucose oxidase (GOx). Enzyme activity assays demonstrated that both ALP and GOx

[*] Reprinted with permission from "Sequential thiol-ene and tetrazine click reactions for the polymerization and functionalization of hydrogel microparticles" by F. Jivan, R. Yegappan, H. Pearce, J. K. Carrow, M. McShane, A. K. Gaharwar, and D. L. Alge. *Biomacromolecules*, 2016, 17, 3516 – 23. Copyright 2016 American Chemical Society.[133]

maintained their bioactivity and imparted tunable bioactivity to the microparticles that depended on the amount of enzyme added. ALP-functionalized microparticles were also observed to initiate calcium phosphate mineralization *in vitro* when incubated with calcium glycerophosphate. Collectively, these results show that protein-functionalized hydrogel microparticles with tunable bioactive properties can be easily synthesized using sequential click chemistry reactions. This approach has potential for future applications in tissue engineering, drug delivery, and biosensing.

2.2. Introduction

Click chemistry is a versatile tool for the synthesis and functionalization of polymeric biomaterials. Click chemistry encompasses a chemical toolkit of highly efficient, specific, and high-yielding reactions that can be performed under mild conditions and produce inoffensive byproducts.[97] Two notable click reactions that are gaining importance for biological applications are the thiol-ene and bioorthogonal tetrazine reactions. The thiol-ene click reaction, which refers to the radical-mediated addition of a thiol to a non-sterically hindered alkene (e.g., norbornene), is being used extensively in polymer synthesis.[134-137] Key advantages of thiol-ene click reactions include their insensitivity to oxygen and the potential for rapid yet stoichiometrically-controlled polymerization, which can be further kinetically controlled via photoinitiation.[138, 139] Thiol-ene click chemistry has also been used to achieve facile incorporation of synthetic peptides and proteins into hydrogel biomaterials, which has led to its broad adoption in the preparation of extracellular matrix mimics for tissue

engineering.[63, 65, 78, 94, 140, 141] Bio-orthogonal tetrazine click reactions are a different class of addition reactions that proceed spontaneously via an inverse electron-demand Diels-Alder cycloaddition between tetrazines and electron rich alkenes, such as norbornene and trans-cyclooctene.[142] Importantly, tetrazine click reactions can proceed with fast reaction rates, do not require radical initiation, can be performed in aqueous conditions at physiologic temperature and pH, and are generally compatible with cells and biologics.[143, 144] Thus, tetrazine click chemistry is considered to be bioorthogonal. Bioorthogonal tetrazine ligation has been used for both in vitro and in vivo cell labelling,[104, 105, 145, 146] polymer coupling,[144] and cell encapsulation within bioactive hydrogels.[106, 147] Tetrazine click chemistry is also synthetically tractable for biomaterials scientists, as gram-scale quantities of asymmetric tetrazines suitable for bioconjugation and polymer functionalization can be readily synthesized.[148] This is an important advantage compared to other bioorthogonal click reactions.

We are interested in applying click chemistry to the development of hydrogel microparticles due to their utilization in a variety of medical and biological applications spanning from drug delivery to tissue engineering and regenerative medicine.[149-152] Griffin *et al.* recently reported using hydrogel microparticles as injectable building blocks for macroporous scaffolds, which they showed accelerated wound healing *in vivo*.[116] This exciting work highlights an emerging application for hydrogel microparticles in the production of 3D scaffolds with enhanced regenerative capabilities, as opposed to their common use as discrete microdevices for drug and cell delivery. Hydrogel microparticles are routinely synthesized by liquid-liquid phase separation using solution, suspension or

emulsion polymerization-based strategies.[153, 154] The general approach of liquid-liquid two phase polymerization is useful because it is simple to perform and can be easily scaled up to quickly produce large batches of microparticles, for example when photopolymerization is employed. Recently, Parlato *et al.* demonstrated the fabrication of hydrolytically- and enzymatically-degradable PEG microparticles that were tens of microns in diameter by vinyl photopolymerization within a water-in-water emulsion.[151] Young *et al.* employed vinyl photopolymerization in combination with submerged electrospraying in oil to produce larger microparticles (hundreds of microns in diameter) under conditions that were suitable for cell encapsulation.[155]

It should be appreciated that the implementation of click chemistry can advance the production of bioactive hydrogel microparticles and lead to new applications in drug delivery and tissue engineering. Indeed, click-based approaches have been used to synthesize hydrogel microparticles incorporating bioactive agents. For example, the previously cited study by Griffin *et al.* used the thiol-vinyl sulfone Michael addition, which is a base-catalyzed click reaction, to make hydrogel microparticles containing peptide sequences that were critical to their microparticle annealing approach.[116] In another recent study, Belair *et al.* used photoinitiated thiol-ene click chemistry to produce peptide-functionalized hydrogel microparticles capable of sequestering and releasing vascular endothelial growth factor.[156] This approach is particularly interesting, as the fast kinetics and efficiency of photoinitiated thiol-ene click chemistry make it well suited for batch microparticle synthesis. Moreover, the use of norbornene as the alkene provides a unique opportunity to combine thiol-ene and tetrazine click reactions for hydrogel

microparticle synthesis and functionalization in a potentially synergistic way by capitalizing on norbornene's reactivity with tetrazines.[104, 106, 144, 146, 147, 157-161] In our opinion, bioorthogonal tetrazine click chemistry is particularly well-suited for functionalizing prefabricated batches of microparticles with bioactive proteins, as this strategy completely avoids exposing the protein to potentially damaging conditions during microparticle fabrication, which could be critical when working with fragile proteins.

Therefore, the objective of this study was to combine thiol-ene and tetrazine click chemistry in a sequential process to develop a versatile and tunable platform for producing protein-functionalized bioactive hydrogel microparticles. The proposed approach combines the benefits of thiol-ene click chemistry (rapid microparticle synthesis, stoichiometric control, tunable material properties, and potential for scale-up) with tetrazine click chemistry to achieve click-mediated protein incorporation into microparticles while preserving native function. To this end, thiol-norbornene and tetrazine-norbornene click reactions were used sequentially to fabricate hydrogel microparticles by performing the thiol-ene polymerization off-stoichiometry (0.75:1.0 thiol-to-norbornene ratio) and then chemically conjugating tetrazine-functionalized proteins to the remaining norbornene groups. PEG concentration was varied to characterize its effect on microparticle size. Efficacy of the tetrazine bioconjugation reaction was then tested using fluorescein-labelled ovalbumin as a model protein. Finally, alkaline phosphatase (ALP) and glucose-oxidase (GOx) were tested to demonstrate utility with bioactive proteins and quantitatively assess microparticle bioactivity.

2.3 Materials and Methods

2.3.1 PEG-Tetra Norbornene (PEG-NB) Synthesis

A PEG-NB precursor for hydrogel microparticles was synthesized according to a previously described method with slight variation.[63] Briefly, 5.0 g PEG macromer (20 kDa, 4-arm PEG-hydroxyl, JenKem), 4-(dimethylamino)pyridine (0.5X to PEG-OH, Sigma-Aldrich), pyridine (5X to PEG-OH, Sigma-Aldrich), and anhydrous dichloromethane (20 mL) were dissolved in round-bottom flask under argon. Separately, 5-Norbornene-2-carboxcylic acid (10 COOH:1 PEG-OH, Alfa Aesar; predominantly endo isomer), diisopropylcarbodiimde (Alfa Aesar) anhydrous dichloromethane (15 mL, Acros) were mixed for 30 min at room temperature in a reaction vessel under argon to generate a dinorbornene anhydride, which was filtered to remove precipitated urea salts and then added to the round-bottom flask containing PEG. The solution was allowed to react overnight at room temperature, after which it was precipitated in 10-fold vol. excess of diethyl ether (Thermo Fisher) and vacuum filtered to yield a white precipitate (PEG-NB). The PEG-NB was subsequently dried under vacuum for 24 h, dialyzed against deionized water for 2 days (MWCO = 10 kDa), and lyophilized to obtain quantitative yield of purified PEG-NB. Analysis by ^{1}H NMR indicated quantitative end-group functionalization with norbornene (**Appendix, Figure VI-1**).

2.3.2 PEG Thiol-ene Microparticle Synthesis and Characterization

Microparticles were synthesized via an aqueous two-phase emulsion system based on bulk phase dextran-disperse phase PEG polymer immiscibility[156] (**Figure II-1**).

Briefly, a dispersed phase consisting of varying wt % PEG-NB macromer (7.5 wt %, 10 wt %, 15 wt %), dithiothreitol (0.75:1.0 thiol−ene, Alfa Aesar) and lithium phenyl-2,4,6-trimethylbenzoylphosphinate photoinitiator (LAP, 2 mM; synthesized as previously described;[162] **Appendix, Figure VI-2**), was emulsified in a bulk phase of dextran (40 wt %, 40 kDa, BioChemica) and LAP (3.125 mM). Emulsions were vortexed and allowed to sit for 10 min to allow for phase separation and then photopolymerized with 365 nm UV light (10 mW/cm^2, 5 min, Lumen Dynamics Omnicure S2000 Series). The resulting microparticles were pelleted via centrifugation (4400 rpm, 10 min) in PBS (30:1 by vol.). The supernatant was decanted and the microparticles were viewed using bright field microscopy (10X, Nikon Eclipse TE2000-S). Microparticle diameters were determined from bright field images analyzed using the ImageJ Particle Analyzer tool (NIH), and a size distribution histogram was plotted for the varying PEG concentrations). Microparticles were stored long-term in PBS and were stable against hydrolysis at neutral pH, as expected.[163] Microparticles prepared with 10 wt % PEG-NB were used for subsequent protein conjugation experiments.

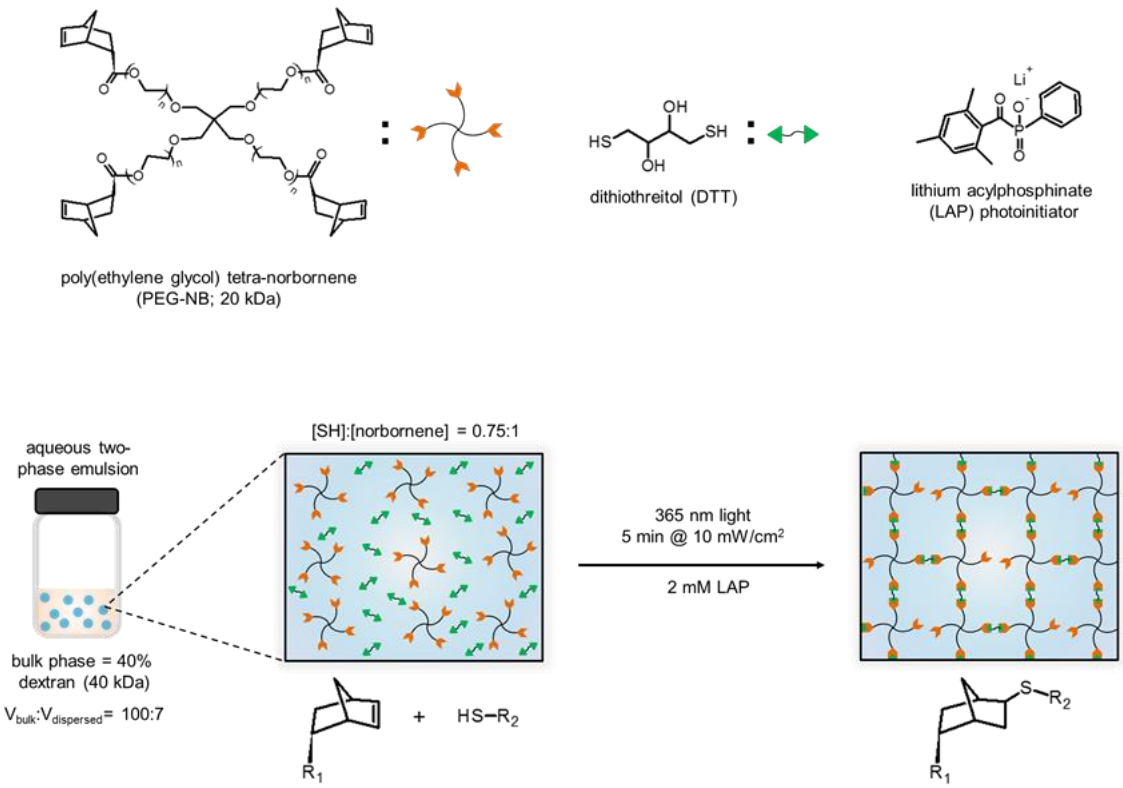

Figure II-1. Chemical structures and schematic of PEG microparticle synthesis using thiol-ene click chemistry. Top Panel: Chemical structures for monomers poly(ethylene glycol) tetra-norbornene (PEG-NB), represented by 4 arm stars, and dithiothreitol (DTT), represented by linear chains, along with photoinitiator lithium acylphosphinate (LAP) are shown. Bottom Panel: A dispersed phase consisting of PEG-NB, DTT (0.75:1 thiol–ene ratio), and LAP were emulsified in a bulk phase consisting of 40 kDa dextran and LAP (100 bulk:7 disperse, by vol.). The emulsion was photopolymerized at 365 nm light for 5 min at 10 mW/cm2 to yield hydrogel microparticles with 25% unreacted norbornene groups. The figure depicts an idealized hydrogel network. Reprinted with permission from "Sequential thiol-ene and tetrazine click reactions for the polymerization and functionalization of hydrogel microparticles" by F. Jivan, R. Yegappan, H. Pearce, J. K. Carrow, M. McShane, A. K. Gaharwar, and D. L. Alge. *Biomacromolecules*, 2016, 17, 3516 – 23. Copyright 2016 American Chemical Society.[133]

2.3.3 Characterization of Norbornene Conversion via Sequential Thiol-ene and Tetrazine Click Reactions

5-(4-(1,2,4,5-Tetrazin-3-yl)benzylamino)-5-oxopentanoic acid was synthesized by reacting 5-(4-(cyano)benzylamino)-5-oxopentanoic acid with hydrazine, formamidine

acetate, and zinc triflate catalyst, as previously described.[104] This tetrazine was subsequently converted to a succinimidyl ester upon reaction with *N,N′*-disuccinimidyl carbonate and trimethylamine in acetonitrile according to the method of Han *et al.*[146] The resulting tetrazine NHS ester (Tz-NHS, **Appendix, Figure VI-3**) was purified by flash chromatography and verified by electrospray ionization mass spectrometry ([M + H] predicted = 399.1, actual = 399.1). To characterize norbornene conversion via sequential thiol−ene and tetrazine click reactions, hydrogels were cross-linked with dithiothreitol and functionalized to varying extents with Tz-NHS. Samples were prepared at 0.75:1 [SH]:[ene] ratio, 0.75:1 [SH]:[ene] ratio followed by 0.25:1 [Tz]:[ene], and 0.75:1 [SH]:[ene] ratio followed by 0.4:1 [Tz]:[ene] (i.e., excess tetrazine). Samples were degraded in 0.01 M sodium hydroxide overnight to hydrolyze ester linkages between norbornene and PEG, pH equilibrated with equimolar hydrochloric acid, then frozen at −80 °C and lyophilized for 2 days. Lyophilized product was dissolved in a mixture of deuterated solvents (50:50, deuterium oxide: dimethyl sulfoxide-d6) and ^{1}H NMR was performed on a 300 MHz instrument to quantify conversion of alkene protons on norbornene.

2.3.4 Protein-Functionalization with Tetrazine Click Chemistry

2.3.4.1 General Approach

For protein functionalization, 100 mM Tz-NHS dissolved in DMSO, was added to the protein of interest (10-fold molar excess tetrazine to protein) in PBS, and allowed to incubate at room temperature for 1 h to allow for tetrazine conjugation to amines of the

protein (Tz-Protein). Subsequent protein functionalization of the microparticles was achieved by incubating pelleted microparticles with Tz-Protein at room temperature for 1 h (**Figure II-2**). Microparticles were then washed three times with PBS (10,000 rpm, 5 min) to remove unconjugated Tz-Protein. The microparticle pellet was resuspended in PBS (600 μL), and further testing was performed based on the conjugated protein of interest.

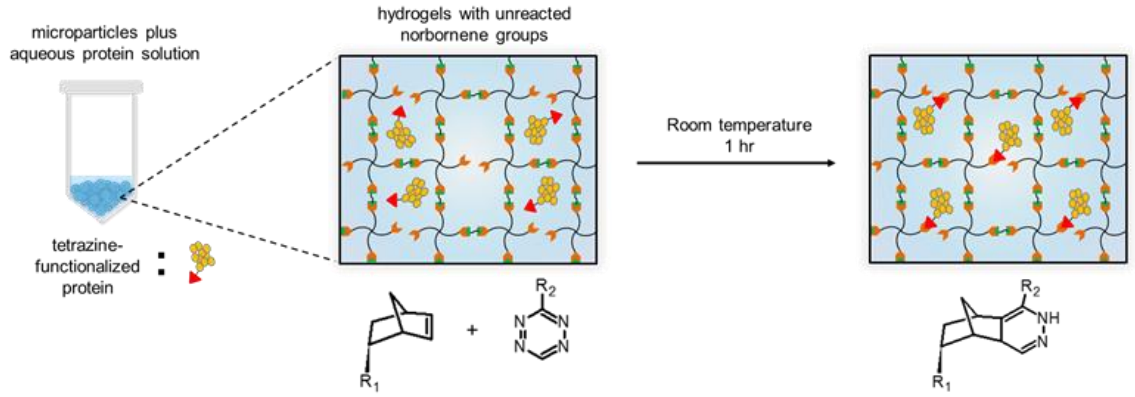

Figure II-2. Chemical structures and schematic of protein-functionalized microparticles using tetrazine-norbornene click chemistry. Pelleted microparticles were incubated for 1 h at room temperature with tetrazine-functionalized protein to allow them to "click" onto the previously unreacted norbornene groups present in the microparticles and yield bioactive, protein-functionalized hydrogel microparticles. The figure depicts an idealized hydrogel network. Reprinted with permission from "Sequential thiol-ene and tetrazine click reactions for the polymerization and functionalization of hydrogel microparticles" by F. Jivan, R. Yegappan, H. Pearce, J. K. Carrow, M. McShane, A. K. Gaharwar, and D. L. Alge. *Biomacromolecules*, 2016, 17, 3516 – 23. Copyright 2016 American Chemical Society.[133]

2.3.4.2 Fluorescein – Ovalbumin

Fluorescein−ovalbumin (5 mg/mL, Life Technologies) in PBS was tetrazine functionalized (Tz-Ovalbumin) and conjugated to the microparticles as described above. Incubation with the microparticle pellet was also performed using fluorescein−ovalbumin

without tetrazine functionalization (NF-Ovalbumin), which served as a negative control for protein tethering with the tetrazine−norbornene click reaction. After the microparticle pellet was resuspended in PBS, the microparticles were imaged using fluorescence microscopy (Nikon Eclipse TE2000-S). Their fluorescence was quantified by analysis on a flow cytometer (BD Accuri C6).

2.3.4.3 Alkaline Phosphatase

Alkaline phosphatase (ALP) from bovine intestinal mucosa (Sigma-Aldrich) was dissolved in PBS (50 mg/mL). Tetrazine functionalization (Tz-ALP) and microparticle conjugation were performed as described above. A negative control for microparticle conjugation was also prepared with non-functionalized ALP (NF-ALP). Prior to microparticle conjugation, Tz-ALP and NF-ALP were compared to ensure tetrazine conjugation did not affect bioactivity (**Appendix, Figure VI-4**).

To study dose-dependent ALP bioactivity, microparticles were loaded with varying amounts of NF-ALP and Tz-ALP (ranging from 0 mg/mL − 25 mg/mL). Microparticles were added to para-nitrophenylphosphate substrate (pNPP, Sigma-Aldrich) in a 96-well plate, and the change in absorbance at 405 nm was monitored over time on a microplate reader (TECAN Infinite M200 Pro). The absorbance increases over time were plotted, and the slopes of the data sets were compared to determine ALP activity.

To demonstrate ALP-induced mineralization, 0.1 M calcium glycerophosphate (Alfa Aesar) dissolved in milli-Q water was incubated with Tz-ALP conjugated

microparticles and control NF-ALP microparticles at 37 °C for 1 h. A negative control of calcium glycerophosphate without microparticles was also tested. Microparticles and any precipitated solids were then centrifuged and washed three times with milli-Q water (10 000 rpm, 5 min) prior to mineralization staining. Alizarin red S (2%, pH 4.2, Electron Microscopy Sciences) was filtered through 25 mm syringe-tip, nylon membrane filter (0.45 μm) and incubated with the microparticles at room temperature for 10 min. The microparticles were subsequently washed three times with milli-Q water and visualized in bright field for red-stained calcium deposits on an inverted microscope (Nikon Eclipse TE2000S). To quantify alizarin red S staining, the microparticles were destained by incubating with 10% glacial acetic acid at room temperature for 30 min, after which the microparticles were pelleted by centrifugation (10 000 rpm, 5 min) and the supernatant was collected. Ten percent ammonium hydroxide was added to the supernatant to return the red color and acidic pH (4.1−4.5). The absorbance at 405 nm was then quantified on a microplate reader.

2.3.4.4 Glucose Oxidase

Glucose oxidase (GOx) was dissolved in PBS (50 mg/mL), functionalized with tetrazine (Tz-GOx), and then conjugated to microparticles, as described above. A negative control for microparticle conjugation was also prepared with non-functionalized GOx (NF-GOx). Prior to microparticle conjugation, Tz-GOx and NF-GOx were compared to ensure tetrazine conjugation did not affect bioactivity (**Appendix, Figure VI-5**).

To study dose-dependent GOx enzyme bioactivity, microparticles were loaded with varying amounts of NF-GOx and Tz-GOx (ranging from 0 mg/mL to 8 mg/mL). Microparticles were washed three times in PBS to remove unconjugated protein, and equilibrated in sodium acetate buffer (pH 5) for 1 h. An adaptation of an established protocol40 was used to quantify GOx bioactivity. Briefly, NF-GOx- and Tz-GOx-conjugated microparticles were incubated in a solution of D-glucose (1.67 wt %), horseradish peroxidase (0.007 mg/mL), and o-dianisidine dye (1.68 μM) in sodium acetate buffer in a 96-well plate, and the change in absorbance at 490 nm was monitored over time on a microplate reader. The absorbance increases over time were plotted, and the slopes of the data sets were compared to determine GOx activity.

2.3.5 Effect of Tetrazine Functionalization on Protein Bioactivity

To evaluate whether or not enzyme functionalization with tetrazine affect bioactivity, 25 mg/mL solutions of NF-ALP and 25 mg/mL Tz-ALP were prepared. Samples were then diluted 1:1000 in a 96-well plate (0.025 mg/mL) and ALP kinetic assay was performed to measure ALP activity of the enzymes in solution. Similarly, 8 mg/mL solutions of NF-GOx and Tz-GOx were prepared. Samples were then added to a 96-well plate, and the GOx kinetic assay was performed to measure GOx activity of the enzymes in solution. The assays were performed as described in the previous experimental sections.

2.3.6 Effect of Norbornene Availability on Protein Conjugation

To demonstrate that norbornene groups are required for protein conjugation, microparticles were prepared with 0.75:1 thiol-ene ratio. Subsequently, these microparticles were incubated with either 25 mg/mL NF-ALP, 25 mg/mL Tz-ALP, or a solution of 5 mM L-Cysteine and 2.9 mM LAP. The microparticles treated with L-Cysteine and LAP were then exposed to UV-365 nm light at 10mW/cm^2 for 5 minutes to initiate a thiol-ene reaction and thereby consume previously unreacted norbornene groups, washed, and then incubated with 25 mg/mL Tz-ALP (this group is referred to as L-Cys + Tz-ALP). All NF-ALP and Tz-ALP incubations were for 1 h at room temperature. The microparticles were subsequently washed and tested for bioactivity as described in the previous experimental sections.

2.3.7 Characterization of Protein Conjugation

ALP and GOx functionalized microparticles were prepared as described in the previous experimental sections. Subsequently, to characterize the amount of protein incorporated by the tetrazine click conjugation reaction, microparticles functionalized with ALP (25 mg/mL) and GOx (8 mg/mL) were degraded via treatment with 0.01M NaOH solution, which hydrolyzed ester linkages between the norbornene and PEG. After being neutralized with equimolar HCl, the concentration of protein in solution was quantified using the CBQCA assay (Thermo Fisher Scientific) according to the manufacturer's protocol.

2.3.8 Statistical Analysis

Particle size data was statistically analyzed in GraphPad Prism 6 using one-way ANOVA followed by post hoc comparisons between PEG weight percentages using Tukey's method. More than 1000 particle diameters were measured from bright field images using ImageJ. Additionally, both ALP and GOx data were statistically using two-way ANOVA with loaded protein concentration and functionalization (i.e., tetrazine-functionalized vs. non-functionalized) as the main effects. Post hoc comparisons between groups were performed using Tukey's method. ALP and GOx data sets were analyzed using results from three independent trials. In all cases, statistically significant data was determined with a p-value of <0.05.

2.4 Results and Discussion

2.4.1 Thiol-ene Polymerization of Hydrogel Microparticles

Key advantages to using photoinitiated thiol−ene click chemistry in conjunction with the emulsion-based microparticle synthesis are the rapid gelation times, stoichiometric control, tunability of material properties, and potential for scale up. We first characterized microparticle size using the thiol−ene polymerization and polymer immiscibility emulsion. Microparticles were synthesized with different concentrations of PEG-NB macromer (7.5, 10, and 15 wt %), and bright field images were analyzed in Image-J to determine average particle size of these different batches. In order to select a maximum number of particles in each image without background interference, a low threshold was set prior to obtaining particle diameters. More than 1000 particles were

analyzed for each PEG-NB wt % variation. The data showed that as PEG-NB wt % increased, average particle size also significantly increased ($p < 0.05$) from 8.88 µm ± 5.28 to 31.7 µm ± 7.03 µm (**Figure II-3**). The increase in particle size could be attributed directly to an increase in PEG content, which increases the volume of polymer as well as the total volume of water in the microparticles at equilibrium swelling. The 15 wt % group also appeared to have lower polydispersity, which could potentially be attributed to a reduction in the occurrence of network non-idealities at higher polymer concentrations.[160, 163, 164]

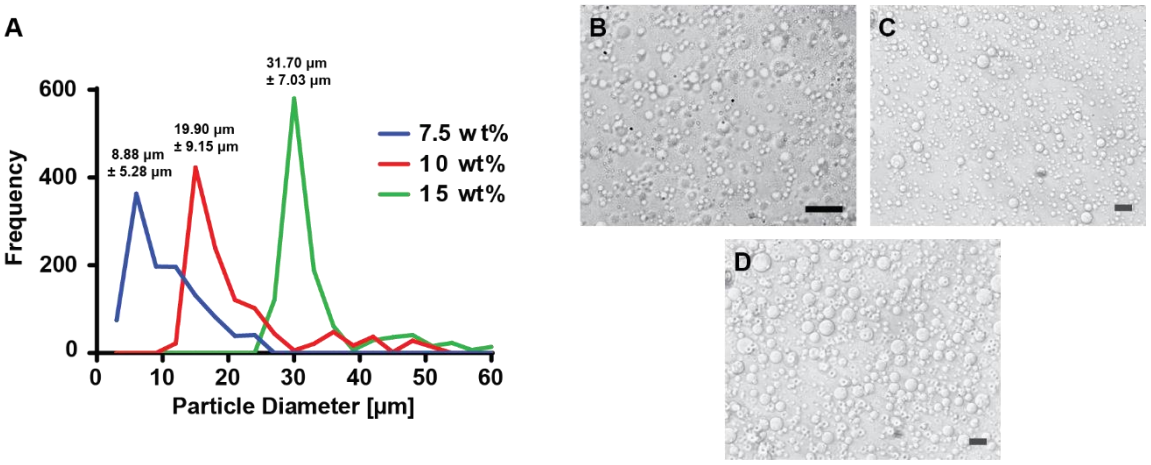

Figure II-3. Microparticle size variation with PEG-NB concentration. (A) Histogram of particle size for microparticles synthesized with each PEG concentration (7.5, 10, 15 wt %) is plotted, along with the calculated average particle size and standard deviation (n = 1124) noted above each peak. Data was analyzed by one-way ANOVA followed by post hoc comparisons (Tukey's method). Statistical analysis showed average particle size significantly increased with PEG concentration ($p < 0.05$). (B–D) Bright-field, grayscale images of microparticles for the increasing PEG concentrations are shown. Scale bars = 50 µm. Reprinted with permission from "Sequential thiol-ene and tetrazine click reactions for the polymerization and functionalization of hydrogel microparticles" by F. Jivan, R. Yegappan, H. Pearce, J. K. Carrow, M. McShane, A. K. Gaharwar, and D. L. Alge. *Biomacromolecules*, 2016, 17, 3516 – 23. Copyright 2016 American Chemical Society.[133]

Hydrogel microparticle size is just one of several important variables that could affect the performance of these materials for applications in tissue engineering and drug delivery. In addition, other variables besides PEG concentration that were not investigated here but could be tuned to modulate the properties of the microparticles include the PEG molecular weight, the PEG-arm functionality, and the length of the dithiol crosslinker. The addition of enzymatically degradable linkers (*i.e.* matrix metalloproteinase degradable peptides) in particular could enhance the utility of these microparticles, for example by facilitating the enzymatically triggered release of a therapeutic growth factor for regenerative medicine.[126, 165-167] Future work will focus on this possibility, as well as increasing average particle size to hundreds of microns in diameter for applications in cell delivery. Additionally, although the polydispersity of the microparticles did not affect other aspects of this project, we will explore methods such as dropwise polymerization from a water-in-oil emulsion (*e.g.* submerged electrospraying,[155] microfluidics[116]) to generate more monodisperse batches without compromising fabrication scalability.

2.4.2 Norbornene Conversion via Sequential Click Reactions

To demonstrate the stoichiometric control of the thiol−ene click and that the unreacted norbornenes can subsequently participate in tetrazine click reactions, norbornene conversion was quantified by ^{1}H NMR and compared to unreacted PEG-NB (**Figure II-4**). Conversion of norbornene groups inversely correlated with the integration of alkene hydrogen peaks. As expected, norbornene conversion was approximately 76.5% at the 0.75:1 [SH]:[ene] ratio. The addition of 0.25 and 0.4 equiv of Tz-NHS relative to

the initial amount of norbornene groups increased the conversion to 89.5% and 94%, respectively. These results demonstrate that unreacted norbornenes are available for tetrazine-mediated functionalization, although a higher than expected amount of tetrazine was required to achieve near complete conversion.

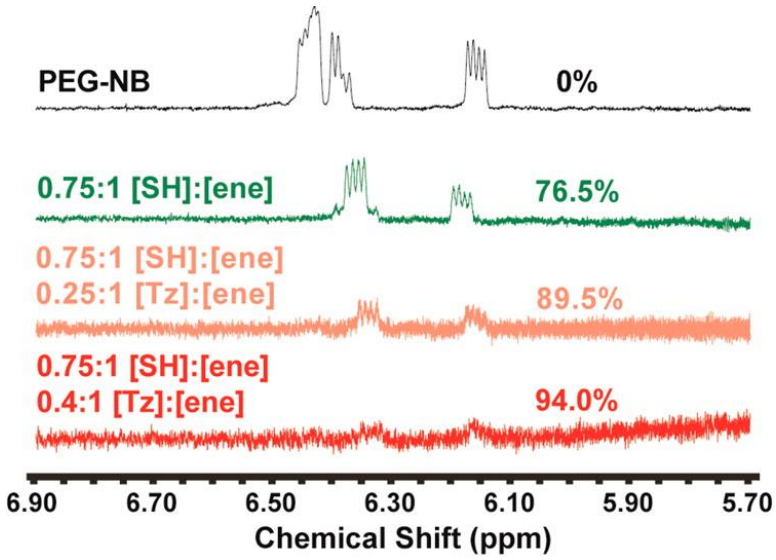

Figure II-4. ^{1}H NMR characterization of norbornene conversion. The peaks corresponding to the alkene protons of norbornene were markedly reduced after cross-linking at a 0.75:1 [SH]:[ene] ratio, and integration relative to the ethylene glycol protons of PEG revealed 76.5% conversion in the thiol–ene click reaction. Subsequent reductions corresponding to 89.5% and 94% conversion were observed when tetrazine was added, indicating that the residual norbornene groups were accessible for tetrazine click functionalization. Reprinted with permission from "Sequential thiol-ene and tetrazine click reactions for the polymerization and functionalization of hydrogel microparticles" by F. Jivan, R. Yegappan, H. Pearce, J. K. Carrow, M. McShane, A. K. Gaharwar, and D. L. Alge. *Biomacromolecules*, 2016, 17, 3516 – 23. Copyright 2016 American Chemical Society.[133]

2.4.3 Fluorescent Protein Conjugation with Tetrazine – Norbornene Click Reaction

To demonstrate the efficacy and selectivity of the tetrazine-norbornene click reaction, fluorescein-labeled ovalbumin was used as a model protein to visualize microparticle biotethering (**Figure II-5 a-d**). Microparticles were clearly seen fluorescing

green under widefield fluorescence microscopy after incubation with tetrazine-functionalized fluorescein ovalbumin (Tz-Oval), indicating successful ovalbumin tethering. In contrast, minimal fluorescence was observed visually when the microparticles were incubated with fluorescein ovalbumin that was not tetrazine-functionalized (NF-Oval), indicating that unconjugated fluorophore was removed during PBS washing steps. The fluorescence of Tz-Oval, NF-Oval, and non-functionalized microparticles was also quantitatively analyzed on a flow cytometer (**Figure II-5 e** and **Appendix, Figure VI-6**). Surprisingly, the NF-Oval microparticles had measurable fluorescence by flow cytometry. Since ovalbumin, which has a hydrodynamic radius of approximately 3 nm, is small enough to diffuse through the polymer mesh, this result suggests that the fluorescent protein was not completely removed after washing. Nevertheless, there was a nearly 5-fold increase in the average fluorescence intensity for the particles treated with Tz-Oval.

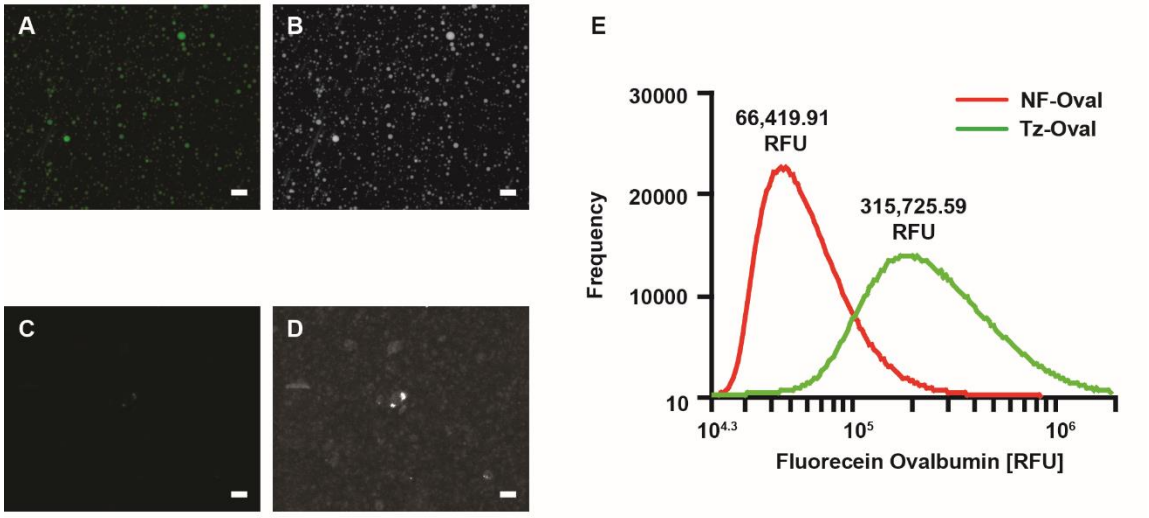

Figure II-5. Selective conjugation of Tz-fluorescein ovalbumin to microparticles. (A,C) Fluorescence images of Tz-Oval microparticles and control NF-Oval microparticles, respectively, showing selective attachment of tetrazine functionalized protein. (B,D) Corresponding contrast-enhanced grayscale images for panels A and C, respectively, showing the presence of microparticles in the control image. Scale bars = 50 μm. (E) Frequency plot of relative fluorescence units (RFU) for both Tz-Oval and NF-Oval microparticles obtained by analysis on a flow cytometer, with average RFU values noted above each peak. A total of 900,000 particles were measured for each sample. Reprinted with permission from "Sequential thiol-ene and tetrazine click reactions for the polymerization and functionalization of hydrogel microparticles" by F. Jivan, R. Yegappan, H. Pearce, J. K. Carrow, M. McShane, A. K. Gaharwar, and D. L. Alge. *Biomacromolecules*, 2016, 17, 3516 – 23. Copyright 2016 American Chemical Society.[133]

2.4.4 Dose-Dependent ALP Bioactivity

To demonstrate conjugation of a bioactive protein we first chose ALP, which is a well-studied and characterized protein related to bone tissue engineering.[168, 169] As previously mentioned, one of the advantages for utilizing the bio-orthogonal tetrazine-norbornene click reaction is the lack of radical production during polymerization, which can affect protein bioactivity. After incubating microparticles with tetrazine-functionalized or non-functionalized ALP (Tz-ALP and NF-ALP, respectively, with NF-

ALP being a negative control) bioactivity was confirmed based on pNPP substrate conversion to *p*-nitrophenol, which was monitored on a microplate reader (**Figure II-6**). Importantly, the microparticles showed dose-dependent bioactivity after incubation with 0 mg/mL to 25 mg/mL of Tz-ALP, as shown by the plots of absorbance versus time. However, minimal bioactivity was observed for microparticles treated with NF-ALP as well as for microparticles that were treated with Tz-ALP but lacked norbornene groups (**Appendix, Figure VI-7**). Quantitative analysis of the ALP activity based on the slopes of the absorbance-versus-time curves showed that the bioactivities of microparticles incubated with 6.25 mg/mL of Tz-ALP and higher concentrations were statistically higher ($p < 0.05$) compared to their negative control counterparts treated with equal NF-ALP concentrations (*). Bioactivity was also significantly increased with increasing Tz-ALP concentrations from 6.25 to 25 mg/mL (‡). These observations indicated increased ALP incorporation for Tz-ALP microparticles compared to NF-ALP microparticles, which was corroborated by protein loading measurements for the highest ALP concentration (**Appendix, Figure VI-8**).

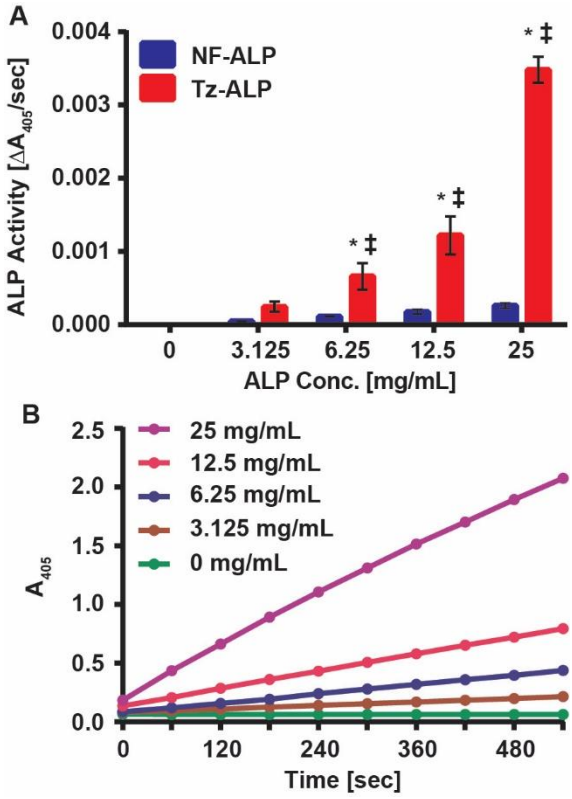

Figure II-6. ALP bioactivity after microparticle functionalization. (A) Average ALP activity of Tz-ALP and NF-ALP microparticles with standard deviations. Data was analyzed by two-way ANOVA followed by post hoc comparisons (Tukey's method). The symbols * and ‡ indicate significant differences between Tz-ALP and NF-ALP and between Tz-ALP concentrations, respectively ($p < 0.05$). (B) Representative curves of absorbance versus time for microparticles functionalized with varying amounts of Tz-ALP and then incubated with the ALP substrate p-nitrophenyl phosphate. Reprinted with permission from "Sequential thiol-ene and tetrazine click reactions for the polymerization and functionalization of hydrogel microparticles" by F. Jivan, R. Yegappan, H. Pearce, J. K. Carrow, M. McShane, A. K. Gaharwar, and D. L. Alge. *Biomacromolecules*, 2016, 17, 3516 – 23. Copyright 2016 American Chemical Society.[133]

In addition to measuring bioactivity via substrate consumption, mineralization is another important and measurable function of ALP bioactivity because of the enzyme's key role in mineralization *in vivo*.[170-173] Thus, mineralization was evaluated by incubating ALP-functionalized microparticles with calcium glycerophosphate and then staining with

alizarin red S. Consistent with the ALP activity data collected using the *p*-nitrophenyl phosphate substrate, Tz-ALP-treated microparticles induced substantial mineralization, as indicated by robust red staining throughout the particles, whereas microparticles incubated with NF-ALP and calcium glycerophosphate control alone were not stained. Quantitative analysis by dye destaining and absorbance measurements confirmed that mineralization was significantly increased for the microparticles functionalized with Tz-ALP (**Figure II-7**). Based on the staining results, the Tz-ALP microparticles appeared to act as nucleation sites for mineralization.

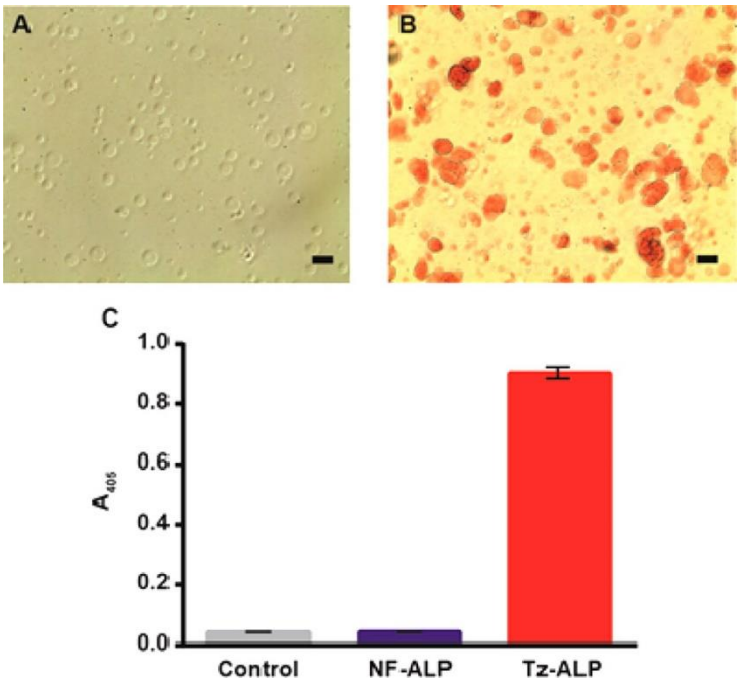

Figure II-7. Quantifying ALP mineralization. (A) Bright field images of 25 mg/mL NF-ALP microparticles and (B) 25 mg/mL Tz-ALP microparticles after alizarin red S staining. Scale bars = 50 μm. (C) Average absorbance measurements at 405 nm after alizarin red S destaining with standard deviations. Statistical analysis confirmed a significant increase in mineralization for 25 mg/mL Tz-ALP group ($p < 0.05$). Reprinted with permission from "Sequential thiol-ene and tetrazine click reactions for the polymerization and functionalization of hydrogel microparticles" by F. Jivan, R. Yegappan, H. Pearce, J. K. Carrow, M. McShane, A. K. Gaharwar, and D. L. Alge. *Biomacromolecules*, 2016, 17, 3516 – 23. Copyright 2016 American Chemical Society.[133]

2.4.5 Dose-Dependent GOx Loading and Bioactivity

To further demonstrate the versatility of our sequential click system, we chose GOx as a second bioactive protein. Importantly, GOx is widely used in glucose biosensing,[174-177] as it catalyzes the oxidation of *D*-glucose to gluconic acid and hydrogen peroxide in the presence of oxygen. This reaction can be quantitatively monitored *in vitro* using horseradish peroxidase and an appropriate colorimetric substrate, such as *o*-dianisidine. Similar to ALP, the bioactivity of microparticles incubated with tetrazine-functionalized GOx (Tz-GOx) was quantified by monitoring the increase in absorbance due to D-glucose consumption/*o*-dianisidine oxidation over time (**Figure II-8**). Similar to what was observed for microparticles functionalized with Tz-ALP, the absorbance-versus-time curves for microparticle bioactivity showed a concentration-dependent increase when functionalized with 0 mg/mL to 8 mg/mL of Tz-GOx. Analysis of the GOx activity, calculated from the slopes of the kinetic curves, showed that 2 mg/mL Tz-GOx and higher concentrations were statistically higher ($p < 0.05$) when compared to their negative control counterparts of equal NF-GOx concentration (*). The increases in enzyme activity as Tz-GOx concentration increased to 2, 4, and 8 mg/mL were also statistically significant (‡). These observations indicated increased GOx incorporation for Tz-GOx compared to NF-GOx, which was supported by protein loading measurements for the highest GOx concentration (**Appendix, Figure VI-9**).

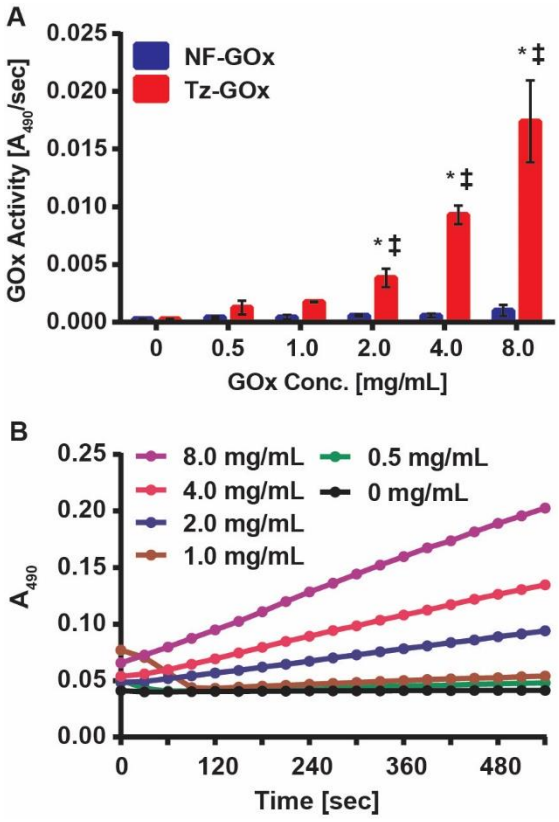

Figure II-8. GOx bioactivity after microparticle functionalization. (A) Average GOx activity of Tz-GOx and NF-GOx microparticles with standard deviations. Data was analyzed by two-way ANOVA followed by post hoc comparisons (Tukey's method). The symbols * and ‡ indicate significant differences between Tz-GOx and NF-GOx and between Tz-GOx concentrations, respectively ($p < 0.05$). (B) Representative curves of absorbance versus time for microparticles functionalized with varying amounts of Tz-GOx and incubated with d-glucose, horseradish peroxidase, and o-dianisidine dye. Reprinted with permission from "Sequential thiol-ene and tetrazine click reactions for the polymerization and functionalization of hydrogel microparticles" by F. Jivan, R. Yegappan, H. Pearce, J. K. Carrow, M. McShane, A. K. Gaharwar, and D. L. Alge. *Biomacromolecules*, 2016, 17, 3516 – 23. Copyright 2016 American Chemical Society.[133]

2.5 Conclusions

This study demonstrates the novel use of sequential thiol−ene and tetrazine−norbornene click reactions to produce protein-functionalized bioactive hydrogel microparticles. The results show that facile control of microparticle size and maintenance

of protein bioactivity/function after conjugation can be achieved. The polymerization and tethering mechanisms used here address the need for versatile, user-controlled chemical tools for synthesizing bioactive polymers. Additionally, because these click reactions are scalable and synthetically tractable for biomaterials, they are amenable to batch fabrication of bioactive materials. Taken together, this strategy of bioactive functionalization is a novel platform that can be employed for theoretically any protein of interest and shows promise for applications in tissue engineering, drug delivery, and biosensing.

CHAPTER III

SEQUENTIAL THIOL-ENE AND TETRAZINE CLICK REACTIONS FOR SYNTHESIZING AND ANNEALING PEG HYDROGEL MICROPARTICLES INTO MICROPOROUS HYDROGELS

3.1 Overview

Microporous annealed particle (MAP) hydrogels are an emerging class of biomaterials with the potential to improve outcomes in tissue repair and regeneration. Here, building upon our previous sequential click platform, a new MAP hydrogel platform comprising PEG hydrogel microparticles that are annealed *in situ* using bio-orthogonal tetrazine click chemistry is reported as a promising tissue engineering platform. Briefly, clickable PEG-peptide hydrogel microparticles with ECM-mimetic peptides to permit cell adhesion and enzymatic degradation were fabricated *via* submerged electrospraying and stoichiometrically controlled thiol-ene click chemistry. Subsequently, unreacted norbornene groups in the microparticles were leveraged for functionalization with bioactive proteins as well as annealing into MAP hydrogels via the tetrazine-norbornene click reaction, which is highly selective and proceeds spontaneously without requiring an initiator or catalyst. Initial mechanical characterization of the novel MAP hydrogel platform was explored with varying tetrazine crosslinker concentrations. The results demonstrate that clickable microparticles can be easily applied to fill a tissue-like defect and rapidly annealed *in situ* to form robust scaffolds with an inherently microporous structure. In addition, the ability to produce MAP hydrogels with heterogeneous properties

by incorporating multiple types of hydrogel microparticles is demonstrated, first with fluorophore-functionalized hydrogel microparticles and then with protein-functionalized hydrogel microparticles. For the latter, tetrazine-modified Texas Red ovalbumin was first demonstrated as a model protein to selectively conjugate to MAP hydrogels, followed by alkaline phosphatase (ALP). Tetrazine-functionalized ALP microparticles were mixed with non-functionalized microparticles to produce MAP hydrogels, which subsequently produced a biomimetic mineralized/non-mineralized interface upon incubation in calcium glycerophosphate. Lastly, human mesenchymal stem cells were encapsulated within tetrazine-crosslinked MAP hydrogels and cell proliferation/spreading were assessed. Overall, these results demonstrate that bio-orthogonally annealed MAP hydrogels are a versatile platform for delivery of stem cells and bioactive growth factors.

3.2 Introduction

Hydrogel microparticles have long been popular materials used for drug/growth factor and cell delivery.[3, 178] Recent emerging strategies in the development of novel biomaterials have demonstrated the use of microparticles as building blocks for microporous annealed particle (MAP) hydrogel scaffolds. While cell culture dimensionality (*i.e.* cell culture in 2-D vs. 3-D) has long been established as an important factor for recapitulating *in vivo*-like mechanical and biochemical conditions within an *in vitro* environment, hydrogel dimensionality or form-factor has recently become an interesting area of exploration for tissue engineering scaffolds. A major advantage of MAP hydrogels is their interconnected microporosity compared to conventional nanoporous

bulk hydrogels which allow for better cell motility and nutrient diffusion.[116, 179] Additionally, cells are able to directly interact with microparticle surfaces rather than being embedded within the hydrogel matrix, resulting in a pseudo-3D platform that can utilize 2D physiochemical properties of microparticles for directing cellular responses.[180] MAP scaffolds fundamentally allow for spatial control by tuning the mechanical and biochemical properties of microparticle building blocks independent of bulk properties, which can be exploited for user-controlled heterogeneity. Lastly, MAP hydrogels can also be assembled *via* precise 3D printing technologies using microparticles are bio-inks, as we have recently shown.[119]

A number of synthetic strategies have been used to anneal microparticles into MAP hydrogels. Seminal work by Griffin *et al*. laid the foundation for annealing microparticles by chemically linking complementary functional groups together, namely lysine and glutamine residues *via* transglutaminase.[116] This enzymatic strategy has continued to be used,[179, 181] but alternative non-enzymatic annealing chemistries have also been reported such as vinyl polymerizations, strain-promoted azide-alkyne cycloadditions,[10, 117, 182] and adamantane-cyclodextrin guest-host interactions.[182, 183] In addition, we recently reported the use of thiol-norbornene click photopolymerization for microparticle synthesis and MAP hydrogel assembly. In our work, we produced poly(ethylene glycol) (PEG) hydrogel microparticles *via* submerged electrospraying and thiol-ene photopolymerization, which allowed us to tune the physicochemical properties of the microparticles to influence how cells responded to the materials.[118] We also controlled the stoichiometry so that the microparticles contained an excess of norbornene groups which enabled facile annealing

with a PEG-di-thiol linker and a secondary thiol-ene reaction. While this approach was effective, the requirement to photoinitiate the annealing reaction could be a barrier to clinical adoption. Thus, we sought to develop an alternative chemical strategy for annealing that would be compatible with our method of producing PEG hydrogel microparticles.

Tetrazine click chemistry is an ideal approach to annealing norbornene-containing hydrogel microparticles into MAP hydrogels. In general, tetrazine click chemistry refers to the inverse-electron demand Diels-Alder reaction between *s*-tetrazines and electron-rich dienophiles, such as norbornene and trans-cyclooctene.[184] Tetrazine click reactions are generally fast, efficient, selective, proceed under physiologic conditions, and produce only nitrogen gas, which is an inoffensive byproduct. Moreover, tetrazine click reactions do not require the addition of an initiator or catalyst, and can be performed in the presence of living cells and even within living animals.[184] Thus, tetrazine click chemistry is regarded as bioorthogonal, which is a key advantage. Importantly, the tetrazine-norbornene reaction has been used as a primary crosslinking chemistry in several studies on hydrogel biomaterials in recent years.[28, 106, 147] We also recently reported on the use of sequential thiol-norbornene and tetrazine-norbornene click reactions to synthesize norbornene-containing PEG hydrogel microparticles and then functionalize them with bioactive proteins, namely alkaline phosphatase (ALP) and glucose oxidase.[133] Based on this prior work, we hypothesized that a di-tetrazine linker could be used analogously to PEG-di-thiol in our previous work to anneal PEG hydrogel microparticles into MAP hydrogels.

The objective of this study was to expand upon our previous work with sequential click reactions for the development of MAP hydrogels for tissue regeneration therapies. We combined the rapid and high-throughput methods of thiol-ene photopolymerization with water-in-oil electrospraying to fabricate off-stoichiometric, norbornene-bearing PEG microparticles. Subsequently, microparticles with free-norbornene groups were conjugated with a tetrazine-functionalized protein and assembled into MAP hydrogels using a PEG-di-tetrazine crosslinker. MAP hydrogel modulus, porosity, degradation and cell spreading were initially assessed with varying tetrazine crosslinker concentrations. Subsequently, we investigated the ability to produce heterogenous and spatially patterned MAP hydrogels, first with fluorophores and then with tetrazine conjugated proteins ovalbumin and ALP. Importantly, tetrazine-ALP functionalized MAP hydrogels were assessed for protein bioactivity after conjugation *via* selective mineralization in calcium glycerophosphate.

3.3 Materials and Methods

3.3.1 PEG-tetra-norbornene Synthesis

PEG-tetra-norbornene (PEG-NB, 5 kDa) was synthesized as previously described. Briefly, PEG-tetra-hydroxyl (JenKem Technology, 5 kDa), 4-(dimethylamino)pyridine (Sigma Aldrich, 0.5 equiv. to PEG-OH), pyridine (Sigma Aldrich, 5 equiv. to PEG-OH), and anhydrous dichloromethane (Acros Organics) were dissolved in a round-bottom flask under argon. Separately, 5-norbornene-2-carboxcylic acid (Alfa Aesar, 10 equiv. to PEG-OH), diisopropylcarbodiimde (Alfa Aesar) and anhydrous dichloromethane were mixed

for 45 min at room temperature in a reaction vessel under argon to generate a di-norbornene anhydride. The resulting product was filtered to remove precipitated urea salts and then added to the round-bottom flask containing dissolved, activated PEG-tetra-hydroxyl. The solution was allowed to react overnight at room temperature, precipitated in cold diethyl ether (Fischer, 10-fold vol. excess) and dried under vacuum for 2 days to yield a white precipitate. The product was further purified by dialysis against deionized water for 2 days (MWCO = 1 kDa) and lyophilized to obtain purified PEG-norbornene. Analysis by ^{1}H NMR indicated quantitative norbornene end group functionalization. ^{1}H NMR (500 MHz, $CDCl_3$, δ): 6.19 – 5.90 (m, 2H), 4.26 – 4.12 (m, 2H), 3.73 – 3.54 (m, ~113H).

3.3.2 PEG-di-Tetrazine Synthesis

PEG-di-tetrazine (PEG-di-Tz, 4.2 kDa) was synthesized from PEG-di-amine (Laysan Bio, 3.4 kDa) and tetrazine carboxylic acid (Tz-COOH) as previously described with slight modification. Briefly, PEG-di-amine was dissolved in 1-methyl-2-pyrrolidinone (NMP, Chem Impex) with diisopropylethylamine (DIEA, 2.5 equiv.) and allowed to stir for 15 min. Separately, 5-(4-(1,2,4,5-Tetrazin-3-yl)benzylamino)-5-oxopentanoic acid (Tz-COOH, Sigma Aldrich, 3 equiv.) was activated with O-(Benzotriazol-1-yl)-N,N,N’,N’-tetramethyl-uronium hexafluorophosphate (HBTU, Chem Impex, 3 equiv.) in NMP for 5 min. The Tz-COOH solution was mixed with the PEG-di-amine solution and allowed to react at room temperature overnight. The reaction mixture was precipitated in cold diethyl ether (10-fold vol. excess), and vacuum dried for 2 days

to yield a pink precipitate. The product was further purified by dialysis against deionized water for 2 days and lyophilized to obtain purified PEG-di-Tz. Analysis by ^{1}H NMR indicated ~85% tetrazine end-group functionalization. ^{1}H NMR (500 MHz, DMSO-d6, δ): 10.57 (s, 1H), 8.45 (d, 2H), 7.54 (d, 2H), 4.40 (s, 2H), 3.65-3.23 (m, ~154H), 2.19-2.11 (m, 4H), 1.76 (m, 2H).

3.3.3 Peptide Synthesis

Peptide synthesis was performed on rink amide resin with a microwave assisted peptide synthesizer (CEM DiscoverBio) using standard Fmoc solid phase peptide synthesis and HBTU activation with DIEA (0.5 M) in NMP. Coupling reactions were generally performed for 8 min at 75 °C, except for cysteine (C) and arginine (R) which were coupled for 8 min at 50 °C, and 25 min at room temperature then 5 min at 75 °C, respectively. Fmoc protecting groups were deprotected with piperidine (20%) in NMP for 6 min at 75 °C, except for aspartic acid (D) containing sequences which used piperazine (5%) with hydroxybenzotriazole (HOBt, 0.1 M) in NMP to prevent aspartimide formation. The peptide was cleaved by treatment with a mixture of trifluoroacetic acid:phenol:triisopropyl silane:water (90:5:2.5:2.5) for 2 hrs at room temperature followed by precipitation in cold diethyl ether. Crude peptide was purified by reverse-phase high performance liquid chromatography (RP-HPLC, Thermo Scientific UltiMate 3000 with Agilent Technologies C18 column, ACN in water with 0.01% TFA). Purified fractions were lyophilized and analyzed via matrix assisted laser desorption ionizaiton time-of-flight mass spectrometry (MALDI-TOF MS) to verify peptide composition. Peptides were

dissolved in PBS and absorbance measurements at 205 nm and 280 nm (Biotek Plate Reader) along with peptide molar absorptivity coefficients were used to calculate the stock concentrations. The MMP-degradable crosslinker (KCGPQGIWGQCK, (MALDI) m/z: $[M + H]^+$ calcd for $C_{56}H_{90}N_{18}O_{14}S_2$, 1303.56; found, 1303.463) was synthesized as described above and purified by RP-HPLC (solvent profile: 95% ACN:5% Water, -1.5% ACN min^{-1} over 8 min). The cell-adhesive, fibronectin-derived peptide (CGRGDS, (MALDI) m/z: $[M + H]^+$ calcd for $C_{20}H_{36}N_{10}O_9S$, 592.62; found, 593.45) was used for incorporation of cell binding domains within microparticles and was synthesized as described above and purified by RP-HPLC (solvent profile: 80% ACN:20% Water, -1.5% ACN min^{-1} over 8 min).

3.3.4 PEG Thiol-ene Microparticle Fabrication via Electrospraying

Thiol-ene microparticles were synthesized using water-in-oil submerged electrospraying combined with UV light for photopolymerization. Briefly, PEG-tetra-norbornene (PEG-NB, 5 kDa, 10 wt%), dithiothreitol (DTT, Sigma Aldrich, 0.75:1 [thiol]:[norbornene]), and photoinitiator lithium acyl phosphinate (LAP, 10 mM, synthesized as previously described[162]) were combined in a pre-polymer solution (300 uL) and electrosprayed into a mineral oil/span 80 mixture (4 kV, 12 mL hr^{-1}). UV-365nm light (60 mW cm^{-2}, 7 min) was exposed onto the sample to induce photoinitiated thiol-norbornene click reaction. PEG microparticles bearing free norbornene groups were isolated via centrifugation and washed with PBS. For all cell studies, microparticles were fabricated with a cell-adhesive peptide (CGRGDS, 1 mM) and an MMP-degradable

peptide crosslinker (KCGPQGIWGQCK) was used instead of DTT (non-degradable) to facilitate long-term cell culture. Additionally, microparticles were sterilized by washing with 70% ethanol followed by two washes in sterile PBS before further use.

3.3.5 Microparticle Size Characterization

Microparticles were incubated with Alexa-488 succinimidyl ester for 1 hr at room temperature. Particles were transferred into a 24-well plate and imaged via fluorescence microscopy (Zeiss Axio Vert A1). Microparticle images were analyzed using FIJI (200 particles analyzed) and particle diameters were binned (20 μm bins) to create a histogram.

3.3.6 Microporous Annealed Particle Hydrogel Fabrication

Microparticles were finally crosslinked to form microporous annealed particle (MAP) hydrogels via tetrazine norbornene click. Briefly, microparticles (50 μL volume, ~13 mM free norbornene) and crosslinker solution containing PEG-di-Tz (12 μL total volume; 0 – 5 mM PEG-di-Tz for rheology, 2 mM PEG-di-Tz for all other experiments unless otherwise specified) were added to a 6 mm mold on glass and allowed to crosslink for 1 hour at 37 °C.

3.3.7 MAP Hydrogel Microporosity

Alexa-488 functionalized microparticles were annealed with various PEG-di-Tz linker concentrations (0 - 5 mM). MAP hydrogels were imaged *via* confocal fluorescence microscopy (Olympus FV1000, 100 μm z-stacks, n = 9 per experimental group) and

porosity was measured using FIJI plugin "Voxel Counter" to measure the percent of porous space in the image stack.

3.3.8 MAP Hydrogel Rheology

Mechanical characterization of MAP hydrogels was performed using *in situ* oscillatory time sweep rheology. Uncrosslinked non-degradable microparticles (50 μL volume) were placed under an 8-mm parallel plate tool and the tool was lowered until the microparticles filled the gap. PEG-di-Tz crosslinker solution was added (0 - 5 mM, 12 μL) prior to lowering the tool to initiate crosslinking. A time sweep within the linear viscoelastic regime (Anton Paar MCR-301, 1% strain, 1 rad/sec angular frequency) was performed during tetrazine-norbornene click reaction until storage modulus bean to plateau (~40 min). Representative *in situ* gelation curves and final storage moduli were plotted.

3.3.9 Collagenase Digestion of MAP Hydrogels

Enzymatic degradation of MAP hydrogels was compared between low and high PEG-di-Tz concentrations (2 mM and 8 mM, respectively) against non-degradable counterparts. MAP hydrogels were placed in cell strainers within a 6-well plate and submerged within a solution of collagenase-B (0.5 mg/mL) in ultra-pure water. The plate was placed in a 37 ℃ bead bath during the degradation study. MAP hydrogels were removed from the plate within the cell strainers, dried, and mass loss was monitored over time.

3.3.10 In situ MAP Hydrogel Annealing in a Tissue-like Defect

To demonstrate *in situ* MAP hydrogel assembly, a tissue-like defect was made at the edge of a plaster block using a small end-mill bit. A glass slide was taped over the edge to provide containment for the microparticle/crosslinker solution as well as provide cross-sectional visibility. Images were taken with a Canon DSLR camera at each step during the MAP hydrogel fabrication process (*i.e.* packing of microparticles, addition of crosslinker solution, etc.). Alexa-548 functionalized microparticles were utilized as they were colored blue under ambient lighting conditions, allowing for easy visibility. After MAP hydrogel crosslinking, the wedge-shaped hydrogel was removed to verify annealing.

3.3.11 Stereomicroscopy Imaging of MAP Hydrogel Patterns

Annealed constructs (6-mm diameter) were imaged under brightfield using a Zeiss SteREO Discovery microscope to show a generic MAP hydrogel. To enable fluorescence visualization, electrosprayed microgels were functionalized by incubation with Alexa-488 NHS Ester or Alexa-548 NHS Ester for 1 hr at room temperature, resulting in fluorophore conjugation to the peptides in the microparticles. Differentially colored microparticles were then combined and added to an 8-mm diameter cylindrical silicone mold to make heterogeneous MAP hydrogels with various patterns (half & half and uniformly mixed). MAP hydrogels were imaged using the Zeiss SteREO microscope in brightfield and using the green fluorescence filter.

3.3.12 Tetrazine-functionalized Protein Conjugation to MAP Hydrogels

3.3.12.1 Texas Red Ovalbumin

Texas Red-labelled Ovalbumin (Life Technologies, 1.5 mg/mL) was reacted with Tz-NHS (10 molar equivalents, Sigma Aldrich) or with dimethyl sulfoxide (non-functionalized protein, NF-Ovalbumin) for 1 hour at room temperature. Tetrazine-functionalized and non-functionalized fluorescent ovalbumin (1 mg/mL) was reacted with norbornene-containing PEG microparticles (50 µL) for 1 hour at room temperature, after which the microparticles were washed with PBS (4 times) and then annealed with PEG-di-Tz (2 mM) for 1 hour at room temperature to form MAP hydrogels. MAP hydrogels were then imaged *via* confocal fluorescence microscopy and FIJI 3D-Viewer plugin was used to generate images and qualitative assess protein conjugation.

3.3.12.2 Alkaline Phosphatase

Tetrazine-functionalized alkaline phosphatase (Tz-ALP) was produced similarly to ovalbumin. Briefly, ALP (25 mg/mL) was incubated with Tz-NHS (10 molar equivalents) for 1 hour at room temperature to yield tetrazine-functionalized ALP (Tz-ALP). Tz-ALP solution was then incubated with a microparticle pellet for 1 hour at 37 °C, to allow for the tetrazine-norbornene reaction to conjugate ALP to the microparticles, followed by four wash steps with PBS to remove unbound protein, before use in mineralization studies.

3.3.13 Mineralization of Tz-ALP-functionalized MAP Hydrogels

To demonstrate formation of a mineralized/non-mineralized interface in MAP hydrogels, a batch of ALP-functionalized microparticles prepared with 10x Tz-NHS functionalized ALP were mixed with ALP-free microparticles. MAP hydrogels were then made in a 6-mm diameter silicone mold as previously described with half of the hydrogel made from Tz-ALP-functionalized microparticles and the other half with ALP-free microparticles. For mineralization, the MAP hydrogels were placed in calcium glycerophosphate (0.1 M in ultrapure water) for 1 hour at 37 °C, and mineralization was visualized using alizarin red S staining and brightfield imaging on a Zeiss SteREO Discovery microscope. Higher magnification images were also taken using brightfield imaging on a Zeiss AxioVert.A1.

3.3.14 hMSC Spreading and Proliferation

Human mesenchymal stem cell (hMSC) spreading and proliferation were compared on degradable MAP hydrogels at low and high PEG-di-Tz concentrations (2 mM and 8 mM, respectively). hMSCs were obtained from the Institute of Regenerative Medicine at Texas A&M University and cultured in α-Minimal essential medium (Gibco) supplemented with 20% v/v fetal bovine serum (Atlanta Biologics), penicillin (50 U/mL), streptomycin (50 µg/mL), and 2 mM Glutamax (Invitrogen) at 5% CO_2 and 37 °C. hMSCs were used at passage 3. For cell encapsulation studies, 2.5 x 10^5 cells were added per microgel scaffold during the crosslinking step. After annealing, scaffolds were placed in hMSC cell culture medium. For cell spreading studies, at 2 days and 8 days, cell-laden

scaffolds were fixed in formaldehyde for 15 min at room temperature followed by washing in PBS. MAP hydrogels were incubated in Triton X (0.1%) for 5 min followed by washing in PBS. F-actin staining with Rhodamine Phalloidin (1:40 in 1% BSA, 165 nM) for 30 min at room temperature. MAP hydrogels were washed in PBS twice. Nuclei staining with DAPI (1:1000 in PBS, 14.3 nM) was performed for 10 min at room temperature followed by washing in PBS. After staining, scaffolds were imaged via fluorescence confocal microscopy. For monitoring cell proliferation in microgel scaffolds, at 2 days and 8 days, scaffolds were washed once with PBS before being added to 300 µL 1x RIPA buffer within microtubes. After centrifugation, cell lytic supernatant was taken for Quant-iT Pico Green assay in order to quantify double-stranded DNA (d.s. DNA) content on the fluorescence plate reader.

3.3.15 Statistical Analysis

Statistical analysis of data was performed in GraphPad Prism 8. For mechanical characterization (n = 3, per experimental group), a one-way ANOVA with post-hoc comparisons (Tukey's method) was performed ($p < 0.05$). For cell spreading and proliferation (n = 3, per experimental group), a two-way ANOVA with post-hoc comparisons (Tukey's method) was performed ($p < 0.05$).

3.4 Results and Discussion

3.4.1 Characterization of Microparticles and MAP Hydrogels

Norbornene-bearing microparticles were produced by off-stoichiometric thiol-ene photopolymerization combined with water-in-oil submerged electrospraying (**Figure III-1 a**). Thiol-ene microparticles were successfully synthesized and isolated with an average particle size of 157 μm and moderate polydispersity with a standard deviation of 28 μm (**Figure III-1 b**).

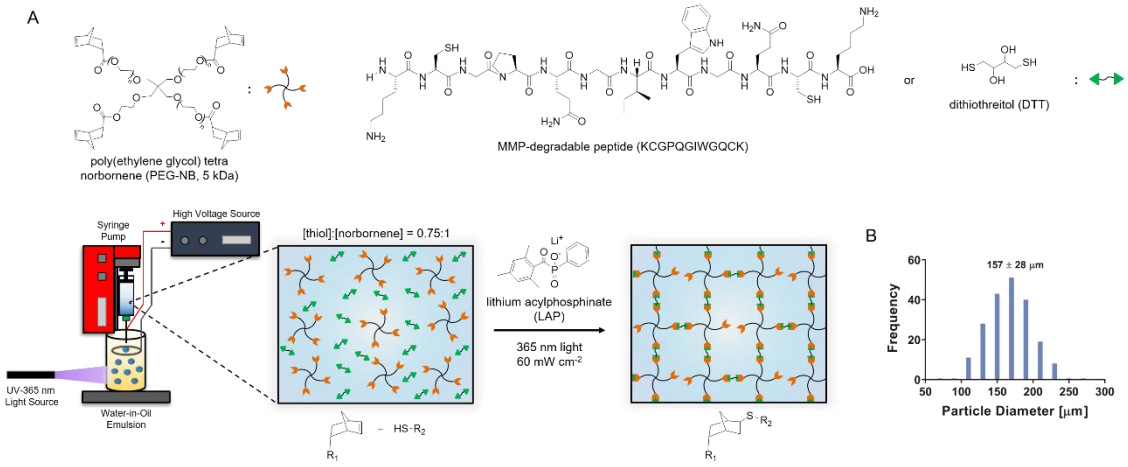

Figure III-1. Microparticle electrospraying and size characterization. Top Panel: Microparticle pre-precursor solution made from polyethylene glycol-tetra norbornene (PEG-NB) represented as 4-arm star, dithiothreitol (DTT) or MMP-degradable peptide crosslinker (KCGPQGIWGQCK) represented as a linear chain, and photoinitiator lithium acylphosphonate (LAP). Bottom Panel: The schematic shows off-stoichiometric, thiol-ene photopolymerization of PEG microparticles via water-in-oil electrospraying to form norbornene-bearing microparticles. The histogram shows average microparticle size (157 μm) and standard deviation (28 μm) after electrospraying (n = 200 particles).

Next, for initial mechanical characterization studies, microparticles were assembled into MAP hydrogels through a PEG-di-Tz crosslinker using bio-orthogonal tetrazine click chemistry (**Figure III-2 a**). MAP scaffold formation using variable PEG-

di-Tz crosslinker concentrations was monitored *in situ* (**Figure III-2 b**). Oscillatory time sweep rheology showed that increasing PEG-di-Tz crosslinker concentration resulted in higher storage moduli scaffolds (**Figure III-2 c**). Additionally, fluorescently-labelled microgel scaffolds were analyzed for differences in microporosity as a result of crosslinker concentration (**Appendix, Figure VI-10**). Analysis from FIJI showed an increase in microporosity with increasing crosslinker concentration, however only the 5 mM PEG-di-Tz scaffold was statistically significant (**Figure III-2 d**).

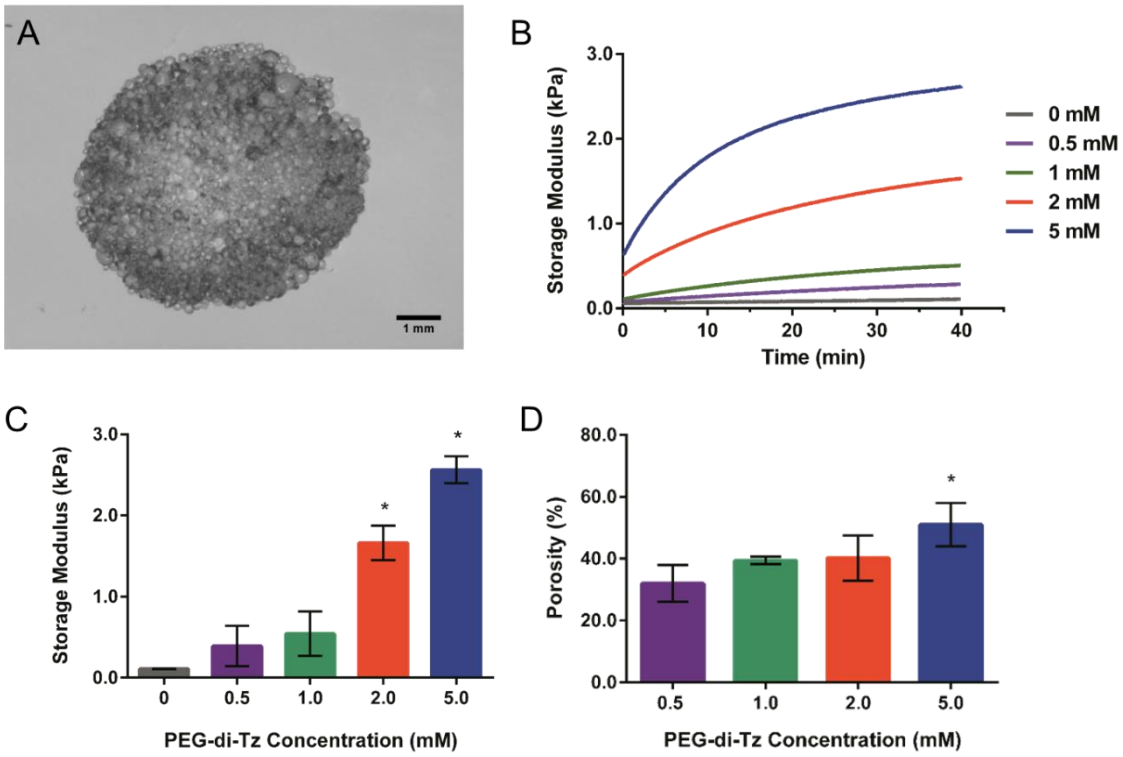

Figure III-2. MAP hydrogel mechanical properties. A) Representative image of a MAP hydrogel. Scale bar = 1 mm B) Representative *in situ* gelation curves from rheology. C) Averaged final storage modulus of MAP hydrogels at various PEG-di-Tz crosslinker concentrations. D) Bar graph of average percent porosity within MAP hydrogels. The symbol * indicates statistical significance with respect to all other PEG-di-Tz concentrations ($p < 0.05$).

3.4.2 MAP Hydrogel Patterning

Heterogeneous MAP hydrogels were produced using fluorophore-labelled microparticles. Incubation of microparticles with Alexa-488 and Alexa-546 NHS esters resulted in distinct color and fluorescence properties due to fluorophore conjugation to amine groups in the peptides. These colored microparticles were easily distinguished from one another in MAP hydrogels when uniformly mixed and when a half/half pattern was produced. In the bright-field images, Alexa-488-labelled microparticles in the MAP hydrogel appeared yellow whereas Alexa-546-labelled particles appeared blue (**Figure III-3 a, b**). Alexa-488-labelled microparticles also fluoresced brightly under the green channel, whereas the Alexa-546-labelled particles appeared dark (**Figure III-3 c, d**).

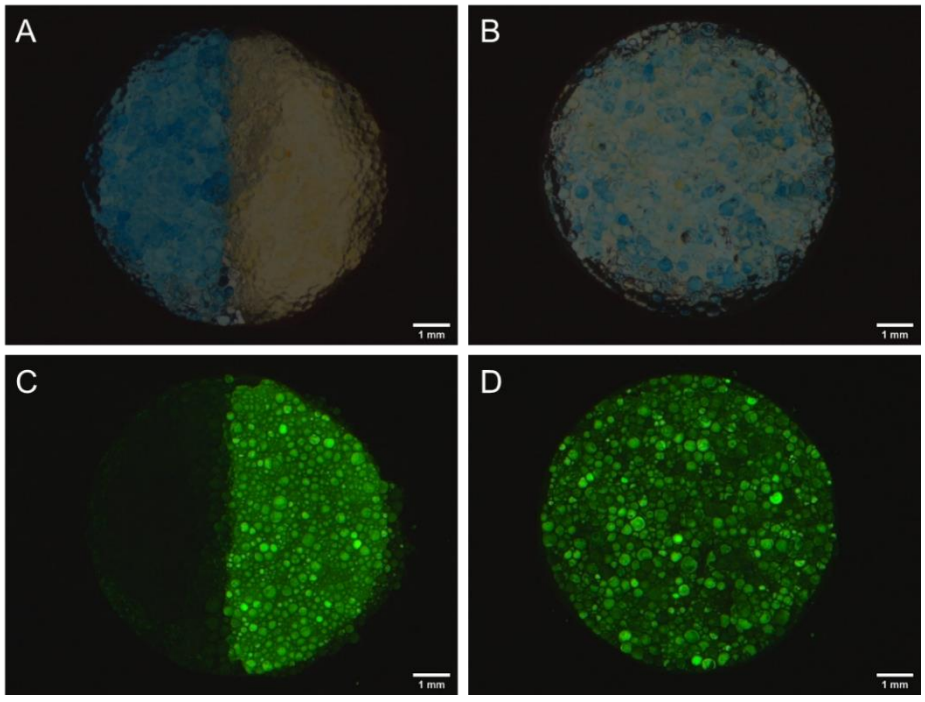

Figure III-3. Heterogeneous MAP hydrogels constructed from fluorophore-labelled PEG microparticles. Brightfield and fluorescence images of TzMAP hydrogels made from A,C) half Alexa-488/half Alexa-548 conjugated microgels and B,D) uniformly mixed Alexa-488 and Alexa-548 microgels. Scale bars = 1 mm.

Lastly for clinical application, we envision the microparticles being applied directly to a tissue defect either via syringe or by being manually scooped/packed-in and then crosslinked *in situ*. To demonstrate the utility of our MAP hydrogel for clinical application towards a periodontal tissue-like defect, microparticles were packed into a wedge-shaped mold and crosslinked with the addition of PEG-di-Tz (**Figure III-4 a-c**). The resulting 3D hydrogel after annealing was well-packed, cohesive, and perfectly matched the wedge defect (**Figure III-4 d**).

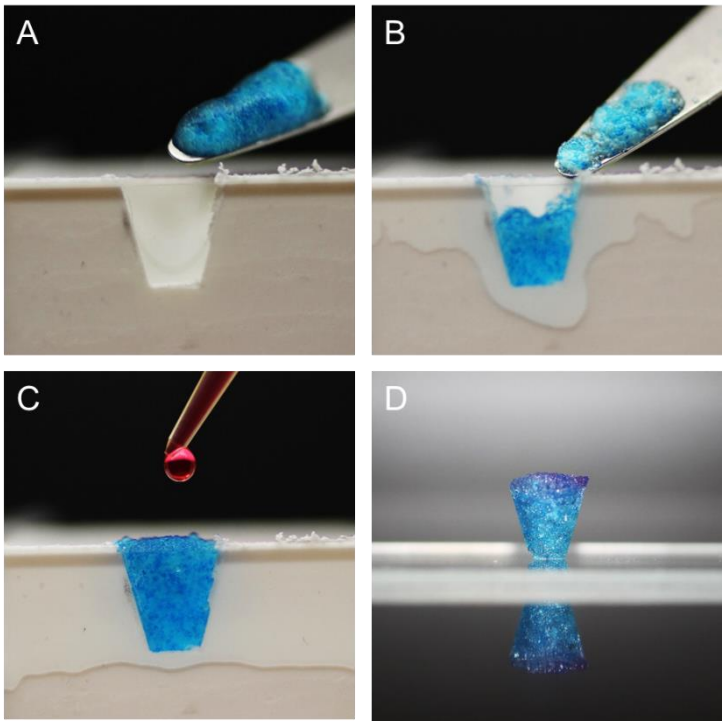

Figure III-4. In situ formation of MAP hydrogel within a tissue-like defect. A-D) Photographs showing formation of a tetrazine-crosslinked MAP hydrogel within a tissue-like defect.

3.4.3 Protein-functionalized MAP hydrogels

Unreacted norbornene groups on microparticles were successfully leveraged for protein functionalization prior to annealing using the same tetrazine click reaction. Texas Red Ovalbumin was reacted with Tz-NHS to form fluorescent tetrazine-modified protein. Non-functionalized protein was used as a control. Subsequently, the protein was incubated with microparticles, which were then annealed into MAP hydrogels. Images obtained from confocal microscopy revealed qualitatively that protein-functionalized MAP hydrogels produced from Tz-NHS demonstrated significantly more fluorescence than non-functionalized counterparts, indicating the importance of the tetrazine moiety (**Figure III-5**).

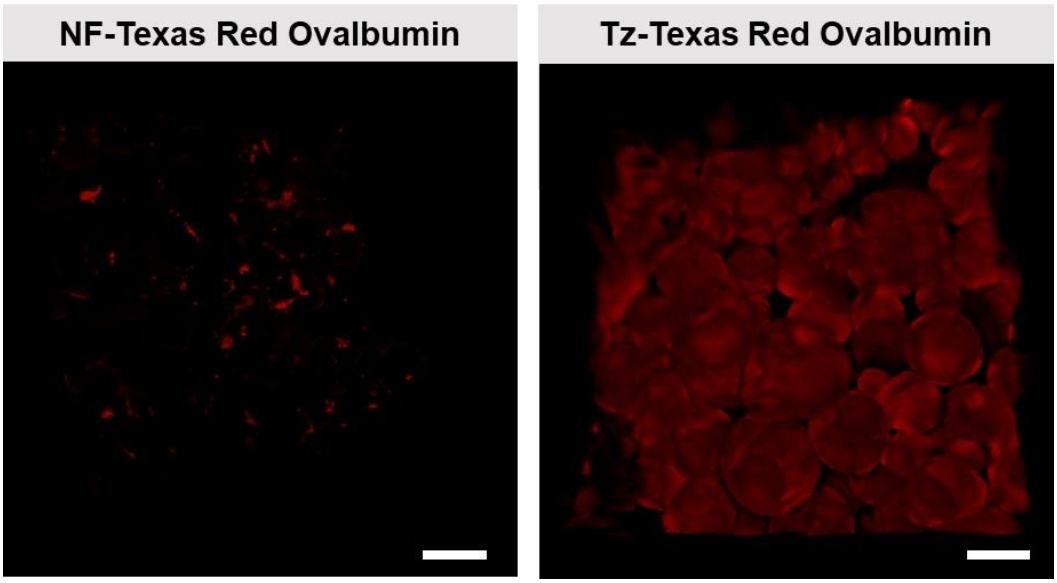

Figure III-5. Tetrazine-mediated protein conjugation to MAP hydrogels. Texas Red-labelled ovalbumin was modified with Tz-NHS and incubated with PEG microgels, which were then used to produce Tz-crosslinked MAP hydrogels. Non-functionalized (NF) Texas Red-labelled ovalbumin was used as a negative control. Scale bars = 200 μm.

Finally, microparticles were utilized to produce heterogeneous MAP hydrogels that were ALP-functionalized on one half and ALP-free on the other. Following incubation with calcium glycerophosphate, these Tz-ALP-functionalized MAP hydrogels were stained with alizarin red to visualize mineralization. Substantial mineralization was observed only on the Tz-ALP-functionalized half of the MAP hydrogels, as indicated by a distinctive red appearance (**Figure III-6 a, b**), while the other half of the MAP hydrogel and control MAP hydrogel (entirely protein free) showed no evidence of mineralization (**Figure III-6 c, d**).

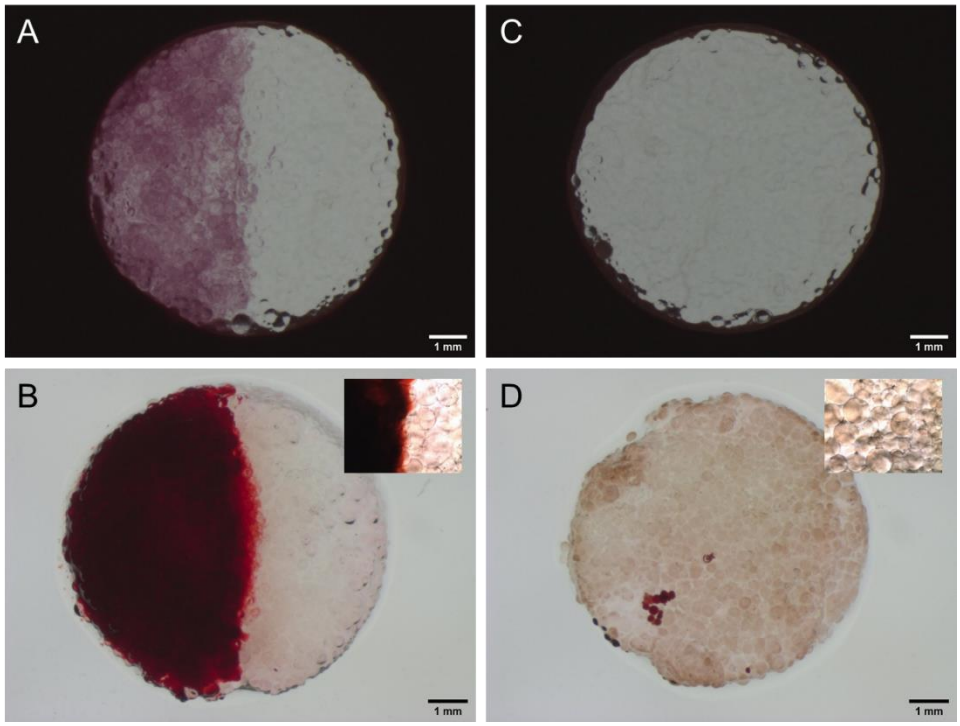

Figure III-6. ALP conjugation and mineralization of MAP hydrogels. Brightfield images of tetrazine-crosslinked MAP hydrogels produced from A) half ALP-functionalized microgels and half non-functionalized microgels, and C) all non-functionalized microgels. Alizarin red (mineralization) staining after 1-hour incubation with calcium glycerophosphate of B) half ALP-functionalized microgels and half non-functionalized microgels and D) all non-functionalized microgels. Scale bars = 1 mm. Insets show higher magnification images.

3.4.4 Tetrazine Click Annealing on hMSC Spreading and Proliferation

While researchers have already shown that the enhanced microporosity within MAP hydrogels provides a permissive microenvironment for cells to spread and proliferate,[116] other factors such as material stiffness and degradability are important to consider for long-term cell growth and viability. Additionally, while tetrazine click reactions have been used in the past for bulk hydrogel crosslinking and cell encapsulation,[106] and direct cell labelling,[105] it was necessary to validate cellular response to annealing of our Tz-crosslinked MAP hydrogels as tissue engineering constructs before proceeding to further cell studies.

Here, MAP hydrogel degradability was compared between a low and high PEG-di-Tz crosslinker concentration and the resulting effects on hMSC spreading and proliferation were measured. After incubation in collagenase-B, MAP hydrogels annealed with 2 mM PEG-di-Tz degraded by 90 min, however MAP hydrogels annealed with 8 mM PEG-di-Tz did not degrade at all (**Figure III-7 a**). This surprising result indicates potential secondary molecular interactions within tetrazine-crosslinked MAP hydrogels that are holding the microparticle network together.

We wanted to further investigate how these differences in degradation profile could affect encapsulated cells (**Figure III-7 b, c**). Within MAP hydrogels annealed with a lower crosslinker concentration, hMSCs were elongated along the surface of the microgels and extended between particles at 2 days (**Figure III-7 d**). By 8 days, cell density appears to have increased and cells have begun to degrade/remodel the MAP hydrogels, likely laying down their own extracellular matrix (ECM) (**Figure III-7 e**). This

increase in proliferation is complemented by d.s. DNA results, showing an increase in average cells per scaffold from 2 days to 8 days. For high crosslinker concentrations, cell number appears to be stunted slightly and show lack of cell spreading at both 2 and 8 days (**Figure III-7 f, g**). In correlation with the degradation results, we know that degradable microparticles crosslinked with a high tetrazine linker concentration cannot degrade, which could explain the lack of cell spreading and ECM remodeling. Thus, despite overcoming the physical restrictions traditionally seen in bulk hydrogels through the use of MAP hydrogels, crosslinker concentration is still an important factor for maintaining a viable cell phenotype. Nonetheless, further investigation into the mechanical stability of highly crosslinked tetrazine MAP hydrogels is still warranted, and additional optimization of cell seeding and perfusion may also be necessary in order to improve cell results.

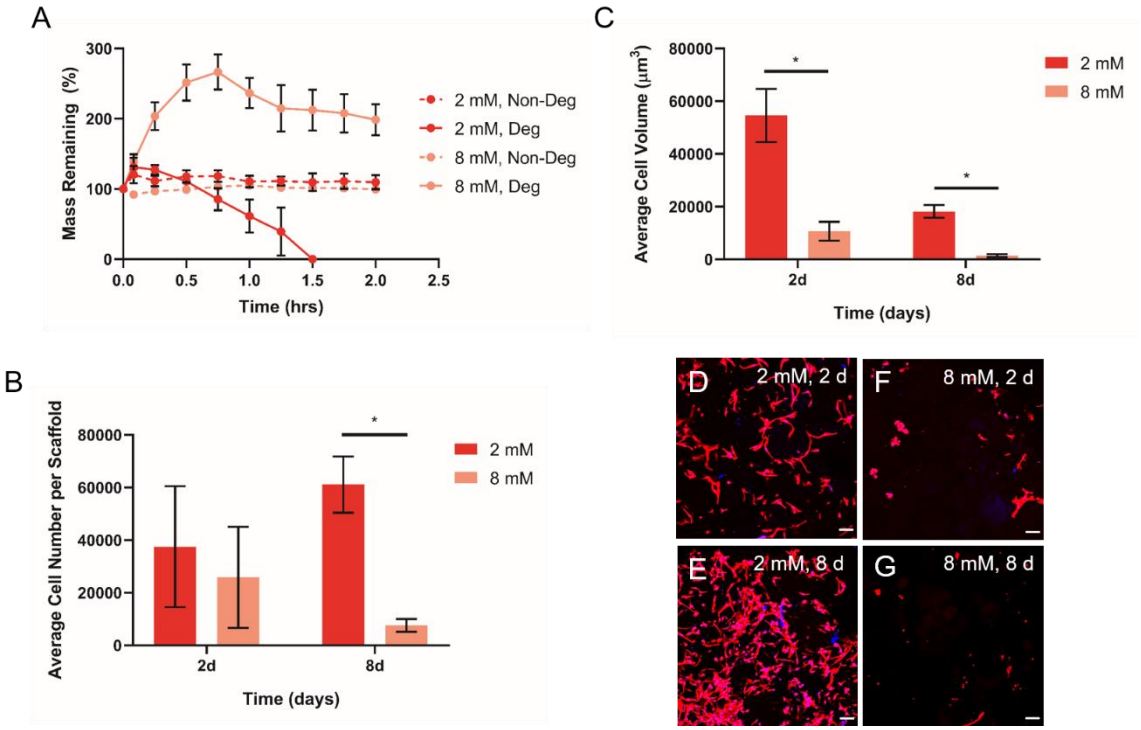

Figure III-7. MAP hydrogel degradation and effect on cell proliferation and spreading. A) Enzymatic degradation of MAP hydrogels crosslinked with low (2 mM) and high (8 mM) PEG-di-Tz crosslinker. B) Average number of hMSCs within MAP hydrogels at 2 days and 8 days. C) Average cell volume within MAP hydrogels at 2 days and 8 days. The symbol * indicates statistical significance between crosslinker concentrations ($p < 0.05$). D-E) Z-projection of representative cell spreading images within 2 mM PEG-di-Tz crosslinked MAP hydrogels and F-G) within 8 mM PEG-di-Tz crosslinked MAP hydrogels. Nuclear DAPI stain is represented in blue and cytoskeletal F-actin stain is represented in red. Scale bar = 100 µm.

3.5 Conclusions

Electrosprayed PEG microparticles prepared *via* off-stoichiometric thiol-norbornene click chemistry were successfully annealed into MAP hydrogels using a PEG-di-Tz linker. MAP hydrogel modulus and degradation were easily tuned with PEG-di-Tz concentration, and the large network of interconnected pores facilitated cell growth and spreading in culture. This approach is amenable to *in situ* MAP hydrogel formation and is

expected to be broadly useful for tissue regeneration and repair. One possibility is to combine MAP hydrogels with tetrazine click-mediated protein conjugation to engineer functional and even heterogenous materials, as demonstrated with ALP. ALP conjugation was specifically leveraged to produce a mineralized/non-mineralized interface, but recent advances in 3D printing MAP hydrogels could enable the production of more sophisticated heterogenous structures. Future studies will also investigate leveraging this conjugation strategy with more sensitive growth factors. Overall, this novel bio-orthogonal approach for the *in situ* assembly of protein-functionalized MAP hydrogels is promising for tissue engineering and "off-the-shelf" type clinical applications.

CHAPTER IV

BIO-ORTHOGONAL, SITE-SELECTIVE PROTEIN CONJUGATION TO MICROPOROUS ANNEALED PARTICLE HYDROGELS

4.1 Overview

Protein conjugation to biomaterial scaffolds is a powerful approach for tissue engineering. However, typical chemical conjugation methods lack site-selectivity and can negatively impact protein bioactivity. To overcome this problem, a site-selective strategy is reported here for installing tetrazine groups on terminal poly-histidines (His-tags) of recombinant proteins. These tetrazine groups are then leveraged for bio-orthogonal conjugation to poly(ethylene glycol) (PEG) hydrogel microparticles, which are subsequently assembled into microporous annealed particle (MAP) hydrogels. Efficacy of the strategy is demonstrated using recombinant, green fluorescent protein with a His tag (His-GFP), which enhanced fluorescence of the MAP hydrogels compared to control protein lacking tetrazine groups. Subsequently, to demonstrate efficacy with a therapeutic protein, recombinant human bone morphogenetic protein-2 (His-BMP2) was conjugated. Human mesenchymal stem cells growing in the MAP hydrogels responded to the conjugated BMP2 and significantly increased mineralization after 21 days compared to controls. Thus, this site-selective protein modification strategy coupled with bio-orthogonal click chemistry is expected to be useful for bone defect repair and regeneration therapies. Broader application to the integration of protein therapeutics with biomaterials is also envisioned.

4.2 Introduction

Protein conjugation to the surface of biomaterials is a powerful approach to engineering therapeutically active materials that are more effective at integrating with the body and promoting healing. However, preserving protein bioactivity and controlling protein presentation are critical to efficacy and are not trivial challenges.[121] Recent advances have been made in protein engineering to create recombinant proteins that are tailored for conjugation,[127, 128, 185-187] but broadly useful strategies that can be applied to proteins in a "plug-and-play" fashion are currently lacking. Rather, to date the field has relied on chemical modification strategies targeting amines (*e.g.* on lysine residues) and thiols (*e.g.* on cysteines).[82, 133, 188-196] While promising results have been achieved with these methods, for example with thiolated transforming growth factor-β,[82, 192-195] the stochastic nature of these modification strategies is an important drawback that leads to heterogeneous mixtures of modified protein and random protein orientation after conjugation. Protein modification can also be detrimental to bioactivity. We have encountered this problem firsthand in efforts to modify bone morphogenetic protein-2 (BMP2) with a tetrazine succinimidyl ester (Tz-NHS), as we found that BMP2 bioactivity decreased as percent tetrazine functionalization increased (**Figure IV-1**).

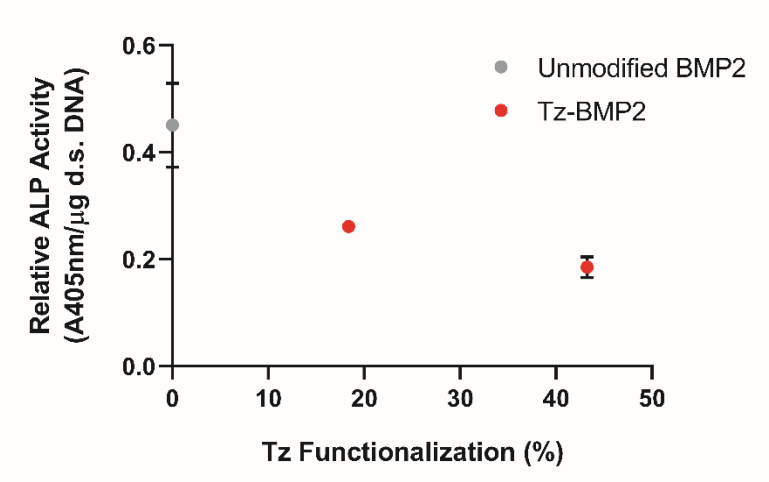

Figure IV-1. Loss of BMP2 bioactivity as a function of tetrazine-BMP2 functionalization. Comparison of BMP2 functionalization by western blot analysis and BMP2 bioactivity results by a W-20-17 reporter cell line show a significant decrease in BMP2 bioactivity with increased Tz-NHS functionalization.

Although they have not yet been used for protein conjugation to biomaterials, interest in PEGylation of protein therapeutics has led to the development of site-selective protein modification strategies that overcome the aforementioned drawbacks,[197] for example using reagents that target specific sites on the protein.[131, 198, 199] Sulfone reagents are particularly intriguing. Bis-sulfones were first reported to site-specifically modify proteins at disulfide bonds through a bis-alkylation reaction without altering protein structure.[130, 200] Subsequent work from Cong *et al.* and Peciak *et al.* reported the use of PEG-bis-sulfone for site-specific PEGylation of interferon α-2a (IFN) at contiguous poly-histidines (His-tags).[131, 132] Protein bioactivity was retained regardless of His-tag location, but favored modification sites such as the C- or N- termini, which are away from the active areas of the protein. This approach could be very promising for conjugating proteins to biomaterials, since many recombinant proteins have His-tags routinely added to the

terminal ends, without detriment to protein activity, as a means for post-translational affinity purification.

Here, we report the use of a 1,2,4,5-tetrazine-PEG-bis-sulfone (Tz-PEG-BS) reagent for site-selective modification of His-tag modified recombinant proteins and subsequent bio-orthogonal conjugation (**Figure IV-2 a**). Briefly, Tz-PEG-BS was converted to Tz-PEG-mono sulfone (Tz-PEG-MS) through the release of sulfonic acid under basic conditions. Tetrazine functionalization was then achieved by reacting Tz-PEG-MS with His-tag modified recombinant proteins through a bis-alkylation reaction. Tetrazine-modified protein was then conjugated to PEG hydrogel microparticles using bio-orthogonal tetrazine-norbornene click chemistry (**Figure IV-2 b**). Tetrazine ligation is a mild-natured click reaction that proceeds spontaneously in aqueous environments under physiologic conditions,[201] which we rationalized would ensure preservation of protein bioactivity. Finally, the protein-functionalized PEG hydrogel microparticles were subsequently linked together using a PEG-di-Tz crosslinker to form microporous annealed particle (MAP) hydrogels (**Figure IV-2 c**), which are currently of high interest as therapeutic biomaterials.[116, 117, 179, 202, 203] To date, MAP hydrogels have only been functionalized with synthetic peptides. Our new method for functionalization with recombinant proteins is expected to enable the development of next-generation MAP hydrogels that are encoded with potent bio-instructive cues.

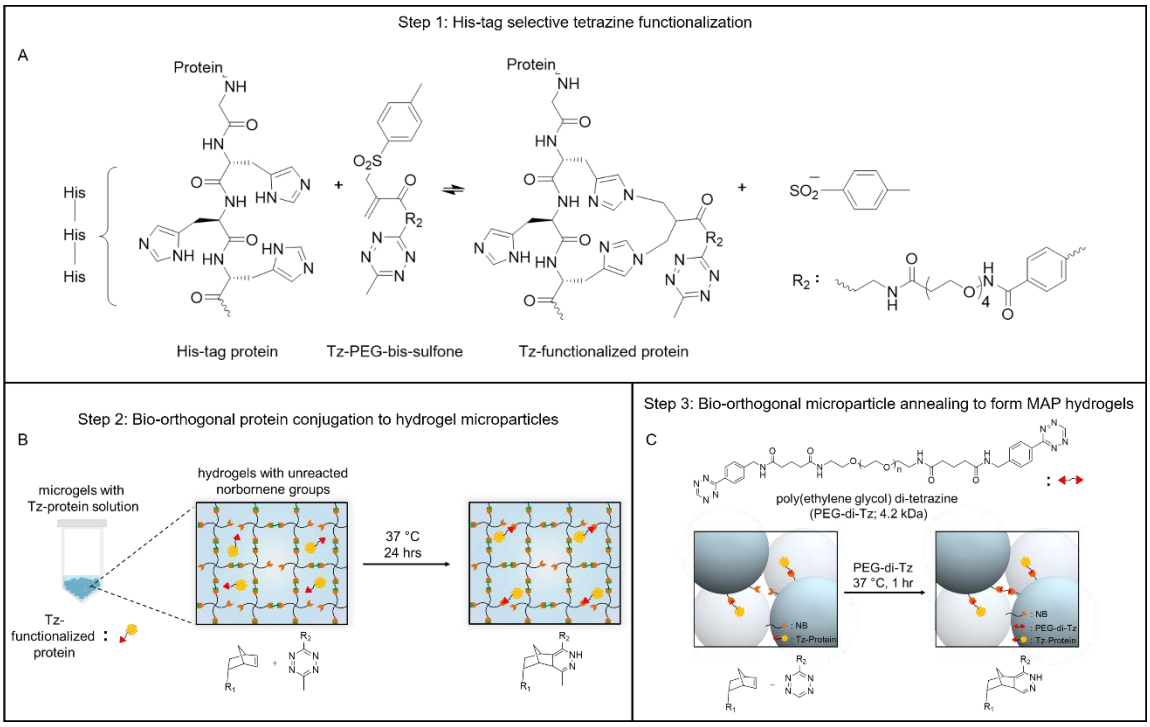

Figure IV-2. Site-selective modification strategy for protein conjugation to MAP hydrogels. A) Chemical scheme for His tag-selective, bis-alkylation reaction of recombinant protein with tetrazine-PEG-bis-sulfone (Tz-PEG-BS) to yield tetrazine-functionalized protein. B) Schematic showing the bio-orthogonal tetrazine click reaction for tetrazine-functionalized protein conjugation to norbornene-bearing microparticles. C) Assembly of microparticles into microporous annealed particle (MAP) hydrogels with PEG-di-tetrazine (PEG-di-Tz) crosslinker.

4.3 Materials and Methods

4.3.1 BMP2 Bioactivity with Respect to Tetrazine Functionalization

In order to first determine tetrazine functionalization, a western blot was performed. BMP2 (R&D Systems, 2 μg/mL) was reacted with various equivalents of tetrazine succinimidyl ester (Tz-NHS, 0 – 30 equiv.) for 1 hr at room temperature. Tz-functionalized BMP2 was further reacted with PEG-di-norbornene (6.5 kDa, 1:1 Tz:ene) for 1 hr at room temperature in order to increase the molecular weight separation between

non-functionalized and Tz-functionalized BMP2. Protein samples were loaded into 14% acrylamide gels and gel electrophoresis was performed (Bio-Rad PowerPac Electrophoresis System). Western blot was performed using mouse monoclonal, anti-human BMP2 (Abcam, 1 μg/mL) and secondary goat, anti-mouse polyclonal antibody with HRP (Abcam, 0.02 μg/mL) on a PDVF membrane. A peroxide solution with chemiluminescent enhancer was added to probe BMP2 protein bands and the membrane was imaged (Li-Cor Western Blot Reader). FIJI was used to measure pixel intensity of protein bands and Tz-functionalized bands were compared to the non-functionalized band to determine percentage of functionalized protein. Secondly, BMP2 bioactivity was confirmed by culturing W-20-17 cells, an alkaline phosphate producing cell line responsive to BMP2 in a dose-dependent manner, in 96-well plates with functionalized BMP2 solutions. Briefly, W-20-17 cells were cultured in low serum media (DMEM with 10% FBS) in a 96-well plate (5000 cells per well) until confluency (~4 days). At day 4, media was removed and replaced with 50% BMP2 sample (500 ng mL^{-1} BMP2 with 0, 10, or 30 equiv. of Tz-NHS) and 50% fresh media and allowed to culture for another 2 days. After 2 days, cells were washed twice with PBS (200 μL) and lysed by freeze/thaw (2 cycles: -80 °C for 45 min, 37 °C for 45 min). ALP activity was measured by incubating PBS supernatant (100 μL) with para-nitrophenyl phosphate solution (100 μL) and absorbance at 405 nm was monitored for 20 min. Additionally, double stranded DNA (d.s. DNA) content was measured using a Quant-iT Pico Green dsDNA assay. PBS supernatant (50 μL) was incubated with TE buffer (10 mM Tris-HCl, 1 mM EDTA, 50 μL), and Pico Green dye (100 μL) for 5 min and fluorescence was measured (Exc: 480nm, Emm: 520nm)

and compared to a d.s. DNA standard curve. ALP activity was normalized to d.s. DNA content to obtain relative ALP activity (A405 nm/ μg d.s. DNA).

4.3.2 Synthesis of Site-Selective, Tetrazine-Functionalized Protein MAP Hydrogels

4.3.2.1 General Approach

Histidine-tagged protein (His-protein) was conjugated with tetrazine-PEG-bis sulfone (Tz-PEG-BS) linker using a method adapted from Cong *et al.*[131] First, Tz-PEG-BS was dissolved in dimethyl sulfoxide at 1 mM concentration. Next, a working solution of Tz-PEG-BS (0.01 mM) was made in PBS, adjusted with triethanolamine (10 mM, pH 8), and allowed to incubate at 4 °C overnight to release sulfonic acid and produce tetrazine-PEG-mono sulfone (Tz-PEG-MS). Next, His-protein was incubated with either Tz-PEG-MS or DMSO (1.5 molar equiv.) overnight at 4 °C to yield tetrazine-functionalized protein (Tz-Protein) or non-functionalized protein (NF-protein), respectively. Thiol-ene microparticles (50 μL volume) were mixed with Tz-Protein (100 μL) for overnight at 37 °C to allow for protein conjugation to microparticles. Microparticles were thoroughly washed by centrifugation with PBS to remove unbound protein and annealed as described above with PEG-di-Tz (2 mM).

4.3.2.2 Green Fluorescent Protein

Recombinant aequorea victoria, his-tagged green fluorescent protein (Sino Biological, His-GFP) was used as a model protein to test Tz-PEG-BS conjugation. His-GFP in PBS (200 μg mL^{-1}) was mixed with Tz-PEG-MS (1.5 molar equiv.) as previously

described, to conjugate the tetrazine linker to GFP (Tz-GFP, 1.5 μg mL^{-1}). Non-functionalized GFP was made by replacing Tz-PEG-MS with DMSO (NF-GFP, 1.5 μg mL^{-1}). Microparticles (50 μL) were conjugated with Tz-GFP or NF-GFP (100 μL, 1.5 μg mL^{-1}) and assembled into MAP hydrogels with PEG-di-Tz crosslinker (2 mM, 12 μL), as described previously. To visualize GFP conjugation, MAP hydrogels were imaged via fluorescence microscopy (Zeiss SteREO and Zeiss Axio Vert A1).

4.3.2.3 Bone Morphogenetic Protein-2

Recombinant, C-terminal, his-tagged bone morphogenetic protein-2 (OriGene, His-BMP2) was used as a growth factor for inducing hMSC osteogenesis. His-BMP2 in PBS (10 μg mL^{-1}) was mixed with Tz-PEG-MS (1.5 molar equiv.) as described above, to conjugate the tetrazine linker to BMP2 (Tz-BMP2, 7.5 μg mL^{-1}). Non-functionalized BMP2 was made by replacing Tz-PEG-MS with DMSO (NF-BMP2, 7.5 μg mL^{-1}). Microparticles (50 μL) were conjugated with Tz-BMP2 or NF-GFP (100 μL, 7.5 μg mL^{-1}) and assembled into MAP hydrogels with PEG-di-Tz crosslinker (2 mM, 12 μL), as described previously.

4.3.3 BMP2 ELISA

A modified surface ELISA was performed on BMP2-functionalized MAP hydrogels to determine differences between Tz-BMP2 functionalized, NF-BMP2 functionalized and blank MAP hydrogels. Briefly, Tz-BMP2 MAP hydrogels, NF-BMP2 MAP hydrogels, and blank MAP hydrogels were placed in 96-well plates and blocked

with blocking buffer (1% BSA in PBS) for overnight at 4 °C. Mouse monoclonal, anti-human BMP2 antibody (Abcam, 100 μL, 0.1 μg mL-1) was incubated within each well for 3 hrs at room temperature. Wells were washed thoroughly with wash buffer (PBS, 0.1% BSA, 0.05% Tween-20). Goat, anti-mouse IgG H&L polyclonal antibody with HRP (Abcam, 100 μL, 0.1 μg mL^{-1}) was incubated within each well for 3 hrs at room temperature. Wells were washed thoroughly with wash buffer. TMB 1-Component liquid substrate (VWR, 100 μL) was added to each well for color development for 20 min. TMB stop solution (100 μL) was added to each well and absorbance was measured at 450 nm and color correction was measured at 620 nm. Color corrected absorbance (A450 nm – A620 nm) was determined and normalized to blank MAP hydrogel values.

4.3.4 BMP2 Induced Osteogenic Differentiation and Mineralization

Bone marrow-derived human mesenchymal stem cells (hMSCs) were acquired from the Institute of Regenerative Medicine at Texas A&M University. The hMSC identity was confirmed by immunophenotypic analysis on positive expression of CD29, CD44, CD146, CD166, HLA ABC, and negative expression of CD11b, CD79a. Osteogenic and adipogenic differentiation potential were also verified. hMSC were cultured in basal cell culture medium (CCM: α-Minimal essential medium (Gibco) supplemented with 20% v/v fetal bovine serum (FBS, Atlanta Biologicals), 2 mM GlutaMAX (Gibco), 50 U mL^{-1} penicillin (Gibco), and 50 μg mL^{-1} streptomycin (Gibco)) at 5% CO_2 and 37 °C in a humidified environment. Passage 3 cells, where 1 passage is equivalent to 8-9 population doublings, were used in this work. Human mesenchymal stem

cells (hMSCs, 2.5 x 10^5 cells per MAP hydrogel) were seeded on MMP-degradable MAP hydrogels during the PEG-di-Tz crosslinking step (50 μL volume of microparticles, 12 μL of crosslinker solution containing containing PEG-di-Tz and hMSCs). After crosslinking, MAP hydrogels were placed in a 24-well plate CCM for 2 days, before being moved to a new 24-well plate and cultured with osteo-base media (OBM: CCM, 50 μg mL^{-1} L-ascorbic acid, 5 mM β-glycerophosphate) or in the case of negative control CCM for the remainder of 21 days, with media replacement occurring every 2 days. At 21 days, MAP hydrogels were rinsed with PBS and fixed in 4% formaldehyde for 15 min. After washing in PBS, MAP hydrogels were dried overnight at 37 °C. Dried MAP hydrogels were incubated with acid solution (0.5M HCl, 100 μL) overnight at 4 °C to solubilize free calcium. Samples were neutralized with base solution (0.5M NaOH, 41 μL), centrifuged (15,000 g, 10 min), and supernatant was removed. MAP hydrogels were placed in *o*-cresolphthalein working detector reagent (Cayman Chemical, 50:50 Calcium Detector R1:R2, 200 μL) for 5 min at room temperature to react with MAP hydrogel-bound calcium. Supernatant (150 uL) was added to a 96-well plate and absorbance was measured at 576 nm to compare mineralization among MAP hydrogels. Six MAP hydrogel groups were compared: MAP hydrogels conjugated with Tz-PEG-BS (1.5 equiv.) modified His-BMP2 (Tz BMP2), non-functionalized His-BMP2 (NF BMP2), Tz-NHS (10 equiv.) modified His-BMP2 (NHS BMP2), exogenously added His-BMP2 solubilized in OBM at day 2 (Sol BMP2), and MAP hydrogels without His-BMP2 cultured in either media (OBM or CCM).

4.3.5 Statistical Analysis

Statistical analysis of data was performed in GraphPad Prism 8. For the BMP2 ELISA studies, a non-parametric t-test was performed ($p < 0.05$). For BMP2 induced mineralization studies (n = 6 for each BMP2-containing experimental group, n = 3 for CCM and OBM controls), a one-way ANOVA with post-hoc comparisons (Tukey's method) was performed ($p < 0.05$).

4.4 Results and Discussion

4.4.1 Site-selective, Bio-orthogonal Protein Conjugation of His-tag Modified Protein to MAP Hydrogels

To demonstrate efficacy of our site-selective bio-orthogonal conjugation strategy, we first explored conjugation of green fluorescent protein (GFP). Importantly, GFP was chosen as a model protein since its fluorescence depends on preservation of the 3D structure of the protein.[204] Tetrazine-functionalized, His-tag GFP was tethered to microparticles and the particles were subsequently annealed into MAP hydrogels. Analysis of fluorescent MAP hydrogel images showed substantially enhanced green fluorescence of Tz-GFP functionalized MAP hydrogels (**Figure IV-3 a, b**), especially evident in higher magnification epifluorescence images, indicating that the protein was successfully tethered and its structure was retained. In contrast, MAP hydrogels formed form microparticles incubated with non-functionalized GFP lacking tetrazine groups (NF-GFP) were less fluorescent macroscopically and exhibited negligible fluorescence at higher magnification (**Figure IV-3 c, d**).

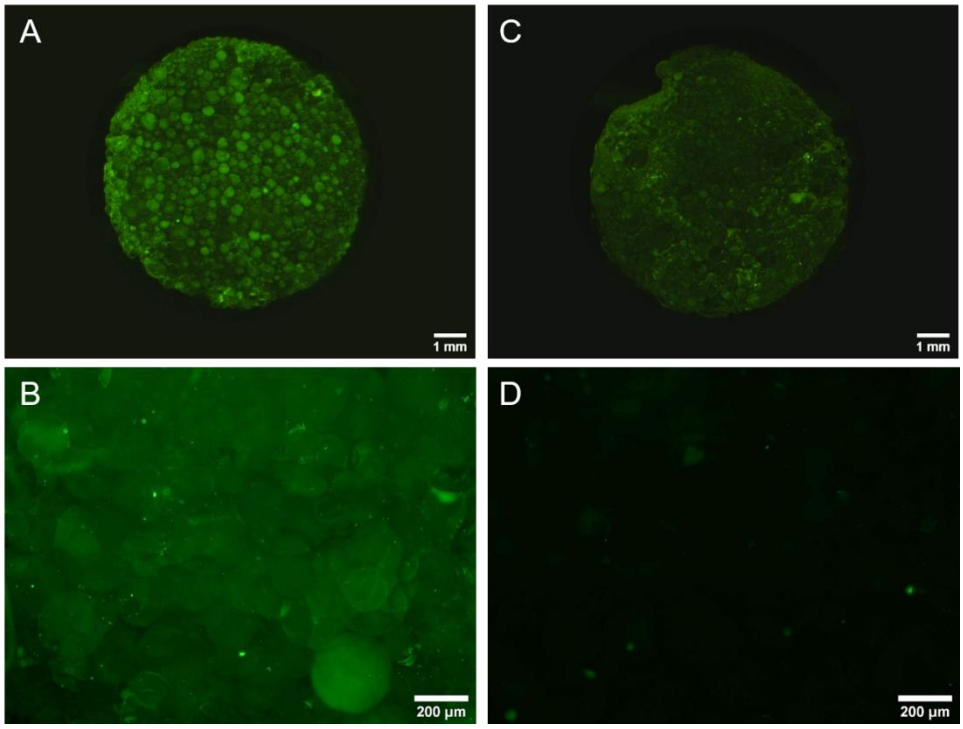

Figure IV-3. Site-selective GFP-functionalized MAP hydrogels. A-B) Fluorescent images of Tz-GFP functionalized MAP hydrogels and C-D) NF-GFP functionalized MAP hydrogels. Tz-GFP functionalized MAP hydrogels show greater protein conjugation and more bioactive fluorescence than NF-GFP functionalized MAP hydrogels. Scale bar = 1 mm for macroscopic fluoresence images and 200 µm for higher magnification images.

4.4.2 BMP2-functionalized MAP Hydrogels for hMSC Osteogenic Differentiation

Based on our promising results with GFP, we hypothesized that our strategy could be leveraged to functionalize MAP hydrogels with BMP2 and enhance human mesenchymal stem cell (hMSC) osteogenic differentiation (**Figure IV-4 a**). Conjugating BMP2 to a biomaterial is expected to be therapeutically advantageous for reducing the off-target effects and complications that have plagued its clinical use. Moreover, compared to our prior work on photocrosslinked MAP hydrogels for hMSC delivery,[118]

using bio-orthogonal tetrazine ligation allows for cell and bioactive therapeutic delivery in a straightforward "mix-and-use" approach to help facilitate clinical translation.

Lastly, recombinant, His-tag, BMP2 (His-BMP2) was conjugated to MAP hydrogels, similar to what was done for GFP. A modified BMP2 ELISA was used to compare relative protein concentration between Tz-BMP2-functionalized MAP hydrogels and control MAP hydrogels that were treated with non-functionalized BMP2 (NF-BMP2). Although some signal was detected when NF-BMP2 was used, the differences in absorbance values between Tz- and NF-BMP2 were statistically significant, indicating Tz-BMP2 functionalized MAP hydrogels had higher protein loading (**Figure IV-4 b**).

Finally, and most importantly, bioactivity of BMP2 functionalized MAP hydrogels was compared *via* biomineralization by hMSCs. Deposition of calcium phosphate minerals is a common late-stage marker of hMSC osteogenesis and thus, served as an indication of retained, long-term BMP2 bioactivity. Importantly, quantitative analysis of calcium content with *o*-cresolphthalein complexone showed that Tz-BMP2 functionalized MAP hydrogels showed enhanced calcium mineralization after 21 days when compared to NF-BMP2 functionalized MAP hydrogels, Tz-NHS BMP2 functionalized MAP hydrogels, as well as negative controls cultured in BMP2-supplemented media, osteo-base media, and basal cell culture media (**Figure IV-4 c**). Moreover, despite the previous results from the modified ELISA showing some retention of unbound protein, NF-BMP2 functionalized MAP hydrogels were ineffective for mineralization and were not significantly different from the controls. This result can be partly attributed to the higher protein loading achieved with Tz-BMP2 functionalized MAP hydrogels, but the sustained

presentation of BMP2 from the materials is also important. Additionally, although there may have been differences in the amount of protein conjugated, the direct comparison between Tz-PEG-BS and Tz-NHS BMP2 modification strategies supports the superiority of the site-selective modification strategy towards maintaining protein bioactivity.

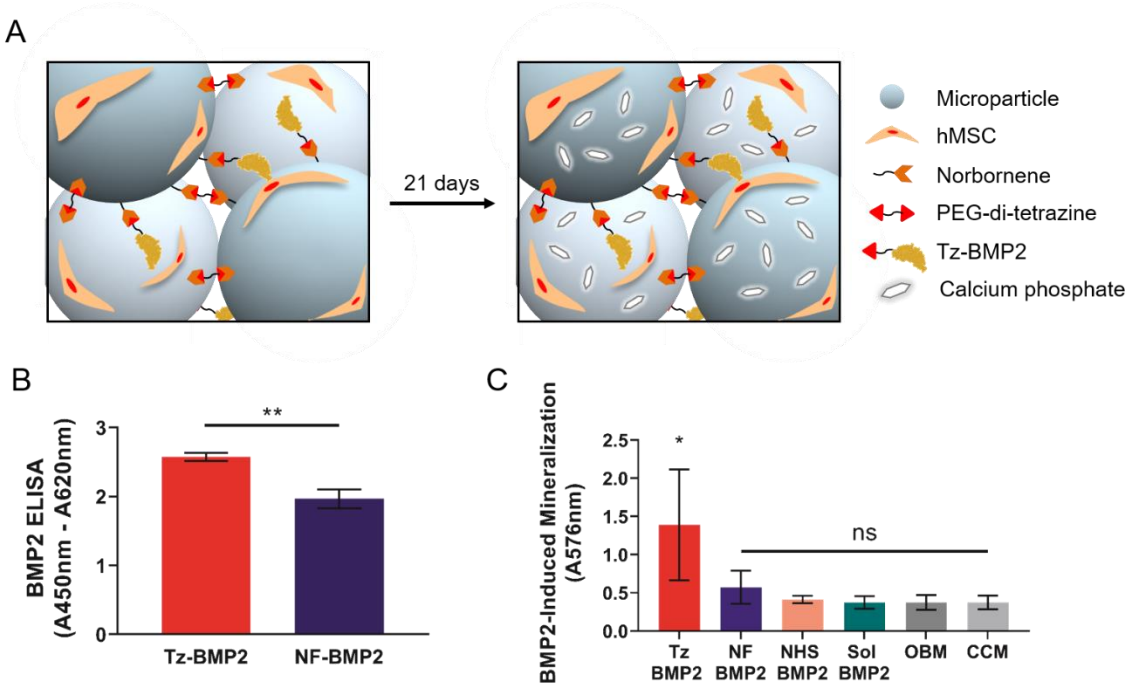

Figure IV-4. Site-selective BMP2-functionalized MAP hydrogels for hMSC osteogenesis. A) Schematic showing Tz-BMP2 functionalized MAP hydrogels with encapsulated hMSCs for a mineralization study. B) Tz-BMP2 and NF-BMP2 (5 μg/mL) functionalized MAP hydrogels compared using a modified surface ELISA (n = 3). Absorbance values demonstrate differences in ELISA development between NF- and Tz-BMP2 MAP hydrogels indicating differences in BMP2 conjugation. The symbol ** indicates statistical significance between groups ($p < 0.01$). C) Comparison of MAP hydrogel-bound calcium mineralization after 21 days (n = 6 for BMP2 samples, n = 3 for media controls). Absorbance values show that only Tz-BMP2 functionalized MAP hydrogels induce hMSC osteogenic mineralization. The symbol * indicates statistical significance between all other experimental groups ($p < 0.05$).

Our success conjugating BMP2 is a significant step toward the development of therapeutic biomaterials. Tethering of fragile signaling proteins has been thought to

improve long-term therapeutic delivery, since naked proteins are sensitive to environmental conditions (*e.g.* pH and temperature) and are susceptible to rapid degradation and clearance *in vivo*. Sustained protein presentation can also help reduce therapeutically delivered doses, since proteins are typically given at high concentrations to account for rapid loss. This could be particularly advantageous for BMPs given the serious negative side effects that can arise from supraphysiological doses.[205-207] Additionally, the His tag-selective nature of our conjugation strategy guarantees that the protein is always presented in the same orientation to bind with cell receptors, which is a significant advantage for ensuring reproducibility and efficacy.

4.5 Conclusions

In summary, we demonstrate here a novel method for bio-orthogonal, site-selective protein conjugation to biomaterials for tissue engineering applications using Tz-PEG-BS, a His tag modifying bis-alkylation reagent. We demonstrated efficacy by conjugating recombinant proteins to Tz-crosslinked MAP hydrogels. Further, MAP hydrogels permitted mesenchymal stem cell growth within the 3D microporous environment and were rendered osteoinductive by BMP2 conjugation. Importantly, this approach circumvents the limitations of traditional amine or thiol-reactive chemistries, which bind non-specifically to potential active sites on the protein, and can result in loss of bioactivity. The BMP2-functionalized MAP hydrogels developed here are expected to be useful as therapeutic materials for bone repair and regeneration. However, the combination of site-selective and bio-orthogonal chemistries introduced here can be applied broadly to

conjugate virtually any recombinant protein-of-interest to any biomaterial that presents norbornene groups. Our method could also be extended to other complimentary pairs within the click chemistry toolkit of reactions simply by substituting the tetrazine and norbornene clickable moieties. Thus, it is a powerful and enabling tool for the development of innovative bio-instructive materials that could be useful for myriad medical applications.

CHAPTER V

SEQUENTIAL CLICK REACTIONS FOR STEP-GROWTH HYDROGEL SYNTHESIS WITHOUT MULTI-ARM PRECURORS[*]

5.1 Overview

Click chemistry reactions have become an important tool for synthesizing user-defined hydrogels consisting of poly(ethylene glycol) (PEG) and bioactive peptides for tissue engineering. However, because click crosslinking proceeds via a step-growth mechanism, multi-arm telechelic precursors are required, which has some disadvantages. Here, we report for the first time that this requirement can be circumvented to create PEG-peptide hydrogels solely from linear precursors through the use of two orthogonal click reactions, the thiol-maleimide Michael addition and thiol-norbornene click reaction. The rapid kinetics of both click reactions allowed for quick formation of norbornene-functionalized PEG-peptide block copolymers *via* Michael addition, which were subsequently photocrosslinked into hydrogels with a dithiol linker. Characterization and in vitro testing demonstrated that the hydrogels have highly tunable physicochemical properties and excellent cytocompatibility. In addition, stoichiometric control over the crosslinking reaction can be leveraged to leave unreacted norbornene groups in the hydrogel for subsequent hydrogel functionalization via bioorthogonal inverse-electron demand Diels-Alder click reactions with *s*-tetrazines. After selectively capping

[*] Reprinted from "Orthogonal click reactions enable the synthesis of ECM-mimetic PEG hydrogels without multi-arm precursors" by F. Jivan, N. Fabela, Z. Davis, and D. L. Alge. *Journal of Materials Chemistry B*, 2018, 6, 4929-36. with permission from The Royal Society of Chemistry.[208]

norbornene groups in a user-defined region with cysteine, this feature was leveraged for protein patterning. Collectively, these results demonstrate that our novel chemical strategy is a simple and versatile approach to the development of hydrogels for tissue engineering that could be useful for a variety of applications.

5.2 Introduction

Hydrogels are crosslinked hydrophilic polymer networks that are considered to be the most tissue-like class of biomaterials, which has led to high interest in their use for tissue engineering.[1, 3, 4] Common crosslinking strategies to fabricate hydrogels include physical crosslinking through polymer chain entanglements or electrostatic interactions, and chemical crosslinking between functional groups. Within chemical crosslinking, chain growth polymerization through rapid propagation of a radical center is widely used with acrylate-containing polymers. However, this approach lacks control and reaction specificity due to the potential for chain transfer events, which can damage proteins and cells.[78, 94, 209] Alternatively, step growth polymerization between two distinct complementary chemical groups allows for more predictable crosslinking and is amenable to a wide range of chemical handles.[210, 211] Click chemistry is widely appreciated as a tool for controlling the step-growth crosslinking of hydrogels. The efficiency, functional group selectivity, and mild nature of click-type reactions makes them particularly well suited for hydrogels being synthesized in the presence of fragile cells or biologics.[97, 98, 212, 213]

There has been considerable innovation in the synthesis of extracellular matrix (ECM)-mimetic hydrogels by click chemistry from both naturally-occurring and synthetic

polymers. Hyaluronic acid and gelatin, both natural polymers which already contain cellular binding domains, have been chemically modified along their respective polymer backbones to incorporate click functional groups for pendant peptide or ECM protein functionalization and to provide numerous crosslinking sites that can be used to independently tune hydrogel mechanical properties.[9, 27, 28, 214-216] Synthetic hydrogels based on poly(ethylene glycol) (PEG) have widely been used in tissue engineering because of their hydrophilicity, tunable tissue-like elasticity, and bio-inertness. PEG hydrogels are also considered to be a "blank slate" platform that can be easily modified with peptides and proteins for drug delivery and cell encapsulation.[217] Notably, the use of photo-initiated thiol-ene click reactions,[63, 78, 81] and Michael addition reactions such as the thiol-vinyl sulfone[100, 102] and thiol-maleimide reactions,[77, 218-220] have become increasingly important in the synthesis of complex, user-controlled hydrogel matrices. Additionally, advances have been made in using biorthogonal, initiator-free click reactions such as oxime ligation,[221, 222] strain promoted azide-alkyne click,[109, 223] and tetrazine-norbornene click reactions[106, 224] for facile incorporation of bioactive ECM-mimetic peptides for cell attachment, cellular degradation or directed differentiation.

Due to the step-growth nature of click cross-linking reactions, the synthesis of ECM mimetic PEG-peptide hydrogels with these chemical strategies requires the use of multi-arm, telechelic PEG precursors. These macromers are synthesized by living ring-opening polymerization of ethylene oxide using multi-functional alcohol cores like pentaerythritol.[225] While they are widely used in hydrogel fabrication, there are important drawbacks. For example, steric hindrance of the growing polymer chain and impurities

such as water can lead to lower extents of polymerization, unpredictable molecular weights and fewer arms than desired. Achieving quantitative functionalization of the end groups with clickable functional handles is also challenging compared to linear PEG precursors and often requires a large excess of functional reagent, which can be costly. Even post-synthesis, the analytical method for determining functionalization, nuclear magnetic resonance spectroscopy (NMR), can provide an incomplete picture of the chemical structure, because of the large discrepancy between the ratio of end group hydrogens compared to hydrogens in the polymer backbone.[226] These drawbacks are important because they can adversely affect hydrogel properties. Reaction stoichiometry is critical in step-growth reactions and click crosslinking, and variability in the functionality of precursors can reduce the number of sites for conjugation, alter crosslinking density, and result in heterogeneous networks or non-idealities within the polymer structure.[160, 164] Additionally, the fact that PEG can only be functionalized on the chain ends means that conjugation of bioactive molecules takes away potential crosslinking sites, thereby limiting the amount that can be added.

To circumvent these challenges, the objective of this work was to develop an alternative strategy for synthesizing ECM-mimetic hydrogels that utilizes only linear precursors. Specifically, we sought to synthesize PEG-peptide block co-polymers (BCPs) via step-growth polymerization of PEG-di-maleimide with di-cysteine peptides. To render these BCPs crosslinkable, we installed norbornene groups on one of the peptides. Since norbornene is an electron-rich alkene, it will not participate in Michael addition reactions but can readily participate in radical initiated thiol-ene reactions as well as inverse electron

demand Diels-Alder reactions with *s*-tetrazines. Here, we demonstrate the ability to tune BCP hydrogel mechanical properties and utilize this versatile platform for cell encapsulation and bioactive protein patterning.

5.3 Materials and Methods

5.3.1 Materials

PEG di-maleimide (5,000 g/mol) and PEG di-thiol (3,400 g/mol) were purchased from Laysan Bio Inc. Rink amide MBHA resin (100-200 mesh) was purchased from Novabiochem. Fmoc protected amino acids, 2-(1H-benzotriazol-1-yl)-1,1,3,3-tetramethyluronium hexauorophosphate (HBTU), and N-methyl-pyroliddinone (NMP) were purchased from Chem-Impex International Inc. Triethanolamine (TEOA), diisopropyl ethylamine (DIEA), deuterium oxide (D2O), 5,5'-dithio-bis-(2-nitrobenzoic acid) (DTNB or Ellman's reagent), phenol, piperidine, triisopropylsilane (TIS), trifluoroacetic acid (TFA) reagent grade and HPLC grade were purchased from Sigma Aldrich. L-cysteine, 5-norbornene 2-carboxcylic acid was purchased from Alfa Aesar. Dichloromethane (DCM), HPLC grade water and acetonitrile (ACN) were purchased from Thermo Fisher Scientific. Dulbecco's Modified Eagle Medium (DMEM) was purchased from Corning. Fetal bovine serum (FBS) was purchased from Atlanta Biologicals. Penicillin streptomyosin (Pen Strep) was purchased from Lonza. Calcein-AM and ethidium homodimer-1 were purchased from Life Technologies.

5.3.2 Synthesis of Peptide Sequences

5.3.2.1 General

Peptide synthesis was performed on Rink amide resin with a microwave assisted peptide synthesizer (CEM DiscoverBio) using standard Fmoc solid phase peptide synthesis and HBTU activation with DIEA (0.5 M) in NMP.[227] Coupling reactions were generally performed for 6 min at 75 °C, except for cysteine (C) and arginine (R) which were coupled for 6 min at 50 °C, and 25 min at room temperature then 5 min at 75 °C, respectively. Fmoc protecting groups were deprotected with piperidine (20%) in NMP for 5 min at 75 °C. The peptide was cleaved by treatment with 90:5:2.5:2.5 (TFA:phenol:TIS:water) for 2 hrs at room temperature followed by precipitation in cold diethyl ether. Crude peptide was purified by reverse-phase high performance liquid chromatography (HPLC, Thermo Scientific UltiMate 3000 with Agilent Technologies C18 column, ACN in water with 0.01% TFA) and lyophilized (**Appendix, Figure VI-11**). Purified product was analyzed via matrix assisted laser desorption ionization time-of-flight mass spectrometry (MALDI-TOF MS) to verify peptide composition (**Appendix, Figure VI-12**). Peptides were dissolved in PBS and absorbance measurements at 205 nm and 280 nm (Thermo Scientific Nanodrop One) were taken to calculate the stock concentrations.[228] MALDI-TOF MS: KCGPQGIAGQCK [M+H] = 1188.513 (expected), 1189 (found); CGRGDSGC [M+H] = 753.242 (expected), 752.9 (found).

5.3.2.2 CGK(NB)GC

Norbornene-containing peptide was synthesized as described above, but with slight variation. A lysine residue with a 4-methyltrityl (Mtt) side protecting group (Fmoc-L-lysine(Mtt)-OH) was used during synthesis instead of the traditional lysine residue (Fmoc-L-lysine). After coupling the K(Mtt) residue, the Mtt protecting group was removed by addition of 1.8% TFA in DCM (9 washes, 3 min each at room temperature). The resin was then washed with DCM followed by NMP. Subsequently, 5-norbornene 2-carboxcylic acid was coupled to the free amine group by HBTU coupling (4:4:1 norbornene acid:HBTU:resin) and DIEA (0.5 M) in NMP. The Fmoc protecting group on the lysine residue was then removed using standard deprotection, and peptide synthesis was completed normally, as described above. MALDI-TOF MS: [M+H] = 586 (expected), 586.396 (found).

5.3.3 Synthesis of PEG-Peptide Block Co-Polymer (BCP) Chains

To prepare the PEG-peptide BCP precursor solution, PEG-di-maleimide was polymerized with di-thiol containing peptide sequences of interest *via* a Michael addition reaction (**Table V.1**).

Table V.1. Concentrations of components for BCP chain formation. Reprinted from "Orthogonal click reactions enable the synthesis of ECM-mimetic PEG hydrogels without multi-arm precursors" by F. Jivan, N. Fabela, Z. Davis, and D. L. Alge. *Journal of Materials Chemistry B*, 2018, 6, 4929-36. with permission from The Royal Society of Chemistry.[208]

Components	Working Concentration of Components	Working Concentration of Click Groups
PEG-Mal	21 mM	42 mM MAL
KCGPQGIAGQCK	5 mM	10 mM SH
CGRGDSGC	1 mM	2 mM SH
CGK(NB)GC	15 mM	30 mM SH and 15 mM NB

A large batch (5 mL) of BCP precursor was prepared from lyophilized PEG and peptides. Briefly, linear bifunctional PEG-maleimide (PEG-Mal, 10.5 wt. %), MMP-degradable di-thiol containing peptide KCGPQGIAGQCK (5 mM), cell-adhesive peptide CGRGDSGC (1 mM), and short peptide with a pendant norbornene group CGK(NB)GC (15 mM), were mixed with TEOA in PBS (1 mM, pH 7-9). The polymer mixture was allowed to polymerize for 30 minutes at room temperature to form PEG-peptide BCP (**Figure V-1**).

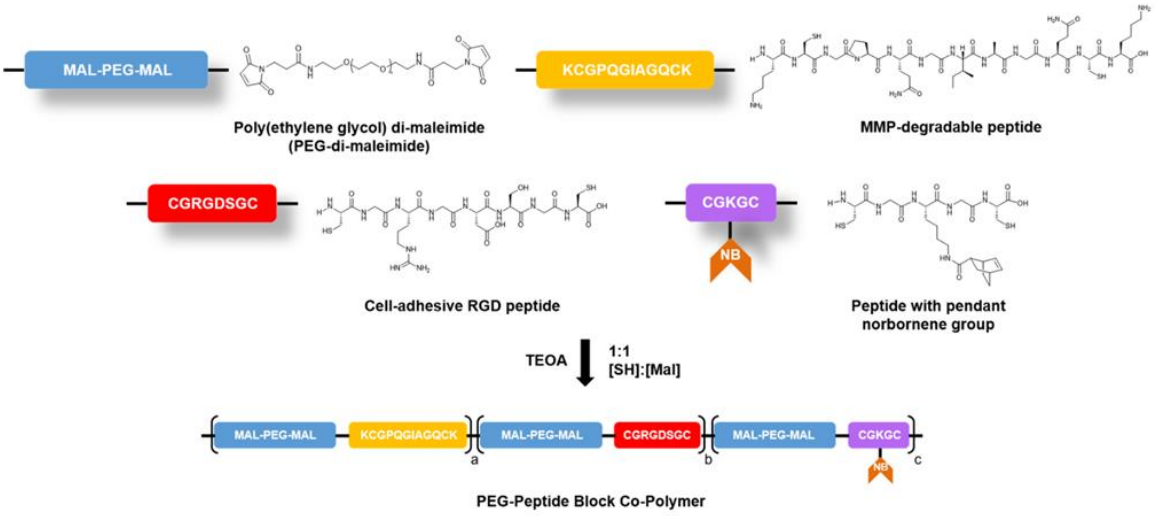

Figure V-1. PEG-peptide block co-polymer assembly via Michael addition. Cartoon representation depicting the assembly process of PEG and peptide subunits into random block-co polymer chains via thiol-maleimide Michael addition of PEG-di-maleimide and di-cysteine containing peptides initiated by triethanolamine. The concentration of each component used to synthesize the block co-polymer chains is shown in Table 1. The subscripts "a – c" correspond to the number of repeat units within the block copolymer (c = 15b = 3a). Reprinted from "Orthogonal click reactions enable the synthesis of ECM-mimetic PEG hydrogels without multi-arm precursors" by F. Jivan, N. Fabela, Z. Davis, and D. L. Alge. *Journal of Materials Chemistry B*, 2018, 6, 4929-36. with permission from The Royal Society of Chemistry.[208]

5.3.4 Synthesis of BCP Hydrogels

PEG-peptide BCP precursor solutions were subsequently crosslinked via thiol-ene click chemistry. Briefly, block co-polymers were combined with a PEG-di-thiol crosslinker ([thiol]:[norbornene] ratio of 1:1) and lithium acylphosphinate photoinitiator (LAP, 2 mM), synthesized as previously described.[162] Varying dilutions of this BCP pre-polymer solution were prepared in PBS to result in different crosslinking (XL) densities (1:1 = high XL, 1:2 = medium XL, and 1:3 = low XL) (**Table V.2**). Pre-polymer solutions (50 μL) were added to 6 mm syringe-tip molds and photopolymerization was achieved using UV light (Omnicure S2000 with a 365 nm filter) at 10 mW/cm^2 for 5 minutes.

Table V.2. Concentration of components for BCP gels. Reprinted from "Orthogonal click reactions enable the synthesis of ECM-mimetic PEG hydrogels without multi-arm precursors" by F. Jivan, N. Fabela, Z. Davis, and D. L. Alge. *Journal of Materials Chemistry B,* 2018, 6, 4929-36. with permission from The Royal Society of Chemistry.[208]

Components	Working Concentration of Click Groups		
	High XL	*Med XL*	*Low XL*
BCP	12 mM NB	6 mM NB	4 mM NB
PEG-di-thiol	12 mM SH	6 mM SH	4 mM SH

5.3.5 Chemical analysis of PEG-Peptide BCP

Thiol conversion during BCP polymerization was monitored *via* Ellman's Assay to determine the extent of the Michael addition polymerization. BCP samples and negative control samples containing PEG-NB instead of PEG-Mal were prepared (n = 3). Samples (10 μL) were taken at various time points (15, 30, 45, and 60 min) and incubated with Ellman's reagent (0.125 mg/mL in PBS, 100 μL). Absorbance measurements at 405 nm were taken, compared to a standard curve of L-cysteine (0 - 2 mM), and thiol concentrations were normalized to negative control sample at 0 minutes. Various sample dilutions were tested to ensure that all measurements taken were within the assay range.

5.3.6 ^{1}H NMR Characterization

^{1}H NMR characterization of the BCP precursor and gels was performed to compare spectra after Michael addition and thiol-ene photopolymerization, respectively. Briefly, BCP Michael addition was performed as previously described and separately a non-gelling photopolymerization BCP reaction with LAP (2 mM) and L-cysteine (15 mM) was

performed to consume norbornenes. Samples were frozen at -80 °C and lyophilized for 2 days. Lyophilized products (10 mg) were dissolved in D_2O, tested using an Inova NMR Spectrometer (500 MHz, 64 scans) and analysed via MestReNova NMR software (Mestralab Research S.L.).

5.3.7 Swelling Ratios of BCP Gels

Hydrogel samples were immersed in 2 mL of PBS for 48 hours to reach equilibrium. Swelling ratios of BCP gels were obtained by measuring the mass of dehydrated gels (W_d) and gels swollen in PBS for 2 days (W_s). The formula for calculating swelling ratio is shown below:

$$Swelling\ Ratio = (W_s - W_d)/W_d \qquad \textbf{(Equation 5.1)}$$

5.3.8 Rheology of BCP Gels

To characterize mechanical properties of BCP gels, amplitude time sweep rheology was performed to measure gelation point and storage modulus. To monitor hydrogel gelation, hydrogels were monitored during crosslinking via in situ photopolymerization rheology. Briefly, pre-polymer solution (50 μL) was added on a peltier rheometer plate (Anton Paar Physica MCR 301) and the 7-mm parallel plate tool was lowered to the measuring position (0.5 mm). A time sweep was performed within the linear viscoelastic regime (1% strain, 1 rad/sec) for 6 minutes with the Omnicure UV-365 nm light source turned on at 30 seconds and photopolymerization occurring for 5 minutes.

Storage (G') and loss moduli (G") were monitored during the time sweep and the gelation point was determined at the time of crossover between the storage and loss moduli (n = 3).

To measure the mechanical properties at equilibrium swelling, BCP gels made in 6 mm syringe-tip molds were swelled in PBS (2 mL) for 2 days before performing amplitude time sweep rheology (1% strain, 1 rad/sec). Amplitude sweeps were performed for 5 minutes and storage moduli were averaged to determine the average storage modulus (n = 3).

5.3.9 Enzymatic Degradation of BCP Gels

To study enzymatic degradation of hydrogels, mass loss of hydrogels incubated in collagenase solution was measured over time. Briefly, pre-swollen hydrogels were first weighed before being placed in 1.5 mL microtubes with collagenase-B solution (1 mg/mL, 1 mL). Microtubes were incubated in a 37 °C water bath to activate enzyme. Gels were removed, dried, and weighed at various time points until complete degradation was observed. Percent remaining mass was calculated at the various time points by normalizing the measured weight to the initial starting gel weight (n =3).

5.3.10 Cell Viability within BCP Matrices

To evaluate cytocompatability of the block co-polymer matrices, NIH 3T3 cells were encapsulated and their viability was assessed after 1 and 5 days of culture. Briefly, 3T3 cells (4.0×10^4 cells/gel) were added to the high XL, BCP solution during

photopolymerization (10 mW/cm^2, 3 min). Gels were cultured in standard DMEM media (DMEM, low glucose, 10% FBS, 1% Pen Strep) for the assigned time at 37 °C, 5% CO_2. Gels were washed with PBS and incubated for 30 min at room temperature with Live/Dead staining solution (2 μM Calcein AM and 4 μM Ethidium homodimer-1 in PBS). Gels were imaged using confocal fluorescent microscopy (Olympus FV1000) and cell viability as well as cell area were quantified using FIJI software (NIH). Fluorescent z-projections are shown for 50 slices (500 μm). For cell area, z-stack projections were manually thresholded to highlight cells and cell size was quantified using FIJI's "Analyze Particles" plugin (50 – 1000 μm^2 pixel size, 0 – 1 circularity). A lower limit of 50 μm^2 (average fibroblast cell area) was set to ensure that measurements were representative of cells fully captured within the z-stack, and an upper limit of 1000 μm^2 was set to exclude cell aggregates.

5.3.11 Protein Patterning on BCP Gels

BCP precursor solution was crosslinked as previously described, but off-stoichiometry ([thiol]:[norbornene] ratio of 0.5:1) to leave residual norbornene groups for protein patterning. Subsequently, the BCP gel was immersed in a solution of L-cysteine (20 mM) and LAP (2 mM) and irradiated with UV light (10 mW/cm^2, 5 min) through a photomask in order to consume norbornene groups on one half of the gel and then rinsed in PBS. Protein conjugation to the remaining norbornene groups was then achieved using bio-orthogonal tetrazine-norbornene click chemistry. First, Texas Red ovalbumin in PBS (1.5 mg/mL) was incubated with tetrazine-N-hydroxy-succinimydl ester (Tz NHS ester, 10 equiv., synthesized as previously described[104, 146]) for 1 hr at room temperature to yield

tetrazine-functionalized Texas Red ovalbumin (Tz-Tx Red Ovalbumin). Tz-Tx Red Ovalbumin (1 mg/mL) was then pipetted on top of the photopatterned BCP gel and allowed to incubate for 1 hr at room temperature to react with free norbornene groups in the unexposed (previously shielded) side of the gel. The BCP gel was then washed in PBS to remove unconjugated protein and imaged via fluorescence microscopy (Zeiss Axio Vert.A1).

5.3.12 Statistical Analysis

For statistical analysis, a standard, unpaired t-test was performed for the Ellman's assay and cell studies ($p < 0.05$). A one-way ANOVA with multiple comparison using Tukey's method was performed for mechanical characterization ($p < 0.05$).

5.4 Results and Discussion

5.4.1 Chemical Characterization of PEG-Peptide Block Co-Polymer (BCP) Precursor and BCP Gel

BCP precursor solution was first formed by thiol-maleimide Michael addition of PEG-di-maleimide and di-thiol peptides. Ellman's assay was used to monitor thiol conversion during Michael addition assembly of BCP chains. Absorbance results for the BCP precursor solution demonstrated complete thiol conversion after 15 minutes of reaction time. Although we did not characterize molecular weight, assuming greater than 99% conversion, we expect a degree of polymerization of 100 based on Carothers' equation for a stoichiometrically balanced step-growth polymerization.[229] Based on the

relative ratios of components within the block co-polymer outlined in Table 1, the number average molecular weight would be approximately 287 kDa. These estimates agree with the results of Miller *et. al.* who demonstrated high conversion of their PEG-peptide polymers *via* thiol-acrylate Michael addition with high molecular weight products (majority of species greater than 500 kDa).[62] Importantly, minimal thiol conversion was observed even after 60 minutes when PEG-NB was substituted for PEG-MAL (**Figure V-2**). This result was expected since norbornene is an electron-rich alkene and should not participate in the Michael addition reaction. The partial thiol conversion in the PEG-NB solution can be attributed to di-sulfide formation of the cysteine-containing peptides.

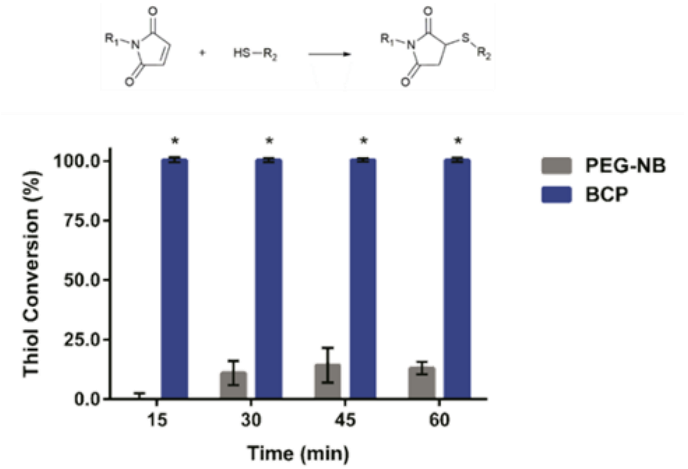

Figure V-2. Characterization of Michael addition versus thiol-ene reaction. Ellman's assay shows rapid thiol conversion for the thiol-maleimide reaction (reaction seen above) and minimal conversion for thiol-ene reaction. BCP percent thiol conversion was statistically significant compared to PEG-NB thiol conversion for all time points ($p < 0.05$, n = 3). Reprinted from "Orthogonal click reactions enable the synthesis of ECM-mimetic PEG hydrogels without multi-arm precursors" by F. Jivan, N. Fabela, Z. Davis, and D. L. Alge. *Journal of Materials Chemistry B*, 2018, 6, 4929-36. with permission from The Royal Society of Chemistry.[208]

Next, because we aimed to leverage pendant norbornenes for hydrogel crosslinking (**Figure V-3 a**), we characterized the BCP assembly by ^{1}H NMR to verify the presence of alkene related hydrogens from the norbornene groups. The results showed the characteristic norbornene peaks (5.9 – 6.3 ppm) were still present after the thiol-maleimide Michael addition but disappeared after adding a thiol source (L-cysteine) and performing thiol-ene photopolymerization (**Figure V-3 b**). Finally, we performed thiol-ene photopolymerization with a PEG-di-thiol crosslinker and used the vial tilt method to confirm that the BCP was capable of hydrogel formation (**Figure V-3 b**).

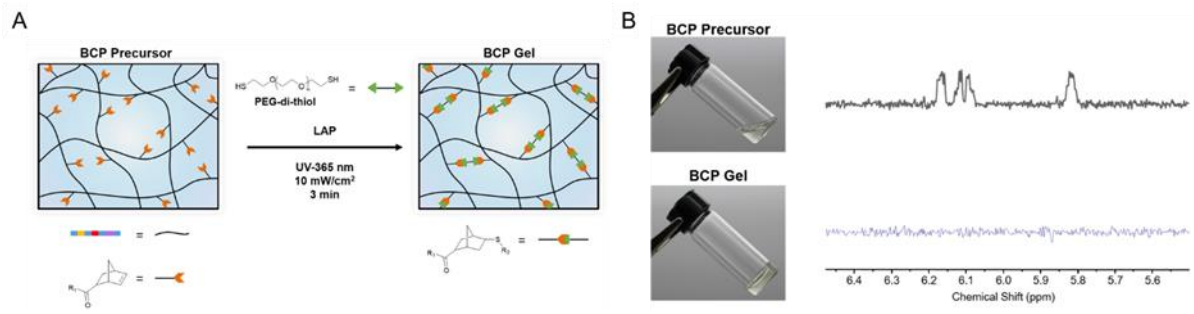

Figure V-3. BCP gelation via thiol-ene photopolymerization. (A) Schematic showing crosslinking of BCP chains through thiol-ene photopolymerization with poly(ethylene glycol)-di-thiol (PEG-di-thiol) . BCP precursor network on the left shows BCP chains that are overlapping but not crosslinked. (B) Tilt test images and corresponding ^{1}H NMR spectra show the uncrosslinked BCP precursor solution still containing the pendant norbornene groups after the thiolmaleimide reaction, while the BCP gel is crosslinked and does not contain norbornene groups after thiol-ene photopolymerization. Reprinted from "Orthogonal click reactions enable the synthesis of ECM-mimetic PEG hydrogels without multi-arm precursors" by F. Jivan, N. Fabela, Z. Davis, and D. L. Alge. *Journal of Materials Chemistry B*, 2018, 6, 4929-36. with permission from The Royal Society of Chemistry.[208]

5.4.2 Characterization of BCP Hydrogel Mechanical Properties, Swelling, and Degradability

After demonstrating photopolymerization of BCP chains with PEG-di-thiol and LAP, hydrogel networks were mechanically characterized *via* time sweep rheology to understand BCP hydrogel properties. First, *in situ* photopolymerization rheology demonstrated rapid gelation with all gel formulations exhibiting similar gel points occurring 10 seconds after photoinitiation (**Appendix, Figure VI-13**) and reaching a stable peak modulus after 3 - 4 min of UV-light exposure (**Figure V-4 a**). Storage modulus of pre-equilibrated BCP hydrogels decreased with increasing dilutions of BCP pre-polymer solution. Hydrogels made with the high XL formulation exhibited a storage modulus of 1036 Pa ± 43 Pa, while medium and low XL gels exhibited a storage modulus of 284 Pa ± 9 Pa and 75 Pa ± 4 Pa, respectively (**Figure V-4 b**). Additionally, swelling ratios inversely correlated with storage moduli as expected. High XL gels had a swelling ratio of 21.99 ± 0.92 while medium and low XL gels had swelling ratios of 33.49 ± 1.21 and 42.45 ± 1.58, respectively (**Figure V-4 c**). Peptide-containing hydrogels were also degraded *via* enzymatic degradation by collagenase-B. High XL BCP gels required 4.5 days to degrade completely, whereas medium and low XL gels degraded by 5 and 1.5 hours, respectively (**Figure V-4 d**). Taken together, these results demonstrate that BCP gels can be rapidly fabricated *via* photopolymerization, tuned over a range of tissue-like stiffness, and are susceptible to enzymatic degradation.

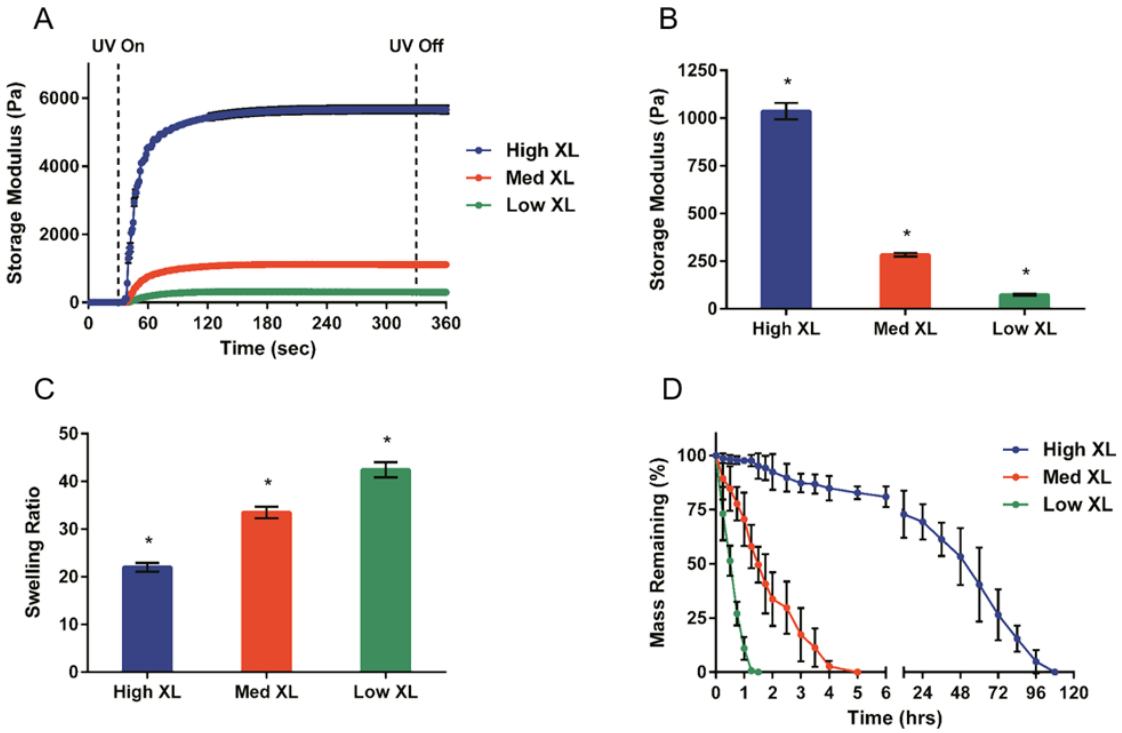

Figure V-4. Mechanical characterization of BCP gels. (A) *In situ* rheology showing gelation kinetics of BCP gelation at low, medium, and high crosslinking formulations. Results are averaged values over multiple runs (n = 3). (B) Storage modulus of pre-equilibrated hydrogels show a trend of decreasing modulus with lower crosslinking density, as expected. Averaged modulus values are all statistically significant with respect to each other ($p < 0.05$, n = 3). (C) Swelling ratios of hydrogels show the expected inverse correlation to the storage modulus data, with swelling ratios increasing with lower crosslinking density. Averaged swelling ratios are statistically significant with respect to each other ($p < 0.05$, n = 3). (D) Degradation of hydrogels in collagenase-B shows increased degradation time with higher crosslinking density. Reprinted from "Orthogonal click reactions enable the synthesis of ECM-mimetic PEG hydrogels without multi-arm precursors" by F. Jivan, N. Fabela, Z. Davis, and D. L. Alge. *Journal of Materials Chemistry B*, 2018, 6, 4929-36. with permission from The Royal Society of Chemistry.[208]

5.4.3 Cell Viability within BCP Hydrogels

To demonstrate the ability of BCP gels to be cytocompatible and a platform for *in vitro* 3-D cell encapsulation, NIH 3T3 fibroblasts were encapsulated within the gels during photopolymerization. Cell viability was then assessed by Live/Dead staining with calcein

AM and ethidium homodimer (**Figure V-5 a, b**). Analysis of confocal fluorescent images showed 78% ± 9% cell viability after 24 hours and 85% ± 12% at 5 days, possibly due to cell proliferation (**Figure V-5 c**). These results were expected given the well-established cytocompatibility of the thiol-norbornene photopolymerization reaction.[94, 209] Cell area was also quantified from confocal images and showed that average cell area statistically increased from 103 to 135 μm^2 from day 1 to day 5, respectively ($p < 0.05$). Additionally, the median and interquartile range for day 5 was larger than day 1 (119 vs. 89, and 80 vs. 55, respectively), indicating that in general the measured cell areas were overall larger on day 5 than day 1 (**Figure V-5 d**). These results were also expected given previous observations of larger cell size and spreading in enzymatically degradable PEG matrices over time.[63, 77] Also, while cell density appears to decrease between 1 day and 5 days, it was noted that BCP gels swelled considerably during culture. This could be a result of cells actively degrading the enzymatically-degradable peptide within the BCP backbone, which would cause the gels to swell in media. Despite this, BCP gels showed good cytocompatability, cell viability, and an increase in cell area throughout the bulk of the matrix.

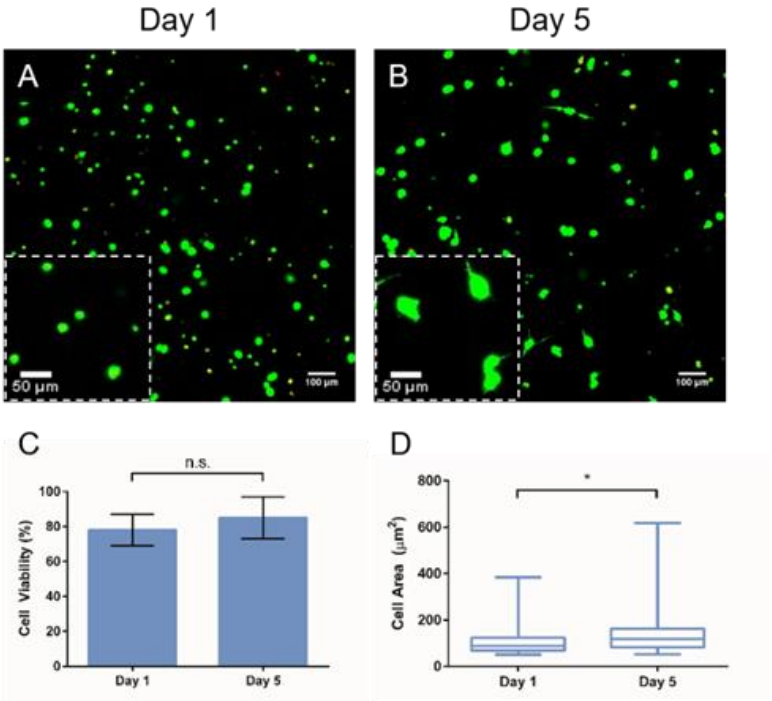

Figure V-5. Cell encapsulation within BCP gels. (A) Z-projection of confocal images of live/dead stained, encapsulated 3T3 fibroblasts at 1 day and (B) 5 days. The inset image shows a magnified area to better visualize cell area and spreading. (C) Analysis of live-dead images (n = 3) shows good cell viability with no difference between days 1 and 5. (D) Box and whisker plot of cell areas calculated from live/dead images (n = 3) shows a greater median and interquartile range at day 5 compared to day 1. Additionally, the average cell area is statistically different between days 1 and 5 ($p < 0.05$). Reprinted from "Orthogonal click reactions enable the synthesis of ECM-mimetic PEG hydrogels without multi-arm precursors" by F. Jivan, N. Fabela, Z. Davis, and D. L. Alge. *Journal of Materials Chemistry B*, 2018, 6, 4929-36. with permission from The Royal Society of Chemistry.[208]

5.4.4 Protein Patterning on BCP Hydrogels

Spatial arrangement of proteins whether discretely or in gradients is of high interest for directing cellular behaviors including attachment, proliferation and differentiation.[230-234] Photolithographic techniques coupled with single or multi-photon light sources offer the ability to easily achieve spatial control in 3-D with a great degree of precision, making

them widely useful for patterning of bulk hydrogels. Typically, peptide and protein-based patterning is performed by phototethering[106, 109, 186, 235-237] or photouncaging[238-240] reactions in order to attach or uncover biological molecules, respectively. While this allows for a high degree of spatial control, exposing biologics to UV light and radical species can compromise their bioactivity, which provides an impetus for developing alternative strategies. Previous work from our lab has demonstrated the ability to sequentially perform click reactions, specifically the thiol-ene and tetrazine-norbornene click reactions, by controlling stoichiometry of reactants.[133] Advantageously, gels can initially be rapidly fabricated using radical photochemistry, while bioconjugation can be performed subsequently, without the use of an initiator, to ensure the bioactivity of sensitive proteins or growth factors. Here, we wanted to demonstrate that this approach can be extended to our BCP gels in order to spatially pattern proteins. After crosslinking BCP chains off-stoichiometry, a photomask was used to selectively cap norbornene groups in one half of the hydrogel with L-cysteine, followed by tetrazine conjugation of ovalbumin to the unexposed half. Fluorescent images showed selective fluorescent ovalbumin conjugation to only half of the BCP gel (**Figure V-6**). Here, we still leverage the control of photopatterning by creating a "negative imprint" and then conjugate protein subsequently with a complimentary and bio-orthogonal chemistry.[230] In the future, this approach could be useful for patterning bioactive growth factors for tissue engineering.

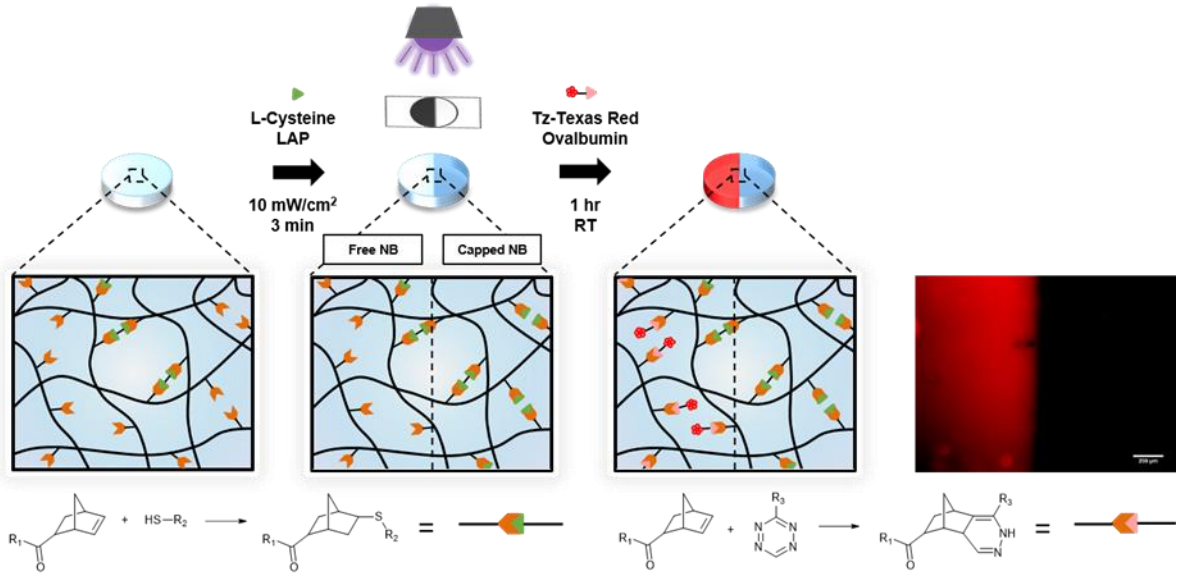

Figure V-6. Protein patterning on BCP gels. Schematic showing the step-by-step process for protein patterning. BCP gels are formed off stoichiometry, followed by thiolene photopolymerization with L-cysteine through a photomask, and finally protein patterning by tetrazine-norbornene click chemistry with tetrazine-functionalized protein. The fluorescent image on the right shows the resulting protein patterning with Tz-Texas Red ovalbumin on the BCP hydrogel. Reprinted from "Orthogonal click reactions enable the synthesis of ECM-mimetic PEG hydrogels without multi-arm precursors" by F. Jivan, N. Fabela, Z. Davis, and D. L. Alge. *Journal of Materials Chemistry B*, 2018, 6, 4929-36. with permission from The Royal Society of Chemistry.[208]

5.5 Conclusions

In summary, our work demonstrates that orthogonal click reactions can be leveraged to synthesize multifunctional and modular PEG-peptide hydrogels can be synthesized from simple linear precursors. The ability to tune mechanical properties within tissue-like ranges, the cytocompatability of the material platform, and the ease of protein attachment make this hydrogel platform broadly useful for tissue engineering applications. While only one BCP precursor composition was used here, the BCP gels can potentially be tailored for a desired application by manipulating the composition of the

BCP components, their molecular weights, or respective working concentrations. Additionally, the ability to mix-and-match BCP precursors of various compositions adds to the versatility of these building blocks and complexity that can be obtained in the resulting BCP gels. In future studies, we will expand this platform to other synthetic precursors and peptide sequences and explore patterning bioactive proteins.

CHAPTER VI

CONCLUSIONS AND FUTURE DIRECTIONS

6.1 Conclusions

Hydrogels are an important class of tissue-like biomaterials with superior hydration and tunable properties, owing to their current widespread use in the biomedical field. For tissue engineering applications, synthetic hydrogels such as PEG have been used as “blank slate” materials and combined with proteins and cells to create bio-instructive materials. However, a major challenge in the development of effective and functional biomaterials is the delivery of bioactive proteins. Tethering proteins to biomaterials has been hypothesized to enhance therapeutic potential by allowing for sustained presentation, reducing concentrations, and localizing cellular effects, Numerous strategies have been used for conjugated protein delivery, however these methods have been shown to either reduce protein bioactivity because of their stochastic nature of functionalization or are generally inaccessible to biomaterial scientists, such as with engineered proteins. Uniquely designed synthetic strategies for material fabrication and protein delivery have the potential to overcome the aforementioned limitations and further the field of tissue engineering. Click chemistry reactions are well poised for addressing these challenges, as their reaction specificity, rapid kinetics, mild nature, and orthogonality have been used to create user-defined hydrogels while maintaining peptide/protein bioactivity.

In this work, novel approaches were developed for the creation of next-generation, bio-instructive PEG-based hydrogels through the use of various sequential click reactions.

In particular, the norbornene functionality was leveraged for its participation in both the thiol-ene and tetrazine click reactions, as described in Chapters II – IV, but also its electron-rich nature precluding it from Michael-type additions as described in Chapter V.

In Chapter II, sequential thiol-norbornene and tetrazine-norbornene click reactions were used for PEG hydrogel microparticle synthesis and subsequent protein functionalization, respectively. Through stoichiometric control over the thiol-ene photopolymerization, free norbornene groups on the microparticles were leveraged for a secondary reaction with tetrazine functionalized proteins. Tetrazine-functionalized ALP and GOx were shown to improve protein loading and remain bioactive in a dose-dependent manner.

In Chapter III, the sequential click paradigm was used for assembling protein-functionalized PEG microparticles into microporous annealed particle (MAP) hydrogels for tissue engineering. As opposed to nanoporous bulk hydrogels, MAP hydrogels allow for spatial patterning of microparticle building blocks and the inherent microporosity allows for enhanced cell proliferation and spreading. Again, norbornene-bearing microparticles were functionalized with tetrazine-modified protein and also annealed using a PEG-di-tetrazine crosslinker through a bio-orthogonal tetrazine click reaction. The results demonstrated that clickable microparticles could be easily applied to a tissue-like defect and annealed into an inherently microporous structure *in situ*. MAP hydrogels were mechanically tuned using the PEG-di-tetrazine concentration and cell proliferation and spreading were found to be crosslinker concentration dependent. Lastly, the heterogeneous assembly of tetrazine-functionalized ALP microparticles within MAP hydrogels resulted

in a biomimetic mineralized/non-mineralized interface after incubation in calcium glycerophosphate, indicating tethered protein remained bioactive.

The focus of Chapter IV was to improve the protein functionalization process to be more site-specific. During the course of our investigation with sensitive proteins like bone morphogenetic protein-2 (BMP2), we found detrimental effects on bioactivity with increased tetrazine modification. As stated previously, protein functionalization strategies that are stochastic in nature (*i.e.* bind ubiquitously across the protein) can disrupt protein structure and function. To address this issue, a tetrazine-bis-sulfone was used to selectively modify proteins at terminal histidine-tags, commonly found on recombinant proteins. This modification strategy allowed for localized protein modification away from active sites on the protein while allowing for amenability with the tetrazine-norbornene click reaction for microparticle functionalization. PEG microparticles were functionalized with BMP2 using this strategy and assembled into MAP hydrogels as described in Chapter III. Tz-BMP2 functionalized MAP hydrogels showed improved protein loading over non-functionalized counterparts. Importantly, when seeded with human mesenchymal stem cells (hMSCs), Tz-BMP2 functionalized MAP hydrogels demonstrated significant calcium mineraliztion after 3 weeks compared to control scaffolds, indicating hMSC osteogenic differentiation.

Lastly in Chapter V, an emphasis was placed on better designing hydrogels by using linear hydrogel precursors rather than macromers. Up to this point, the PEG hydrogels we had been using were made from multi-arm PEG precursors, which can be more challenging to synthesize, poorly functionalized with reactive end-groups, and have limited space for both peptide/protein conjugation and hydrogel crosslinking. To

circumvent these challenges, linear PEG-di-maleimide and di-thiol peptide sequences were assembled *via* thiol-maleimide Michael addition to form PEG-peptide block co-polymers (BCPs). Importantly, the Michael addition reaction proceeded in the presence of a short peptide sequence containing pendant electron-rich norbornene groups, which in turn resulted in free pendant norbornene groups along the PEG-peptide BCP backbone. BCP precursors were crosslinked into BCP hydrogels using a photoinitiated thiol-norbornene click reaction with a PEG-di-thiol crosslinker. Mechanical characterization and cytocompatabiliy tests were performed to evaluate the use of BCP gels for tissue engineering applications. Again, stoichiometric control of the thiol-ene crosslinking reaction was leveraged for protein patterning *via* a subsequent bio-orthogonal click reaction with tetrazine-modified protein. The ability to create ECM-mimetic hydrogels using this tri-click system from only simple linear precursors, opens the possibilities to customizable scaffolds for tissue engineering.

6.2 Future Directions

The sequential click paradigm is a unique platform that is not limited to just thiol-ene and tetrazine click reactions, but rather can be applied to any set of complimentary reaction pairs, even those outside of the click toolbox. For example, thiol Michael additions can be combined with vinyl polymerizations or alkynes, and copper catalyzed azide-alkyne reactions can be combined with strain promoted reactions. A list of some reactions utilizing similar reactants is shown below in **Table VI.1**.[241]

Table VI.1. Click chemistry toolkit of reactions showing complimentary reactants. Reprinted from "Click chemistry beyong Metal-catalyzed cycloaddition" by C. R. Becer, R. Hoogenboom, and U. S. Schubert. *Angewandte Chemie*. 2009, 48, 4900-08. with permission from John Wiley and Sons.[241]

	Reagent A	Reagent B	Mechanism
0	Azide	Alkyne	Cu-catalyzed [3+2] azide-alkyne cycloaddition (CuAAC)
1	Azide	Cyclooctyne	Strain promoted [3+2] azide-alkyne cycloaddition
2	Azide	Activated-alkyne	[3+2] Huisgen cycloaddition
3	Azide	Electron deficient alkyne	[3+2] Cycloaddition
4	Azide	Aryne	[3+2] Cycloaddition
5	Tetrazine	Alkene	Diels-Alder Retro-[4+2] cycloaddition
6	Tetrazole	Alkene	1,3-Dipolar cycloaddition (photo click)
7	Dithioester	Diene	Hetero Diels-Alder cycloaddition
8	Anthracene	Maleimide	[4+2] Diels-Alder reaction
9	Thiol	Alkene	Radical addition or Michael addition (thio-click)
10	Thiol	Enone	Michael addition
11	Thiol	Maleimide	Michael addition
12	Thiol	*para*-Fluoro	Nucleophilic substitution
13	Amine	*para*-Fluoro	Nucleophilic substitution
14	Thiol	Bromo	Thioetherification
15	Thiol	Alkyne	Radical addition
16	Nitrile oxide	Alkyne	Dipolar cycloaddition

Taking a page out of the bioconjugate chemistry handbook, Chapter IV described the site-selective modification of His-tag recombinant proteins with tetrazine using a bis-sulfone reagent. This powerful modification strategy was initially used for PEGylation, however here we applied it for protein conjugation to biomaterials for the first time. Similar to protein loading experiments that were performed in Chapter II and bioacitivty experiments with tetrazine functionalization performed in Chapter IV, further characterization of tetrazine functionalization using Tz-PEG-bis sulfone is necessary to achieve optimal modification conditions. Additionally, while the current calcium mineralization results with BMP2 conjugation are promising, further characterization of

osteogenic markers (RUNX2, osteoprotegrin, alkaline phosphatase, collagen-1α osteopontin, osteocalcin) is still necessary to verify hMSC osteogenesis *in vitro*.

Since protein modification using bis-sulfones is a reagent-based strategy that targets His-tags commonly found on commercially available recombinant proteins, it is more accessible to biomaterial scientists and amenable to theoretically any recombinant protein of interest. This opens the possibility for co-delivery of other sensitive growth factors in conjunction with BMP2, for example other potent BMPs (BMP4, BMP7, BMP9) for osteogenesis, transforming growth factor-beta (TGF-β) for osteogenesis/chondrogenesis, vascular endothelial growth factor (VEGF) for stimulating angiogenesis, epidermal growth factor (EGF) or fibroblast growth factor (FGF) for cell growth and proliferation.

For applications outside of osteogenesis, developing immunomodulatory materials is of great interest in the evolving field of immunology.[242] Until only recently, biomaterial scientists have sought to minimize the immune response of implantable materials, however engineering biomaterials that can manipulate the immune system or illicit a desired immune response can be important for not only improving drug/vaccine efficacy but also allowing us to better understand the immune system and its components (*e.g.* cells and secreted factors). Tumor necrosis factor-alpha (TNFα) and interferon-gamma (IFNγ) have both been implicated in activation of macrophages in a pro-inflammatory manner within the body.[243] TNFα is released at the site of tissue injury or infection and is pivotal in orchestrating the pro-inflammatory immune response including macrophage cytokine cascades and inflammatory cell recruitment. Addition of exogenous TNFα relies on cross-

talk with IFNγ for inducing macrophage activation and leading to enhanced autocrine signaling. Due to its role as a master regulator, TNFα is thought to play a critical role in the development of chronic inflammatory diseases (*e.g.* rheumatoid arthritis, inflammatory bowel disease, atherosclerosis) making it a therapeutic target.[244-246] Thus, from a fundamentally biological and immunological perspective, studying these inflammatory agents in a controlled system *in vitro* could help to further understand their roles in the complex signaling cascade of immune response. Additionally, bioactive delivery of these factors within a hydrogel platform in conjugation with macrophages could serve to aid patients fighting immunological insults or with immunodeficiencies.

REFERENCES

1. Hoffman, A. S., Hydrogels for biomedical applications. *Adv. Drug Deliv. Rev.*, **2002,** *54* (1), 3-12.

2. Kirschner, C. M.; Anseth, K. S., Hydrogels in healthcare: from static to dynamic material microenvironments. *Acta Materialia*, **2013,** *61* (3), 931-44.

3. Lee, K. Y.; Mooney, D. J., Hydrogels for tissue engineering. *Chem. Rev.*, **2001,** *101* (7), 1869-80.

4. Drury, J. L.; Mooney, D. J., Hydrogels for tissue engineering: scaffold design variables and applications. *Biomaterials*, **2003,** *24* (24), 4337-51.

5. Buwalda, S. J.; Boere, K. W.; Dijkstra, P. J.; Feijen, J.; Vermonden, T.; Hennink, W. E., Hydrogels in a historical perspective: from simple networks to smart materials. *J. Control Release*, **2014,** *190*, 254-73.

6. Kharkar, P. M.; Kiick, K. L.; Kloxin, A. M., Designing degradable hydrogels for orthogonal control of cell microenvironments. *Chem. Soc. Rev.*, **2013,** *42* (17), 7335-72.

7. Rowley, J. A.; Madlambayan, G.; Mooney, D. J., Alginate hydrogels as synthetic extracellular matrix materials. *Biomaterials*, **1999,** *20* (1), 45-53.

8. Liu, L.; Liu, Y.; Li, J.; Du, G.; Chen, J., Microbial production of hyaluronic acid: current state, challenges, and perspectives. *Microb. Cell Fact.*, **2011,** *10*, 99-99.

9. Gramlich, W. M.; Kim, I. L.; Burdick, J. A., Synthesis and orthogonal photopatterning of hyaluronic acid hydrogels with thiol-norbornene chemistry. *Biomaterials*, **2013,** *34* (38), 9803-11.

10. Sideris, E.; Griffin, D. R.; Ding, Y.; Li, S.; Weaver, W. M.; Di Carlo, D.; Hsiai, T.; Segura, T., Particle hydrogels based on hyaluronic acid building blocks. *ACS Biomater. Sci. Eng.*, **2016,** *2* (11), 2034-41.

11. Prestwich, G. D.; Marecak, D. M.; Marecek, J. F.; Vercruysse, K. P.; Ziebell, M. R., Controlled chemical modification of hyaluronic acid: synthesis, applications, and biodegradation of hydrazide derivatives. *J. Control Release,* **1998,** *53* (1-3), 93-103.

12. Vercruysse, K. P.; Marecak, D. M.; Marecek, J. F.; Prestwich, G. D., Synthesis and in vitro degradation of new polyvalent hydrazide cross-linked hydrogels of hyaluronic acid. *Bioconjug. Chem.*, **1997,** *8* (5), 686-94.

13. Segura, T.; Anderson, B. C.; Chung, P. H.; Webber, R. E.; Shull, K. R.; Shea, L. D., Crosslinked hyaluronic acid hydrogels: a strategy to functionalize and pattern. *Biomaterials,* **2005,** *26* (4), 359-71.

14. Lee, K. Y.; Mooney, D. J., Alginate: properties and biomedical applications. *Prog. Polym. Sci.*, **2012,** *37* (1), 106-26.

15. Kim, W. S.; Mooney, D. J.; Arany, P. R.; Lee, K.; Huebsch, N.; Kim, J., Adipose tissue engineering using injectable, oxidized alginate hydrogels. *Tissue Eng. Part A,* **2012,** *18* (7-8), 737-43.

16. Shoichet, M. S.; Li, R. H.; White, M. L.; Winn, S. R., Stability of hydrogels used in cell encapsulation: an in vitro comparison of alginate and agarose. *Biotechnol. Bioeng.*, **1996,** *50* (4), 374-81.

17. Lee, K. Y.; Rowley, J. A.; Eiselt, P.; Moy, E. M.; Bouhadir, K. H.; Mooney, D. J., Controlling mechanical and swelling properties of alginate hydrogels independently by cross-linker type and cross-linking density. *Macromolecules,* **2000,** *33* (11), 4291-94.

18. Parenteau-Bareil, R.; Gauvin, R.; Berthod, F., Collagen-based biomaterials for tissue engineering applications. *Materials,* **2010,** *3* (3), 1863-87.

19. Kang, H.; Bayless, K. J.; Kaunas, R., Fluid shear stress modulates endothelial cell invasion into three-dimensional collagen matrices. *Am. J. Physiol. Heart. Circ. Physiol.,* **2008,** *295* (5), H2087-97.

20. Kang, H.; Kwak, H. I.; Kaunas, R.; Bayless, K. J., Fluid shear stress and sphingosine 1-phosphate activate calpain to promote membrane type 1 matrix metalloproteinase (MT1-MMP) membrane translocation and endothelial invasion into three-dimensional collagen matrices. *J. Biol. Chem.,* **2011,** *286* (49), 42017-26.

21. Hinton, T. J.; Jallerat, Q.; Palchesko, R. N.; Park, J. H.; Grodzicki, M. S.; Shue, H. J.; Ramadan, M. H.; Hudson, A. R.; Feinberg, A. W., Three-dimensional printing of complex biological structures by freeform reversible embedding of suspended hydrogels. *Sci. Adv.,* **2015,** *1* (9), e1500758.

22. Xavier, J. R.; Thakur, T.; Desai, P.; Jaiswal, M. K.; Sears, N.; Cosgriff-Hernandez, E.; Kaunas, R.; Gaharwar, A. K., Bioactive nanoengineered hydrogels for bone tissue engineering: a growth-factor-free approach. *ACS Nano.,* **2015,** *9* (3), 3109-18.

23. Paul, A.; Hasan, A.; Kindi, H. A.; Gaharwar, A. K.; Rao, V. T.; Nikkhah, M.; Shin, S. R.; Krafft, D.; Dokmeci, M. R.; Shum-Tim, D.; Khademhosseini, A., Injectable

graphene oxide/hydrogel-based angiogenic gene delivery system for vasculogenesis and cardiac repair. *ACS Nano.*, **2014,** *8* (8), 8050-62.

24. Billiet, T.; Gevaert, E.; De Schryver, T.; Cornelissen, M.; Dubruel, P., The 3D printing of gelatin methacrylamide cell-laden tissue-engineered constructs with high cell viability. *Biomaterials*, **2014,** *35* (1), 49-62.

25. Nichol, J. W.; Koshy, S. T.; Bae, H.; Hwang, C. M.; Yamanlar, S.; Khademhosseini, A., Cell-laden microengineered gelatin methacrylate hydrogels. *Biomaterials,* **2010,** *31* (21), 5536-44.

26. Bertlein, S.; Brown, G.; Lim, K. S.; Jungst, T.; Boeck, T.; Blunk, T.; Tessmar, J.; Hooper, G. J.; Woodfield, T. B.; Groll, J., Thiol–ene clickable gelatin: a platform bioink for multiple 3D biofabrication technologies. *Adv. Mater.*, **2017,** *29* (44), 1703404.

27. Truong, V. X.; Tsang, K. M.; Simon, G. P.; Boyd, R. L.; Evans, R. A.; Thissen, H.; Forsythe, J. S., Photodegradable gelatin-based hydrogels prepared by bioorthogonal click chemistry for cell encapsulation and release. *Biomacromolecules,* **2015,** *16* (7), 2246-53.

28. Koshy, S. T.; Desai, R. M.; Joly, P.; Li, J.; Bagrodia, R. K.; Lewin, S. A.; Joshi, N. S.; Mooney, D. J., Click-crosslinked injectable gelatin hydrogels. *Adv. Healthcare Mater.,* **2016,** *5* (5), 541-47.

29. Ratner, B. D.; Hoffman, A. S., Synthetic hydrogels for biomedical applications. *Hydrogels for Medical and Related Applications*, ACS, **1976**, *31*, 1-36.

30. Wichterle, O.; Lim, D., Hydrophilic gels for biological use. *Nature*, **1960,** *185* (4706), 117-18.

31. Garrett, Q.; Laycock, B.; Garrett, R. W., Hydrogel lens monomer constituents modulate protein sorption. *Invest. Ophthalmol. Vis. Sci.*, **2000,** *41* (7), 1687-95.

32. Hassan, C. M.; Peppas, N. A., Structure and applications of poly (vinyl alcohol) hydrogels produced by conventional crosslinking or by freezing/thawing methods. *Biopolymers· PVA Hydrogels, Anionic Polymerisation Nanocomposites*, Springer, **2000**, 37-65.

33. Stauffer, S. R.; Peppas, N. A., Poly (vinyl alcohol) hydrogels prepared by freezing-thawing cyclic processing. *Polymer,* **1992,** *33* (18), 3932-36.

34. Morimoto, K.; Fukanoki, S.; Morisaka, K.; Hyon, S.-H.; Ikada, Y., Design of polyvinyl alcohol hydrogel as a controlled-release vehicle for rectal administration of dl-propranolol-HCl and atenolol. *Chem. Pharm. Bull.,* **1989,** *37* (9), 2491-95.

35. Peppas, N. A.; Mongia, N. K., Ultrapure poly(vinyl alcohol) hydrogels with mucoadhesive drug delivery characteristics. *Eur. J. Pharm. Biopharm.,* **1997,** *43* (1), 51-58.

36. Bray, J. C.; Merrill, E. W., Poly(vinyl alcohol) hydrogels for synthetic articular cartilage material. *J. Biomed. Mater. Res.,* **1973,** *7* (5), 431-43.

37. Hyon, S.-H.; Cha, W.-I.; Ikada, Y.; Kita, M.; Ogura, Y.; Honda, Y., Poly (vinyl alcohol) hydrogels as soft contact lens material. *J. Biomater. Sci. Polym. Ed.,* **1994,** *5* (5), 397-406.

38. Schnaar, R. L.; Weigel, P. H.; Kuhlenschmidt, M. S.; Lee, Y. C.; Roseman, S., Adhesion of chicken hepatocytes to polyacrylamide gels derivatized with N-acetylglucosamine. *J. Biol. Chem.,* **1978,** *253* (21), 7940-51.

39. Beningo, K. A.; Lo, C.-M.; Wang, Y.-L., Flexible polyacrylamide substrata for the analysis of mechanical interactions at cell-substratum adhesions. *Methods Cell Biol.*, **2002**, *69*, 325-39.

40. Lo, C.-M.; Wang, H.-B.; Dembo, M.; Wang, Y.-L., Cell movement is guided by the rigidity of the substrate. *Biophs. J.*, **2000,** *79* (1), 144-52.

41. Engler, A. J.; Sen, S.; Sweeney, H. L.; Discher, D. E., Matrix elasticity directs stem cell lineage specification. *Cell*, **2006,** *126* (4), 677-89.

42. Reinhart-King, C. A.; Dembo, M.; Hammer, D. A., The dynamics and mechanics of endothelial cell spreading. *Biophys. J.*, **2005,** *89* (1), 676-89.

43. Pelham, R. J.; Wang, Y.-l., Cell locomotion and focal adhesions are regulated by substrate flexibility. *Proc. Natl. Acad. Sci.*, **1997,** *94* (25), 13661-65.

44. Kandow, C. E.; Georges, P. C.; Janmey, P. A.; Beningo, K. A., Polyacrylamide hydrogels for cell mechanics: steps toward optimization and alternative uses. *Methods Cell Biol.*, **2007,** *83*, 29-46.

45. Damljanovic, V.; Christoffer Lagerholm, B.; Jacobson, K., Bulk and micropatterned conjugation of extracellular matrix proteins to characterized polyacrylamide substrates for cell mechanotransduction assays. *BioTechniques*, **2005,** *39* (6), 847-51.

46. Yang, T.-H., Recent applications of polyacrylamide as biomaterials. *Recent Pat. Mater. Sci.*, **2008,** *1* (1), 29-40.

47. Dembo, M.; Wang, Y.-L., Stresses at the cell-to-substrate interface during locomotion of fibroblasts. *Biophs. J.*, **1999,** *76* (4), 2307-16.

48. Pelham Jr, R. J.; Wang, Y.-L., High resolution detection of mechanical forces exerted by locomoting fibroblasts on the substrate. *Mol. Biol. Cell,* **1999,** *10* (4), 935-45.

49. Reinhart-King, C. A.; Dembo, M.; Hammer, D. A., Endothelial cell traction forces on RGD-derivatized polyacrylamide substrata. *Langmuir,* **2003,** *19* (5), 1573-79.

50. Johnson, K. A.; Gorzinski, S. J.; Bodner, K. M.; Campbell, R. A.; Wolf, C. H.; Friedman, M. A.; Mast, R. W., Chronic toxicity and oncogenicity study on acrylamide incorporated in the drinking water of Fischer 344 rats. *Toxicol. Appl. Pharmacol.,* **1986,** *85* (2), 154-68.

51. Awad, M.; Abdel-Rahman, M.; Hassan, S., Acrylamide toxicity in isolated rat hepatocytes. *Toxicol. In Vitro,* **1998,** *12* (6), 699-704.

52. Beningo, K. A.; Wang, Y. L., Double-hydrogel substrate as a model system for three-dimensional cell culture. *Adhesion Protein Protocols*, Springer, **2007**, 203-11.

53. Feil, H.; Bae, Y. H.; Feijen, J.; Kim, S. W., Effect of comonomer hydrophilicity and ionization on the lower critical solution temperature of N-isopropylacrylamide copolymers. *Macromolecules,* **1993,** *26* (10), 2496-500.

54. Zhang, X.-Z.; Yang, Y.-Y.; Chung, T.-S.; Ma, K.-X., Preparation and characterization of fast response macroporous poly (N-isopropylacrylamide) hydrogels. *Langmuir,* **2001,** *17* (20), 6094-99.

55. Stile, R. A.; Burghardt, W. R.; Healy, K. E., Synthesis and characterization of injectable poly (N-isopropylacrylamide)-based hydrogels that support tissue formation in vitro. *Macromolecules,* **1999,** *32* (22), 7370-79.

56. Stile, R. A.; Healy, K. E., Poly (N-isopropylacrylamide)-based semi-interpenetrating polymer networks for tissue engineering applications. 1. effects of linear poly (acrylic acid) chains on phase behavior. *Biomacromolecules*, **2002,** *3* (3), 591-600.

57. Okuyama, Y.; Yoshida, R.; Sakai, K.; Okano, T.; Sakurai, Y., Swelling controlled zero order and sigmoidal drug release from thermo-responsive poly(N-isopropylacrylamide-co-butyl methacrylate) hydrogel. *J. Biomater. Sci. Polym. Ed.*, **1993,** *4* (5), 545-56.

58. Yamada, N.; Okano, T.; Sakai, H.; Karikusa, F.; Sawasaki, Y.; Sakurai, Y., Thermo-responsive polymeric surfaces; control of attachment and detachment of cultured cells. *Macromol. Rapid Commun.*, **1990,** *11* (11), 571-76.

59. Kim, M. R.; Jeong, J. H.; Park, T. G., Swelling induced detachment of chondrocytes using RGD-modified poly(N-isopropylacrylamide) hydrogel beads. *Biotechnol. Prog*., **2002,** *18* (3), 495-500.

60. Means, A. K.; Dong, P.; Clubb, F. J.; Friedemann, M. C.; Colvin, L. E.; Shrode, C. A.; Coté, G. L.; Grunlan, M. A., A self-cleaning, mechanically robust membrane for minimizing the foreign body reaction: towards extending the lifetime of sub-Q glucose biosensors. *J. Mater. Sci Mater.Med.*, **2019,** *30* (79), 1-11.

61. Hern, D. L.; Hubbell, J. A., Incorporation of adhesion peptides into nonadhesive hydrogels useful for tissue resurfacing. *J. Biomed. Mater. Res.*, **1998,** *39* (2), 266-76.

62. Miller, J. S.; Shen, C. J.; Legant, W. R.; Baranski, J. D.; Blakely, B. L.; Chen, C. S., Bioactive hydrogels made from step-growth derived PEG–peptide macromers. *Biomaterials*, **2010,** *31* (13), 3736-43.

63. Fairbanks, B. D.; Schwartz, M. P.; Halevi, A. E.; Nuttelman, C. R.; Bowman, C. N.; Anseth, K. S., A versatile synthetic extracellular matrix mimic via thiol-norbornene photopolymerization. *Adv. Mater.,* **2009,** *21* (48), 5005-10.

64. Benton, J. A.; Fairbanks, B. D.; Anseth, K. S., Characterization of valvular interstitial cell function in three dimensional matrix metalloproteinase degradable PEG hydrogels. *Biomaterials,* **2009,** *30* (34), 6593-603.

65. Anderson, S. B.; Lin, C.-C.; Kuntzler, D. V.; Anseth, K. S., The performance of human mesenchymal stem cells encapsulated in cell-degradable polymer-peptide hydrogels. *Biomaterials,* **2011,** *32* (14), 3564-74.

66. Raza, A.; Ki, C. S.; Lin, C.-C., The influence of matrix properties on growth and morphogenesis of human pancreatic ductal epithelial cells in 3D. *Biomaterials,* **2013,** *34* (21), 5117-27.

67. Stringer, J. L.; Peppas, N. A., Diffusion of small molecular weight drugs in radiation-crosslinked poly(ethylene oxide) hydrogels. *J. Control. Release,* **1996,** *42* (2), 195-202.

68. Kofinas, P.; Athanassiou, V.; Merrill, E. W., Hydrogels prepared by electron irradiation of poly(ethylene oxide) in water solution: unexpected dependence of cross-link density and protein diffusion coefficients on initial PEO molecular weight. *Biomaterials,* **1996,** *17* (15), 1547-50.

69. Peppas, N. A.; Keys, K. B.; Torres-Lugo, M.; Lowman, A. M., Poly(ethylene glycol)-containing hydrogels in drug delivery. *J. Control. Release,* **1999,** *62* (1), 81-87.

70. Panayotov, I. M.; Belcheva, N.; Stamenova, R.; Tsvetanov, C.; Lambov, N.; Tsankov, S.; Smid, J., Crosslinked poly(ethylene oxide) for drug release systems. *Macromol. Symp.,* **1996,** *103* (1), 193-211.

71. Bromberg, L., Crosslinked poly (ethylene glycol) networks as reservoirs for protein delivery. *J. Appl. Polym. Sci.,* **1996,** *59* (3), 459-66.

72. Elisseeff, J.; McIntosh, W.; Anseth, K.; Riley, S.; Ragan, P.; Langer, R., Photoencapsulation of chondrocytes in poly (ethylene oxide)-based semi-interpenetrating networks. *J. Biomed. Mater. Res.,* **2000,** *51* (2), 164-71.

73. Hill-West, J. L.; Chowdhury, S. M.; Slepian, M. J.; Hubbell, J. A., Inhibition of thrombosis and intimal thickening by in situ photopolymerization of thin hydrogel barriers. *Proc. Natl. Acad. Sci.,* **1994,** *91* (13), 5967-71.

74. West, J. L.; Hubbell, J. A., Polymeric biomaterials with degradation sites for proteases involved in cell migration. *Macromolecules,* **1999,** *32* (1), 241-44.

75. Rydholm, A. E.; Bowman, C. N.; Anseth, K. S., Degradable thiol-acrylate photopolymers: polymerization and degradation behavior of an in situ forming biomaterial. *Biomaterials,* **2005,** *26* (22), 4495-506.

76. Tibbitt, M.; Kloxin, A; Sawicki, L; Anseth, K. S., Mechanical properties and degradation of chain and step-polymerized photodegradable hydrogels. *Macromolecules,* **2013,** *46* (7), 2785-92.

77. Phelps, E. A.; Enemchukwu, N. O.; Fiore, V. F.; Sy, J. C.; Murthy, N.; Sulchek, T. A.; Barker, T. H.; Garcia, A. J., Maleimide cross-linked bioactive PEG hydrogel

exhibits improved reaction kinetics and cross-linking for cell encapsulation and in situ delivery. *Adv. Mater.,* **2012,** *24* (1), 64-70, 2-12.

78. McCall, J. D.; Anseth, K. S., Thiol-ene photopolymerizations provide a facile method to encapsulate proteins and maintain their bioactivity. *Biomacromolecules,* **2012,** *13* (8), 2410-17.

79. Rehmann, M. S.; Skeens, K. M.; Kharkar, P. M.; Ford, E. M.; Maverakis, E.; Lee, K. H.; Kloxin, A. M., Tuning and predicting mesh size and protein release from step growth hydrogels. *Biomacromolecules,* **2017,** *18* (10), 3131-42.

80. Lin, C.-C.; Anseth, K. S., PEG hydrogels for the controlled release of biomolecules in regenerative medicine. *Pharm. Res.,* **2009,** *26* (3), 631-43.

81. Aimetti, A. A.; Machen, A. J.; Anseth, K. S., Poly(ethylene glycol) hydrogels formed by thiol-ene photopolymerization for enzyme-responsive protein delivery. *Biomaterials,* **2009,** *30* (30), 6048-54.

82. McCall, J. D.; Luoma, J. E.; Anseth, K. S., Covalently tethered transforming growth factor beta in PEG hydrogels promotes chondrogenic differentiation of encapsulated human mesenchymal stem cells. *Drug Deliv. Transl. Res.,* **2012,** *2* (5), 305-12.

83. Peppas, N. A., Physiologically responsive hydrogels. *J. Bioact. Compat. Polym.,* **1991,** *6* (3), 241-46.

84. Wilson, S. A.; Cross, L. M.; Peak, C. W.; Gaharwar, A. K., Shear-thinning and thermo-reversible nanoengineered inks for 3D bioprinting. *ACS Appl. Mater. Interfaces,* **2017,** *9* (50), 43449-58.

85. Chimene, D.; Peak, C. W.; Gentry, J. L.; Carrow, J. K.; Cross, L. M.; Mondragon, E.; Cardoso, G. B.; Kaunas, R.; Gaharwar, A. K., Nanoengineered ionic-covalent entanglement (NICE) bioinks for 3D bioprinting. *ACS Appl. Mater. Interfaces,* **2018,** *10* (12), 9957-68.

86. Osada, Y., Equilibrium study of polymer–polymer complexation of poly(methacrylic acid) and poly(acrylic acid) with complementary polymers through cooperative hydrogen bonding. *J. Polym. Sc. Polym. Chem. Ed.,* **1979,** *17* (11), 3485-98.

87. Hu, X.; Vatankhah-Varnoosfaderani, M.; Zhou, J.; Li, Q.; Sheiko, S. S., Weak hydrogen bonding enables hard, strong, tough, and elastic hydrogels. *Adv. Mater.,* **2015,** *27* (43), 6899-905.

88. Zhang, J.; Wang, N.; Liu, W.; Zhao, X.; Lu, W., Intermolecular hydrogen bonding strategy to fabricate mechanically strong hydrogels with high elasticity and fatigue resistance. *Soft Matter,* **2013,** *9* (27), 6331-37.

89. Peppas, N. A., Turbidimetric studies of aqueous poly (vinyl alcohol) solutions. *Macromol. Chem. Phys.,* **1975,** *176* (11), 3433-40.

90. Zhang, H.; Cooper, A. I., Aligned porous structures by directional freezing. *Adv. Mater.,* **2007,** *19* (11), 1529-33.

91. Shirwaiker, R. A.; Purser, M. F.; Wysk, R. A., Scaffolding hydrogels for rapid prototyping based tissue engineering. *Rapid Prototyping of Biomaterials*, Narayan, R., Ed. Woodhead Publishing, **2014**, 176-200.

92. Southorn, P. A.; Powis, G., Free radicals in medicine. I. chemical nature and biologic reactions. *Mayo Clin. Proc.,* **1988,** *63* (4), 381-89.

93. Roberts, J. J.; Bryant, S. J., Comparison of photopolymerizable thiol-ene PEG and acrylate-based PEG hydrogels for cartilage development. *Biomaterials,* **2013,** *34* (38), 9969-79.

94. Lin, C. C.; Raza, A.; Shih, H., PEG hydrogels formed by thiol-ene photo-click chemistry and their effect on the formation and recovery of insulin-secreting cell spheroids. *Biomaterials,* **2011,** *32* (36), 9685-95.

95. Lee, T. Y.; Guymon, C. A.; Jönsson, E. S.; Hoyle, C. E., The effect of monomer structure on oxygen inhibition of (meth)acrylates photopolymerization. *Polymer,* **2004,** *45* (18), 6155-62.

96. Ligon, S. C.; Husár, B.; Wutzel, H.; Holman, R.; Liska, R., Strategies to reduce oxygen inhibition in photoinduced polymerization. *Chem. Rev.*, **2014,** *114* (1), 557-89.

97. Kolb, H. C.; Finn, M. G.; Sharpless, K. B., Click chemistry: diverse chemical function from a few good reactions. *Angew. Chem.*, **2001,** *40* (11), 2004-21.

98. Nair, D. P.; Podgorski, M.; Chatani, S.; Gong, T.; Xi, W. X.; Fenoli, C. R.; Bowman, C. N., The thiol-michael addition click reaction: a powerful and widely used tool in materials chemistry. *Chem. Mater.,* **2014,** *26* (1), 724-44.

99. Elbert, D. L.; Hubbell, J. A., Conjugate addition reactions combined with free-radical cross-linking for the design of materials for tissue engineering. *Biomacromolecules,* **2001,** *2* (2), 430-41.

100. Lutolf, M.; Hubbell, J., Synthesis and physicochemical characterization of end-linked poly (ethylene glycol)-co-peptide hydrogels formed by Michael-type addition. *Biomacromolecules,* **2003,** *4* (3), 713-22.

101. Lutolf, M. P.; Tirelli, N.; Cerritelli, S.; Cavalli, L.; Hubbell, J. A., Systematic modulation of Michael-type reactivity of thiols through the use of charged amino acids. *Bioconjug. Chem.,* **2001,** *12* (6), 1051-56.

102. Lutolf, M. P..; Lauer-Fields, J.; Schmoekel, H.; Metters, A. T.; Weber, F.; Fields, G.; Hubbell, J. A., Synthetic matrix metalloproteinase-sensitive hydrogels for the conduction of tissue regeneration: engineering cell-invasion characteristics. *Proc. Natl. Acad. Sci.,* **2003,** *100* (9), 5413-18.

103. Sawicki, L. A.; Kloxin, A. M., Design of thiol-ene photoclick hydrogels using facile techniques for cell culture applications. *Biomater. Sci.,* **2014,** *2* (11), 1612-26.

104. Devaraj, N. K.; Weissleder, R.; Hilderbrand, S. A., Tetrazine-based cycloadditions: application to pretargeted live cell imaging. *Bioconjug. Chem.,* **2008,** *19* (12), 2297-99.

105. Devaraj, N. K.; Upadhyay, R.; Haun, J. B.; Hilderbrand, S. A.; Weissleder, R., Fast and sensitive pretargeted labeling of cancer cells through a tetrazine/trans-cyclooctene cycloaddition. *Angew. Chem. Int. Ed.,* **2009,** *48* (38), 7013-16.

106. Alge, D. L.; Azagarsamy, M. A.; Donohue, D. F.; Anseth, K. S., Synthetically tractable click hydrogels for three-dimensional cell culture formed using tetrazine–norbornene chemistry. *Biomacromolecules,* **2013,** *14* (4), 949-53.

107. Mabry, K. M.; Lawrence, R. L.; Anseth, K. S., Dynamic stiffening of poly(ethylene glycol)-based hydrogels to direct valvular interstitial cell phenotype in a three-dimensional environment. *Biomaterials*, **2015,** *49*, 47-56.

108. Khetan, S.; Katz, J. S.; Burdick, J. A., Sequential crosslinking to control cellular spreading in three-dimensional hydrogels. *Soft Matter,* **2009,** *5* (8), 1601-06.

109. DeForest, C. A.; Polizzotti, B. D.; Anseth, K. S., Sequential click reactions for synthesizing and patterning three-dimensional cell microenvironments. *Nat. Mater.,* **2009,** *8* (8), 659-64.

110. Guvendiren, M.; Molde, J.; Soares, R. M.; Kohn, J., Designing biomaterials for 3D printing. *ACS Biomater. Sci. Eng.,* **2016,** *2* (10), 1679-93.

111. Mannoor, M. S.; Jiang, Z.; James, T.; Kong, Y. L.; Malatesta, K. A.; Soboyejo, W. O.; Verma, N.; Gracias, D. H.; McAlpine, M. C., 3D printed bionic ears. *Nano Lett.,* **2013,** *13* (6), 2634-39.

112. Wu, W.; DeConinck, A.; Lewis, J. A., Omnidirectional printing of 3D microvascular networks. *Adv. Mater.,* **2011,** *23* (24), H178-83.

113. Highley, C. B.; Rodell, C. B.; Burdick, J. A., Direct 3D printing of shear-thinning hydrogels into self-healing hydrogels. *Adv. Mater.,* **2015,** *27* (34), 5075-79.

114. Arcaute, K.; Mann, B. K.; Wicker, R. B., Stereolithography of three-dimensional bioactive poly(ethylene glycol) constructs with encapsulated cells. *Ann. Biomed. Eng.,* **2006,** *34* (9), 1429-41.

115. Grigoryan, B.; Paulsen, S. J.; Corbett, D. C.; Sazer, D. W.; Fortin, C. L.; Zaita, A. J.; Greenfield, P. T.; Calafat, N. J.; Gounley, J. P.; Ta, A. H.; Johansson, F.; Randles, A.; Rosenkrantz, J. E.; Louis-Rosenberg, J. D.; Galie, P. A.; Stevens, K. R.; Miller, J. S., Multivascular networks and functional intravascular topologies within biocompatible hydrogels. *Science,* **2019,** *364* (6439), 458-64.

116. Griffin, D. R.; Weaver, W. M.; Scumpia, P. O.; Di Carlo, D.; Segura, T., Accelerated wound healing by injectable microporous gel scaffolds assembled from annealed building blocks. *Nat. Mater.*, **2015,** *14* (7), 737-44.

117. Caldwell, A. S.; Campbell, G. T.; Shekiro, K. M. T.; Anseth, K. S., Clickable microgel scaffolds as platforms for 3D cell encapsulation. *Adv. Healthcare Mater.,* **2017,** *6* (15), 1700254 (1-8).

118. Xin, S.; Wyman, O. M.; Alge, D. L., Assembly of PEG microgels into porous cell-instructive 3D scaffolds via thiol-ene click chemistry. *Adv. Healthcare Mater.,* **2018,** *7* (11), 1800160 (1-7).

119. Xin, S.; Chimene, D.; Garza, J. E.; Gaharwar, A. K.; Alge, D. L., Clickable PEG hydrogel microspheres as building blocks for 3D bioprinting. *Biomater. Sci.,* **2019,** *7* (3), 1179-87.

120. Schmedlen, R. H.; Masters, K. S.; West, J. L., Photocrosslinkable polyvinyl alcohol hydrogels that can be modified with cell adhesion peptides for use in tissue engineering. *Biomaterials,* **2002,** *23* (22), 4325-32.

121. Fisher, S. A.; Baker, A. E. G.; Shoichet, M. S., Designing peptide and protein modified hydrogels: selecting the optimal conjugation strategy. *J. Am. Chem. Soc.,* **2017,** *139* (22), 7416-27.

122. McGann, C. L.; Levenson, E. A.; Kiick, K. L., Resilin-based hybrid hydrogels for cardiovascular tissue engineering. *Macromolecules,* **2013,** *214* (2), 203-13.

123. Lutolf, M. P.; Raeber, G. P.; Zisch, A. H.; Tirelli, N.; Hubbell, J. A., Cell-responsive synthetic hydrogels. *Adv. Mater.,* **2003,** *15* (11), 888-92.

124. Kuhl, P. R.; Griffith-Cima, L. G., Tethered epidermal growth factor as a paradigm for growth factor-induced stimulation from the solid phase. *Nat. Med.,* **1996,** *2* (9), 1022-27.

125. Mann, B. K.; Schmedlen, R. H.; West, J. L., Tethered-TGF-beta increases extracellular matrix production of vascular smooth muscle cells. *Biomaterials,* **2001,** *22* (5), 439-44.

126. Seliktar, D.; Zisch, A. H.; Lutolf, M. P.; Wrana, J. L.; Hubbell, J. A., MMP-2 sensitive, VEGF-bearing bioactive hydrogels for promotion of vascular healing. *J. Biomed. Mater. Res. A,* **2004,** *68* (4), 704-16.

127. Cambria, E.; Renggli, K.; Ahrens, C. C.; Cook, C. D.; Kroll, C.; Krueger, A. T.; Imperiali, B.; Griffith, L. G., Covalent modification of synthetic hydrogels with bioactive proteins via sortase-mediated ligation. *Biomacromolecules,* **2015,** *16* (8), 2316-26.

128. Shadish, J. A.; Benuska, G. M.; DeForest, C. A., Bioactive site-specifically modified proteins for 4D patterning of gel biomaterials. *Nat. Mater.,* **2019**, *18,* 1005-14.

129. Kwiatkowski, W.; Gray, P. C.; Choe, S., Engineering TGF-beta superfamily ligands for clinical applications. *Trends Pharmacol. Sci.,* **2014,** *35* (12), 648-57.

130. Balan, S.; Choi, J. W.; Godwin, A.; Teo, I.; Laborde, C. M.; Heidelberger, S.; Zloh, M.; Shaunak, S.; Brocchini, S., Site-specific PEGylation of protein disulfide bonds using a three-carbon bridge. *Bioconjug. Chem.,* **2007,** *18* (1), 61-76.

131. Cong, Y.; Pawlisz, E.; Bryant, P.; Balan, S.; Laurine, E.; Tommasi, R.; Singh, R.; Dubey, S.; Peciak, K.; Bird, M.; Sivasankar, A.; Swierkosz, J.; Muroni, M.; Heidelberger, S.; Farys, M.; Khayrzad, F.; Edwards, J.; Badescu, G.; Hodgson, I.; Heise, C.;

Somavarapu, S.; Liddell, J.; Powell, K.; Zloh, M.; Choi, J. W.; Godwin, A.; Brocchini, S., Site-specific PEGylation at histidine tags. *Bioconjug. Chem.,* **2012,** *23* (2), 248-63.

132. Peciak, K.; Laurine, E.; Tommasi, R.; Choi, J. W.; Brocchini, S., Site-selective protein conjugation at histidine. *Chem. Sci.,* **2019,** *10* (2), 427-39.

133. Jivan, F.; Yegappan, R.; Pearce, H.; Carrow, J. K.; McShane, M.; Gaharwar, A. K.; Alge, D. L., Sequential thiol–ene and tetrazine click reactions for the polymerization and functionalization of hydrogel microparticles. *Biomacromolecules,* **2016,** *17* (11), 3516-23.

134. Hoyle, C. E.; Lowe, A. B.; Bowman, C. N., Thiol-click chemistry: a multifaceted toolbox for small molecule and polymer synthesis. *Chem. Soc. Rev.,* **2010,** *39* (4), 1355-87.

135. Kade, M. J.; Burke, D. J.; Hawker, C. J., The power of thiol-ene chemistry. *J. Polym. Sci. A Polym. Chem.,* **2010,** *48* (4), 743-50.

136. Killops, K. L.; Campos, L. M.; Hawker, C. J., Robust, efficient, and orthogonal synthesis of dendrimers via thiol-ene "click" chemistry. *J. Am. Chem. Soc.,* **2008,** *130* (15), 5062-64.

137. Lowe, A. B., Thiol-ene "click" reactions and recent applications in polymer and materials synthesis. *Polym. Chem.,* **2010,** *1* (1), 17-36.

138. Hoyle, C. E.; Bowman, C. N., Thiol-ene click chemistry. *Angew. Chem.,* **2010,** *49* (9), 1540-73.

139. Cramer, N. B.; Davies, T.; O'Brien, A. K.; Bowman, C. N., Mechanism and modeling of a thiol−ene photopolymerization. *Macromolecules,* **2003,** *36* (12), 4631-36.

140. Gould, S. T.; Darling, N. J.; Anseth, K. S., Small peptide functionalized thiol–ene hydrogels as culture substrates for understanding valvular interstitial cell activation and de novo tissue deposition. *Acta Biomater.,* **2012,** *8* (9), 3201-09.

141. Sawicki, L. A.; Kloxin, A. M., Design of thiol-ene photoclick hydrogels using facile techniques for cell culture applications. *Biomater. Sci.,* **2014,** *2* (11), 1612-26.

142. Blackman, M. L.; Royzen, M.; Fox, J. M., Tetrazine ligation: fast bioconjugation based on inverse-electron-demand Diels− Alder reactivity. *J. Am. Chem. Soc.,* **2008,** *130* (41), 13518-19.

143. Saracoglu, N., Recent advances and applications in 1,2,4,5-tetrazine chemistry. *Tetrahedron,* **2007,** *63* (20), 4199-236.

144. Hansell, C. F.; Espeel, P.; Stamenovic, M. M.; Barker, I. A.; Dove, A. P.; Du Prez, F. E.; O'Reilly, R. K., Additive-free clicking for polymer functionalization and coupling by tetrazine-norbornene chemistry. *J. Am. Chem. Soc.,* **2011,** *133* (35), 13828-31.

145. Carlson, J. C.; Meimetis, L. G.; Hilderbrand, S. A.; Weissleder, R., BODIPY–tetrazine derivatives as superbright bioorthogonal turn-on probes. *Angew. Chem.,* **2013,** *125* (27), 7055-58.

146. Han, H. S.; Devaraj, N. K.; Lee, J.; Hilderbrand, S. A.; Weissleder, R.; Bawendi, M. G., Development of a bioorthogonal and highly efficient conjugation method for quantum dots using tetrazine-norbornene cycloaddition. *J. Am. Chem. Soc.,* **2010,** *132* (23), 7838-39.

147. Desai, R. M.; Koshy, S. T.; Hilderbrand, S. A.; Mooney, D. J.; Joshi, N. S., Versatile click alginate hydrogels crosslinked via tetrazine–norbornene chemistry. *Biomaterials*, **2015,** *50*, 30-37.

148. Alge, D. L.; Donohue, D. F.; Anseth, K. S., Facile and efficient Lewis acid catalyzed synthesis of an asymmetric tetrazine useful for bio-orthogonal click chemistry applications. *Tetrahedron Lett.*, **2013,** *54* (41), 5639-41.

149. van Hooy-Corstjens, C. S. J.; Saralidze, K.; Knetsch, M. L. W.; Emans, P. J.; de Haan, M. W.; Magusin, P. C. M. M.; Mezari, B.; Koole, L. H., New intrinsically radiopaque hydrophilic microspheres for embolization: synthesis and characterization. *Biomacromolecules*, **2008,** *9* (1), 84-90.

150. Secret, E.; Kelly, S. J.; Crannell, K. E.; Andrew, J. S., Enzyme-responsive hydrogel microparticles for pulmonary drug delivery. *ACS Appl. Mater. Interfaces*, **2014,** *6* (13), 10313-21.

151. Parlato, M.; Johnson, A.; Hudalla, G. A.; Murphy, W. L., Adaptable poly(ethylene glycol) microspheres capable of mixed-mode degradation. *Acta Biomater.*, **2013,** *9* (12), 9270-80.

152. Utech, S.; Prodanovic, R.; Mao, A. S.; Ostafe, R.; Mooney, D. J.; Weitz, D. A., Microfluidic generation of monodisperse, structurally homogeneous alginate microgels for cell encapsulation and 3D cell culture. *Adv. Healthcare Mater.*, **2015**, *4* (11), 1628-33.

153. Elbert, D. L., Liquid-liquid two-phase systems for the production of porous hydrogels and hydrogel microspheres for biomedical applications: a tutorial review. *Acta Biomater.*, **2011,** *7* (1), 31-56.

154. Liu, A. L.; García, A. J., Methods for generating hydrogel particles for protein delivery. *Ann. Biomed. Eng.*, **2016,** *44* (6), 1946-58.

155. Young, C. J.; Poole-Warren, L. A.; Martens, P. J., Combining submerged electrospray and UV photopolymerization for production of synthetic hydrogel microspheres for cell encapsulation. *Biotechnol. Bioeng.*, **2012,** *109* (6), 1561-70.

156. Belair, D. G.; Khalil, A. S.; Miller, M. J.; Murphy, W. L., Serum-dependence of affinity-mediated VEGF release from biomimetic microspheres. *Biomacromolecules*, **2014,** *15* (6), 2038-48.

157. Kawamoto, K.; Grindy, S. C.; Liu, J.; Holten-Andersen, N.; Johnson, J. A., Dual role for 1,2,4,5-tetrazines in polymer networks: combining Diels–Alder reactions and metal coordination to generate functional supramolecular gels. *ACS Macro Lett.*, **2015,** *4* (4), 458-61.

158. Zhou, H.; Johnson, J. A., Photo-controlled growth of telechelic polymers and end-linked polymer gels. *Angew. Chem.*, **2013,** *125* (8), 2291-94.

159. Cok, A. M.; Zhou, H.; Johnson, J. A., Synthesis of model network hydrogels via tetrazine-olefin inverse electron demand Diels-Alder cycloaddition. *Macromol. Symp.*, **2013,** *329* (1), 108-12.

160. Zhou, H.; Woo, J.; Cok, A. M.; Wang, M.; Olsen, B. D.; Johnson, J. A., Counting primary loops in polymer gels. *Proc. Natl. Acad. Sci.*, **2012,** *109* (47), 19119-24.

161. Zhou, H.; Schon, E. M.; Wang, M.; Glassman, M. J.; Liu, J.; Zhong, M.; Diaz Diaz, D.; Olsen, B. D.; Johnson, J. A., Crossover experiments applied to network formation reactions: improved strategies for counting elastically inactive molecular

defects in PEG gels and hyperbranched polymers. *J. Am. Chem. Soc.*, **2014,** *136* (26), 9464-70.

162. Fairbanks, B. D.; Schwartz, M. P.; Bowman, C. N.; Anseth, K. S., Photoinitiated polymerization of PEG-diacrylate with lithium phenyl-2,4,6-trimethylbenzoylphosphinate: polymerization rate and cytocompatibility. *Biomaterials,* **2009,** *30* (35), 6702-07.

163. Shih, H.; Lin, C. C., Cross-linking and degradation of step-growth hydrogels formed by thiol-ene photoclick chemistry. *Biomacromolecules,* **2012,** *13* (7), 2003-12.

164. Kawamoto, K.; Zhong, M.; Wang, R.; Olsen, B. D.; Johnson, J. A., Loops versus branch functionality in model click hydrogels. *Macromolecules,* **2015,** *48* (24), 8980-88.

165. Zisch, A. H.; Lutolf, M. P.; Ehrbar, M.; Raeber, G. P.; Rizzi, S. C.; Davies, N.; Schmokel, H.; Bezuidenhout, D.; Djonov, V.; Zilla, P.; Hubbell, J. A., Cell-demanded release of VEGF from synthetic, biointeractive cell ingrowth matrices for vascularized tissue growth. *FASEB J.,* **2003,** *17* (15), 2260-62.

166. Tokatlian, T.; Shrum, C. T.; Kadoya, W. M.; Segura, T., Protease degradable tethers for controlled and cell-mediated release of nanoparticles in 2- and 3-dimensions. *Biomaterials,* **2010,** *31* (31), 8072-80.

167. Van Hove, A. H.; Antonienko, E.; Burke, K.; Brown, E., 3rd; Benoit, D. S., Temporally tunable, enzymatically responsive delivery of proangiogenic peptides from poly(ethylene glycol) hydrogels. *Adv. Healthcare Mater.,* **2015,** *4* (13), 2002-11.

168. Beertsen, W.; van den Bos, T., Alkaline phosphatase induces the mineralization of sheets of collagen implanted subcutaneously in the rat. *J. Clin. Invest.,* **1992,** *89* (6), 1974-80.

169. Douglas, T. E.; Messersmith, P. B.; Chasan, S.; Mikos, A. G.; de Mulder, E. L.; Dickson, G.; Schaubroeck, D.; Balcaen, L.; Vanhaecke, F.; Dubruel, P.; Jansen, J. A.; Leeuwenburgh, S. C., Enzymatic mineralization of hydrogels for bone tissue engineering by incorporation of alkaline phosphatase. *Macromol. Biosci.,* **2012,** *12* (8), 1077-89.

170. Robison, R., The possible significance of hexosephosphoric esters in ossification. *Biochem. J.,* **1923,** *17* (2), 286-93.

171. Henrichsen, E., Alkaline phosphatase and calcification; histochemical investigations on the relationship between alkaline phosphatase and calcification. *Acta Orthop. Scand. Suppl.,* **1958,** *34*, 1-82.

172. Hessle, L.; Johnson, K. A.; Anderson, H. C.; Narisawa, S.; Sali, A.; Goding, J. W.; Terkeltaub, R.; Millan, J. L., Tissue-nonspecific alkaline phosphatase and plasma cell membrane glycoprotein-1 are central antagonistic regulators of bone mineralization. *Proc. Natl. Acad. Sci.,* **2002,** *99* (14), 9445-49.

173. Narisawa, S.; Yadav, M. C.; Millan, J. L., In vivo overexpression of tissue-nonspecific alkaline phosphatase increases skeletal mineralization and affects the phosphorylation status of osteopontin. *J. Bone Miner. Res.,* **2013,** *28* (7), 1587-98.

174. Unruh, R. M.; Roberts, J. R.; Nichols, S. P.; Gamsey, S.; Wisniewski, N. A.; McShane, M. J., Preclinical evaluation of poly(HEMA-co-acrylamide) hydrogels

encapsulating glucose oxidase and palladium benzoporphyrin as fully implantable glucose sensors. *J. Diabetes Sci. Technol.,* **2015,** *9* (5), 985-92.

175. Roberts, J. R.; Park, J.; Helton, K.; Wisniewski, N.; McShane, M. J., Biofouling of polymer hydrogel materials and its effect on diffusion and enzyme-based luminescent glucose sensor functional characteristics. *J. Diabetes Sci. Technol.,* **2012,** *6* (6), 1267-75.

176. Brahim, S.; Narinesingh, D.; Guiseppi-Elie, A., Kinetics of glucose oxidase immobilized in p(HEMA)-hydrogel microspheres in a packed-bed bioreactor. *J. Mol. Catal. B Enzym.,* **2002,** *18* (1), 69-80.

177. Guiseppi-Elie, A.; Brahim, S.; Slaughter, G.; Ward, K. R., Design of a subcutaneous implantable biochip for monitoring of glucose and lactate. *IEEE Sens. J.*, **2005,** *5* (3), 345-55.

178. Nguyen, K. T.; West, J. L., Photopolymerizable hydrogels for tissue engineering applications. *Biomaterials,* **2002,** *23* (22), 4307-14.

179. Nih, L. R.; Sideris, E.; Carmichael, S. T.; Segura, T., Injection of microporous annealing particle (MAP) hydrogels in the stroke cavity reduces gliosis and inflammation and promotes NPC migration to the lesion. *Adv. Mater.*, **2017,** *29* (32), 1606471 (1-8).

180. Guvendiren, M.; Burdick, J. A., Engineering synthetic hydrogel microenvironments to instruct stem cells. *Curr. Opin. Biotechnol.,* **2013,** *24* (5), 841-46.

181. Darling, N. J.; Sideris, E.; Hamada, N.; Carmichael, S. T.; Segura, T., Injectable and spatially patterned microporous annealed particle (MAP) hydrogels for tissue repair applications. *Adv. Sci.,* **2018,** *5* (11), 1801046 (1-8).

182. Mealy, J. E.; Chung, J. J.; Jeong, H. H.; Issadore, D.; Lee, D.; Atluri, P.; Burdick, J. A., Injectable granular hydrogels with multifunctional properties for biomedical applications. *Adv. Mater.,* **2018,** *30* (20), 1705912 (1-7).

183. Chen, M. H.; Chung, J. J.; Mealy, J. E.; Zaman, S.; Li, E. C.; Arisi, M. F.; Atluri, P.; Burdick, J. A., Injectable supramolecular hydrogel/microgel composites for therapeutic delivery. *Macromol. Biosci.,* **2019,** *19* (1), 1800248 (1-12).

184. Oliveira, B. L.; Guo, Z.; Bernardes, G. J. L., Inverse electron demand Diels-Alder reactions in chemical biology. *Chem. Soc. Rev.,* **2017,** *46* (16), 4895-950.

185. Headen, D. M.; Woodward, K. B.; Coronel, M. M.; Shrestha, P.; Weaver, J. D.; Zhao, H.; Tan, M.; Hunckler, M. D.; Bowen, W. S.; Johnson, C. T.; Shea, L.; Yolcu, E. S.; García, A. J.; Shirwan, H., Local immunomodulation with Fas ligand-engineered biomaterials achieves allogeneic islet graft acceptance. *Nat. Mater.,* **2018,** *17* (8), 732-39.

186. Wylie, R. G.; Ahsan, S.; Aizawa, Y.; Maxwell, K. L.; Morshead, C. M.; Shoichet, M. S., Spatially controlled simultaneous patterning of multiple growth factors in three-dimensional hydrogels. *Nat. Mater.,* **2011,** *10* (10), 799-806.

187. Seeherman, H. J.; Berasi, S. P.; Brown, C. T.; Martinez, R. X.; Juo, Z. S.; Jelinsky, S.; Cain, M. J.; Grode, J.; Tumelty, K. E.; Bohner, M.; Grinberg, O.; Orr, N.; Shoseyov, O.; Eyckmans, J.; Chen, C.; Morales, P. R.; Wilson, C. G.; Vanderploeg, E. J.; Wozney, J. M., A BMP/activin A chimera is superior to native BMPs and induces bone repair in nonhuman primates when delivered in a composite matrix. *Sci. Transl. Med.* **2019,** *11* (489), eaar4953 (1-20).

188. Basle, E.; Joubert, N.; Pucheault, M., Protein chemical modification on endogenous amino acids. *Chem. Biol.,* **2010,** *17* (3), 213-27.

189. Engler, A. J.; Sen, S.; Sweeney, H. L.; Discher, D. E., Matrix elasticity directs stem cell lineage specification. *Cell,* **2006,** *126* (4), 677-89.

190. Leight, J. L.; Wozniak, M. A.; Chen, S.; Lynch, M. L.; Chen, C. S., Matrix rigidity regulates a switch between TGF-beta1-induced apoptosis and epithelial-mesenchymal transition. *Mol. Biol. Cell,* **2012,** *23* (5), 781-91.

191. Wei, S. C.; Fattet, L.; Tsai, J. H.; Guo, Y.; Pai, V. H.; Majeski, H. E.; Chen, A. C.; Sah, R. L.; Taylor, S. S.; Engler, A. J.; Yang, J., Matrix stiffness drives epithelial-mesenchymal transition and tumour metastasis through a TWIST1-G3BP2 mechanotransduction pathway. *Nat, Cell Biol.,* **2015,** *17* (5), 678-88.

192. Hume, P. S.; He, J.; Haskins, K.; Anseth, K. S., Strategies to reduce dendritic cell activation through functional biomaterial design. *Biomaterials,* **2012,** *33* (14), 3615-25.

193. Grim, J. C.; Brown, T. E.; Aguado, B. A.; Chapnick, D. A.; Viert, A. L.; Liu, X.; Anseth, K. S., A reversible and repeatable thiol-ene bioconjugation for dynamic patterning of signaling proteins in hydrogels. *ACS Cent. Sci.,* **2018,** *4* (7), 909-16.

194. Bock, T.; Schill, V.; Krahnke, M.; Steinert, A. F.; Tessmar, J.; Blunk, T.; Groll, J., TGF-beta1-modified hyaluronic acid/poly(glycidol) hydrogels for chondrogenic differentiation of human mesenchymal stromal cells. *Macromol. Biosci.,* **2018,** *18* (7), 1700390 (1-13).

195. Palumbo, F. S.; Agnello, S.; Fiorica, C.; Pitarresi, G.; Puleio, R.; Loria, G. R.; Giammona, G., Spray dried hyaluronic acid microparticles for adhesion controlled

aggregation and potential stimulation of stem cells. *Int. J. Pharm.,* **2017,** *519* (1-2), 332-42.

196. Li, W.; Lee, S.; Ma, M.; Kim, S. M.; Guye, P.; Pancoast, J. R.; Anderson, D. G.; Weiss, R.; Lee, R. T.; Hammond, P. T., Microbead-based biomimetic synthetic neighbors enhance survival and function of rat pancreatic beta-cells. *Sci. Rep.,* **2013,** *3*, 2863 (1-10).

197. Meldal, M.; Schoffelen, S., Recent advances in covalent, site-specific protein immobilization. *F1000Res.,* **2016,** *5*, 1-11.

198. Johnson, J. A.; Lu, Y. Y.; Van Deventer, J. A.; Tirrell, D. A., Residue-specific incorporation of non-canonical amino acids into proteins: recent developments and applications. *Curr. Opin. Chem. Biol.,* **2010,** *14* (6), 774-80.

199. MacDonald, J. I.; Munch, H. K.; Moore, T.; Francis, M. B., One-step site-specific modification of native proteins with 2-pyridinecarboxyaldehydes. *Nat. Chem. Biol.,* **2015,** *11* (5), 326-31.

200. Shaunak, S.; Godwin, A.; Choi, J. W.; Balan, S.; Pedone, E.; Vijayarangam, D.; Heidelberger, S.; Teo, I.; Zloh, M.; Brocchini, S., Site-specific PEGylation of native disulfide bonds in therapeutic proteins. *Nat. Chem. Biol.,* **2006,** *2* (6), 312-13.

201. Knall, A. C.; Slugovc, C., Inverse electron demand Diels-Alder (iEDDA)-initiated conjugation: a (high) potential click chemistry scheme. *Chem. Soc. Rev.,* **2013,** *42* (12), 5131-42.

202. Truong, N. F.; Lesher-Pérez, S. C.; Kurt, E.; Segura, T., Pathways governing polyethylenimine polyplex transfection in microporous annealed particle scaffolds. *Bioconju. Chem.,* **2019,** *30* (2), 476-86.

203. Hou, S.; Lake, R.; Park, S.; Edwards, S.; Jones, C.; Jeong, K. J., Injectable macroporous hydrogel formed by enzymatic cross-linking of gelatin microgels. *ACS Appl. Bio. Mater.*, **2018,** *1* (5), 1430-39.

204. Zimmer, M., Green fluorescent protein (GFP): applications, structure, and related photophysical behavior. *Chem. Rev.,* **2002,** *102* (3), 759-81.

205. Epstein, N. E., Complications due to the use of BMP/INFUSE in spine surgery: The evidence continues to mount. *Surg. Neurol. Int.*, **2013,** *4*, 343-52.

206. McKay, W. F.; Peckham, S. M.; Badura, J. M., A comprehensive clinical review of recombinant human bone morphogenetic protein-2 (INFUSE® Bone Graft). *Int. Orthop.,* **2007,** *31* (6), 729-34.

207. Haidar, Z. S.; Hamdy, R. C.; Tabrizian, M., Delivery of recombinant bone morphogenetic proteins for bone regeneration and repair. part A: current challenges in BMP delivery. *Biotechnol. Lett.,* **2009,** *31* (12), 1817-24.

208. Jivan, F.; Fabela, N.; Davis, Z.; Alge, D. L., Orthogonal click reactions enable the synthesis of ECM-mimetic PEG hydrogels without multi-arm precursors. *J. Mater. Chem. B,* **2018,** *6* (30), 4929-36.

209. Shubin, A. D.; Felong, T. J.; Graunke, D.; Ovitt, C. E.; Benoit, D. S. W., Development of poly(ethylene glycol) hydrogels for salivary gland tissue engineering applications. *Tissue Eng. Part A,* **2015,** *21* (11-12), 1733-51.

210. Malkoch, M.; Vestberg, R.; Gupta, N.; Mespouille, L.; Dubois, P.; Mason, A. F.; Hedrick, J. L.; Liao, Q.; Frank, C. W.; Kingsbury, K.; Hawker, C. J., Synthesis of well-defined hydrogel networks using click chemistry. *Chem. Commun.,* **2006,** (26), 2774-76.

211. Lee, S.; Tong, X.; Yang, F., Effects of the poly(ethylene glycol) hydrogel crosslinking mechanism on protein release. *Biomater. Sci.,* **2016,** *4* (3), 405-11.

212. Binder, W. H.; Sachsenhofer, R., 'Click'chemistry in polymer and materials science. *Macromol. Rapid Commun.,* **2007,** *28* (1), 15-54.

213. Nimmo, C. M.; Shoichet, M. S., Regenerative biomaterials that "click": simple, aqueous-based protocols for hydrogel synthesis, surface immobilization, and 3D patterning. *Bioconjug. Chem.,* **2011,** *22* (11), 2199-209.

214. Owen, S. C.; Fisher, S. A.; Tam, R. Y.; Nimmo, C. M.; Shoichet, M. S., Hyaluronic acid click hydrogels emulate the extracellular matrix. *Langmuir,* **2013,** *29* (24), 7393-400.

215. Nimmo, C. M.; Owen, S. C.; Shoichet, M. S., Diels-Alder click cross-linked hyaluronic acid hydrogels for tissue engineering. *Biomacromolecules,* **2011,** *12* (3), 824-30.

216. Munoz, Z.; Shih, H.; Lin, C. C., Gelatin hydrogels formed by orthogonal thiol-norbornene photochemistry for cell encapsulation. *Biomater Sci.,* **2014,** *2* (8), 1063-72.

217. Magin, C. M.; Alge, D. L.; Anseth, K. S., Bio-inspired 3D microenvironments: a new dimension in tissue engineering. *Biomed. Mater.,* **2016,** *11* (2), 022001 (1-12).

218. Kharkar, P. M.; Kiick, K. L.; Kloxin, A. M., Design of thiol-and light-sensitive degradable hydrogels using Michael-type addition reactions. *Polym. Chem.,* **2015,** *6* (31), 5565-74.

219. Liu, Z.; Lin, Q.; Sun, Y.; Liu, T.; Bao, C.; Li, F.; Zhu, L., Spatiotemporally controllable and cytocompatible approach builds 3D cell culture matrix by photo-uncaged-thiol Michael addition reaction. *Adv. Mater.,* **2014,** *26* (23), 3912-17.

220. Fu, Y.; Kao, W. J., In situ forming poly (ethylene glycol)-based hydrogels via thiol-maleimide Michael-type addition. *J. Biomed. Mater. Res. Part A,* **2011,** *98* (2), 201-11.

221. Grover, G. N.; Lam, J.; Nguyen, T. H.; Segura, T.; Maynard, H. D., Biocompatible hydrogels by oxime click chemistry. *Biomacromolecules,* **2012,** *13* (10), 3013-17.

222. Lin, F.; Yu, J.; Tang, W.; Zheng, J.; Defante, A.; Guo, K.; Wesdemiotis, C.; Becker, M. L., Peptide functionalized oxime hydrogels with tunable mechanical properties and gelation behavior. *Biomacromolecules,* **2013,** *14* (10), 3749-58.

223. Zheng, J.; Smith Callahan, L. A.; Hao, J.; Guo, K.; Wesdemiotis, C.; Weiss, R.; Becker, M. L., Strain-promoted cross-linking of PEG-based hydrogels via copper-free cycloaddition. *ACS Macro Lett.,* **2012,** *1* (8), 1071-73.

224. Carthew, J.; Frith, J. E.; Forsythe, J. S.; Truong, V. X., Polyethylene glycol-gelatin hydrogels with tuneable stiffness prepared by horseradish peroxidase-activated tetrazine-norbornene ligation. *J. Mater. Chem. B,* **2018,** *6* (9), 1394-401.

225. Lapienis, G., Star-shaped polymers having PEO arms. *Prog. Polym. Sci.*, **2009,** *34* (9), 852-92.

226. Myers, B. K.; Zhang, B.; Lapucha, J. E.; Grayson, S. M., The characterization of dendronized poly(ethylene glycol)s and poly(ethylene glycol) multi-arm stars using matrix-assisted laser desorption/ionization time-of-flight mass spectrometry. *Anal. Chim. Acta,* **2014,** *808*, 175-189.

227. Chan, W. C.; White, P. D., Fmoc solid phase peptide synthesis : a practical approach. *Oxford University Press*, **1999**, *222*, 1-346.

228. Anthis, N. J.; Clore, G. M., Sequence-specific determination of protein and peptide concentrations by absorbance at 205 nm. *Protein Sci.,* **2013,** *22* (6), 851-58.

229. Carothers, W. H., Polymers and polyfunctionality. *Trans. Faraday Soc.,* **1936,** *32*, 39-49.

230. Luo, Y.; Shoichet, M. S., A photolabile hydrogel for guided three-dimensional cell growth and migration. *Nat. Mater.,* **2004,** *3*, 249-53.

231. Luo, Y.; Shoichet, M. S., Light-activated immobilization of biomolecules to agarose hydrogels for controlled cellular response. *Biomacromolecules,* **2004,** *5* (6), 2315-23.

232. Lee, S.-H.; Moon, J. J.; West, J. L., Three-dimensional micropatterning of bioactive hydrogels via two-photon laser scanning photolithography for guided 3D cell migration. *Biomaterials,* **2008,** *29* (20), 2962-68.

233. Cosson, S..; Kobel, S. A.; Lutolf, M. P., Capturing complex protein gradients on biomimetic hydrogels for cell-based ssays. *Adv. Funct. Mater.,* **2009,** *19* (21), 3411-19.

234. Hernandez, D. S.; Ritschdorff, E. T.; Seidlits, S. K.; Schmidt, C. E.; Shear, J. B., Functionalizing micro-3D-printed protein hydrogels for cell adhesion and patterning. *J. Mater. Chem. B,* **2016,** *4* (10), 1818-26.

235. Wylie, R. G.; Shoichet, M. S., Three-dimensional spatial patterning of proteins in hydrogels. *Biomacromolecules,* **2011,** *12* (10), 3789-96.

236. Farahani, P. E.; Adelmund, S. M.; Shadish, J. A.; DeForest, C. A., Photomediated oxime ligation as a bioorthogonal tool for spatiotemporally-controlled hydrogel formation and modification. *J. Mater. Chem. B,* **2017,** *5* (23), 4435-42.

237. DeForest, C. A.; Tirrell, D. A., A photoreversible protein-patterning approach for guiding stem cell fate in three-dimensional gels. *Nat. Mater.*, **2015,** *14* (5), 523-31.

238. Polizzotti, B. D.; Fairbanks, B. D.; Anseth, K. S., Three-dimensional biochemical patterning of click-based composite hydrogels via thiolene photopolymerization. *Biomacromolecules,* **2008,** *9* (4), 1084-87.

239. DeForest, C. A.; Anseth, K. S., Photoreversible patterning of biomolecules within click-based hydrogels. *Angew. Chem. Int. Ed.*, **2012,** *51* (8), 1816-19.

240. DeForest, C. A.; Anseth, K. S., Cytocompatible click-based hydrogels with dynamically tunable properties through orthogonal photoconjugation and photocleavage reactions. *Nat. Chem.*, **2011,** *3* (12), 925-31.

241. Becer, C. R.; Hoogenboom, R.; Schubert, U. S., Click chemistry beyond metal-catalyzed cycloaddition. *Angew. Chem. Int. Ed.*, **2009,** *48* (27), 4900-08.

242. Hubbell, J. A.; Thomas, S. N.; Swartz, M. A., Materials engineering for immunomodulation. *Nature,* **2009,** *462* (7272), 449-60.

243. Parameswaran, N.; Patial, S., Tumor necrosis factor-alpha signaling in macrophages. *Crit. Rev. Eukaryot. Gene Expr.*, **2010,** *20* (2), 87-103.

244. Flavell, R. A., The relationship of inflammation and initiation of autoimmune disease: role of TNF super family members. *Curr. Top. Microbiol. Immunol.*, **2002,** *266*, 1-9.

245. Isomaki, P.; Punnonen, J., Pro- and anti-inflammatory cytokines in rheumatoid arthritis. *Ann. Med.*, **1997,** *29* (6), 499-507.

246. Kollias, G.; Douni, E.; Kassiotis, G.; Kontoyiannis, D., On the role of tumor necrosis factor and receptors in models of multiorgan failure, rheumatoid arthritis, multiple sclerosis and inflammatory bowel disease. *Immunol. Rev.*, **1999,** *169*, 175-94.

APPENDIX A

Chapter II

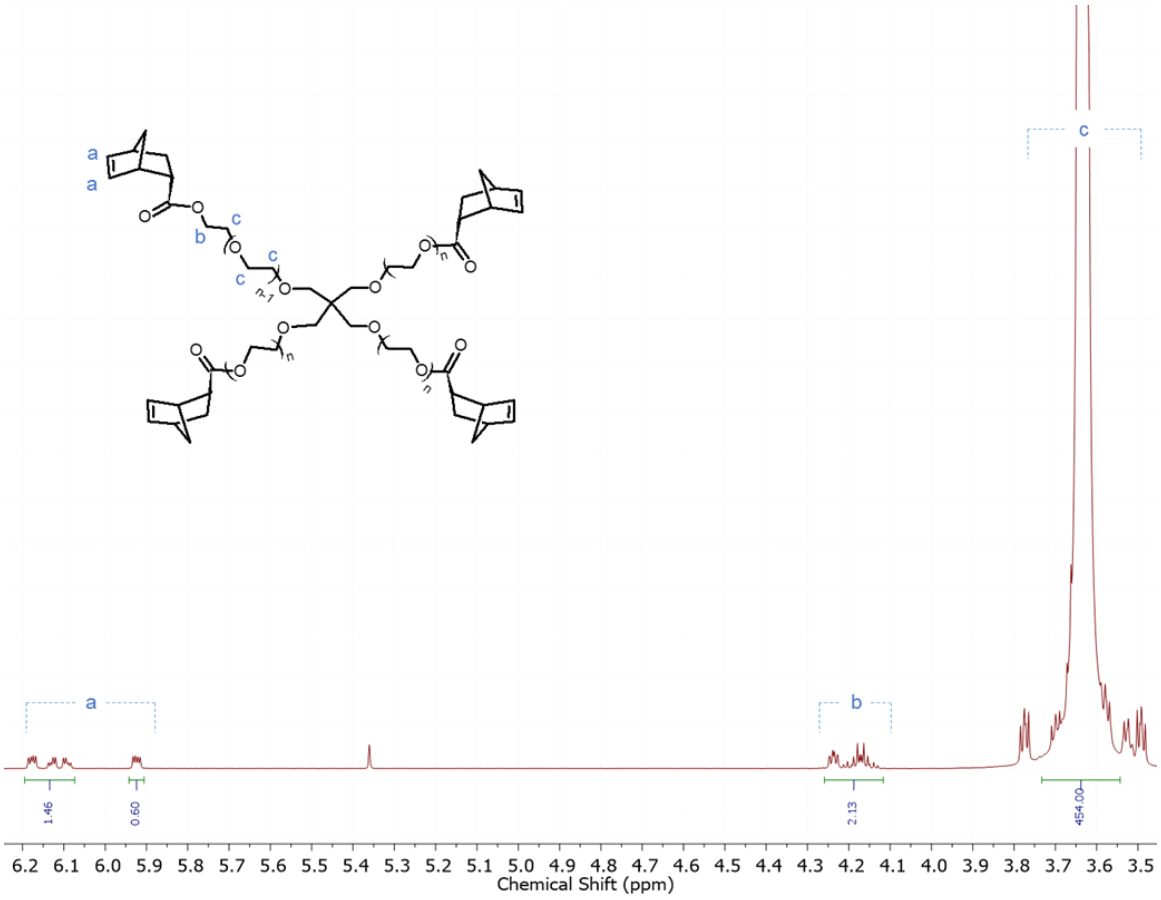

Figure VI-1. ^{1}H NMR of polyethylene glycol tetra-norbornene (PEG-NB). ^{1}H NMR (500MHz, $CDCl_3$) δ 6.19 – 5.90 (m, 2H), 4.26 – 4.12 (m, 2H), 3.73 – 3.54 (m, 454H). NMR shows quantitative norbornene functionalization based on a comparison of the alkene protons from norbornene to the theoretically expected number of alkene protons, using the ethylene glycol protons as a reference. Reprinted with permission from "Sequential thiol-ene and tetrazine click reactions for the polymerization and functionalization of hydrogel microparticles" by F. Jivan, R. Yegappan, H. Pearce, J. K. Carrow, M. McShane, A. K. Gaharwar, and D. L. Alge. *Biomacromolecules*, 2016, 17, 3516 – 23. Copyright 2016 American Chemical Society.[133]

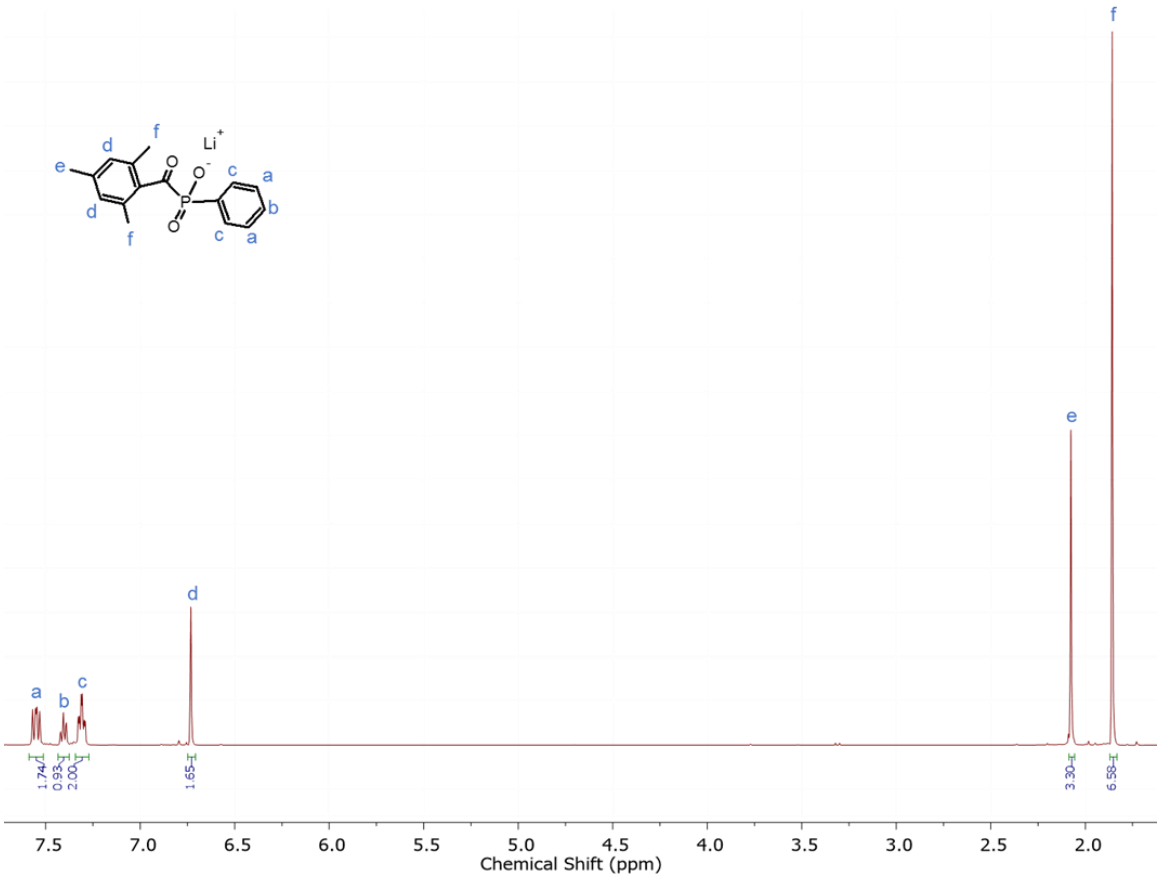

Figure VI-2. ^{1}H NMR of lithium acylphosphinate (LAP). ^{1}H NMR (500MHz, D2O) δ 7.55 (m, 2H), 7.41 (m, 1H), 7.31 (m, 2H), 6.73 (s, 2H), 2.08 (s, 3H), 1.86 (s, 6H). Reprinted with permission from "Sequential thiol-ene and tetrazine click reactions for the polymerization and functionalization of hydrogel microparticles" by F. Jivan, R. Yegappan, H. Pearce, J. K. Carrow, M. McShane, A. K. Gaharwar, and D. L. Alge. *Biomacromolecules*, 2016, 17, 3516 – 23. Copyright 2016 American Chemical Society.[133]

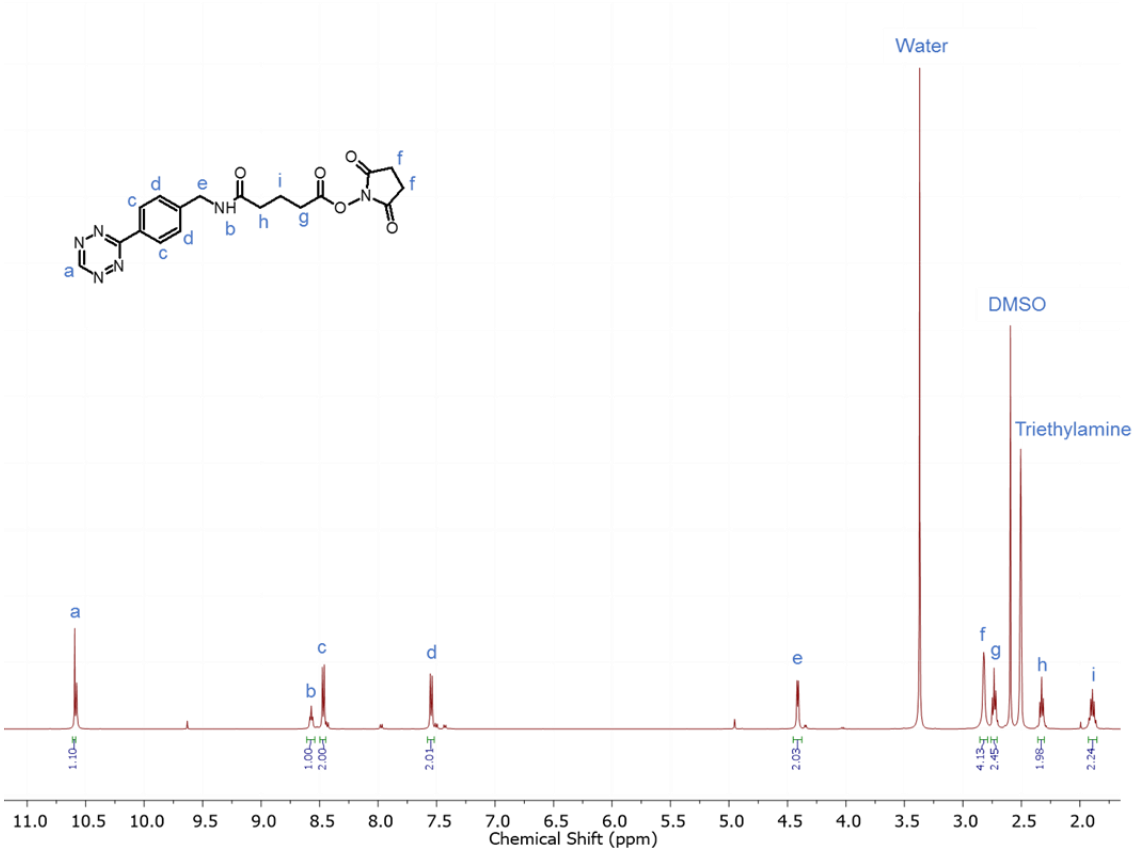

Figure VI-3. ^{1}H NMR of tetrazine-N-hydroxy-succinimydl ester (Tz-NHS Ester). ^{1}H NMR (500 MHz, DMSO-d6) δ 10.59 (s, 1H), 8.57 (m, 1H), 8.47 (d, 2H), 7.55 (d, 2H), 4.41 (d, 1H), 2.82 (d, 4H), 2.73 (t, 2H), 2.33 (t, 2H), 1.89 (m, 2H). Reprinted with permission from "Sequential thiol-ene and tetrazine click reactions for the polymerization and functionalization of hydrogel microparticles" by F. Jivan, R. Yegappan, H. Pearce, J. K. Carrow, M. McShane, A. K. Gaharwar, and D. L. Alge. *Biomacromolecules*, 2016, 17, 3516 – 23. Copyright 2016 American Chemical Society.[133]

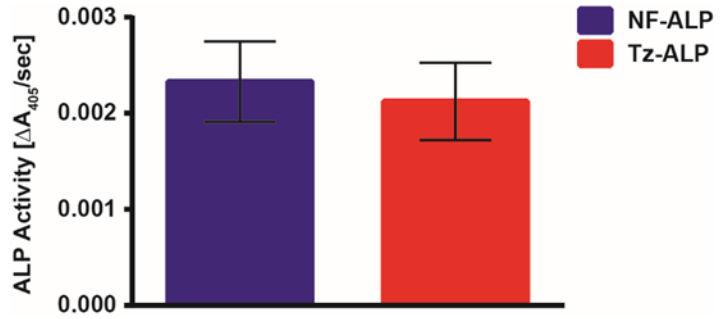

Figure VI-4. Effect of Tetrazine Functionalization on ALP Activity. ALP activity with standard deviations is shown (n = 3). Data was analyzed by non-parametric t-test and results showed that differences between NF-ALP and Tz-ALP samples were not significant ($p > 0.05$), indicating that ALP bioactivity was maintained after tetrazine functionalization. Reprinted with permission from "Sequential thiol-ene and tetrazine click reactions for the polymerization and functionalization of hydrogel microparticles" by F. Jivan, R. Yegappan, H. Pearce, J. K. Carrow, M. McShane, A. K. Gaharwar, and D. L. Alge. *Biomacromolecules*, 2016, 17, 3516 – 23. Copyright 2016 American Chemical Society.[133]

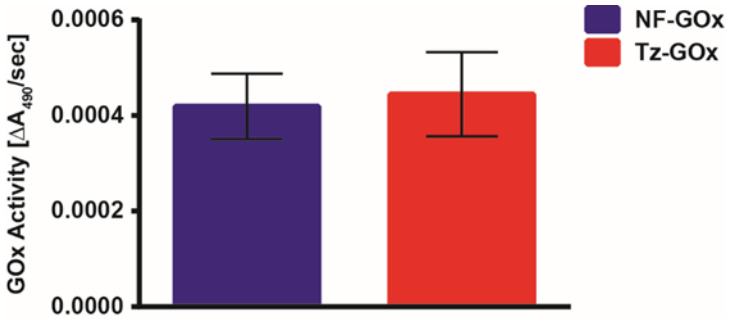

Figure VI-5. Effect of Tetrazine Functionalization on GOx Activity. GOx activity with standard deviations is shown (n = 3). Data was analyzed by non-parametric t-test and results showed that differences between NF-GOx and Tz-GOx samples were not significant ($p > 0.05$), indicating that GOx bioactivity was maintained after tetrazine functionalization. Reprinted with permission from "Sequential thiol-ene and tetrazine click reactions for the polymerization and functionalization of hydrogel microparticles" by F. Jivan, R. Yegappan, H. Pearce, J. K. Carrow, M. McShane, A. K. Gaharwar, and D. L. Alge. *Biomacromolecules*, 2016, 17, 3516 – 23. Copyright 2016 American Chemical Society.[133]

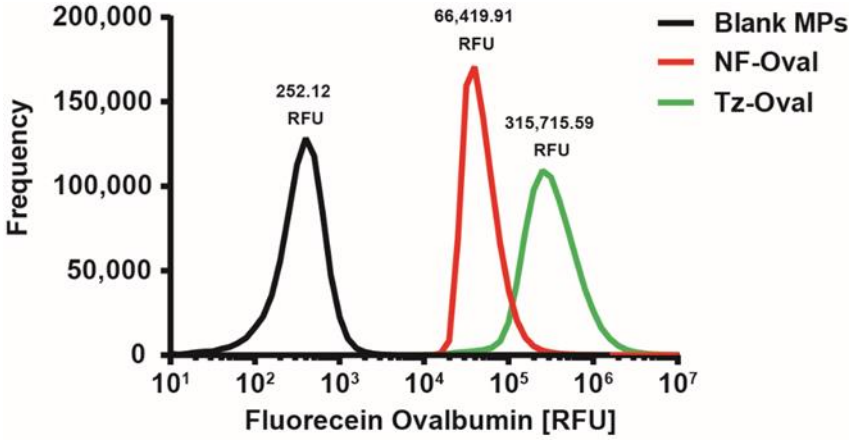

Figure VI-6. Fluorescence Histograms for Blank, NF-Ovalbumin, and Tz-Ovalbumin Microparticles. All curves from flow cytometry are shown: Blank microparticles without ovalbumin, NF-Ovalbumin microparticles, and Tz-Ovalbumin microparticles are shown with associated average RFU values above each peak. Reprinted with permission from "Sequential thiol-ene and tetrazine click reactions for the polymerization and functionalization of hydrogel microparticles" by F. Jivan, R. Yegappan, H. Pearce, J. K. Carrow, M. McShane, A. K. Gaharwar, and D. L. Alge. *Biomacromolecules*, 2016, 17, 3516 – 23. Copyright 2016 American Chemical Society.[133]

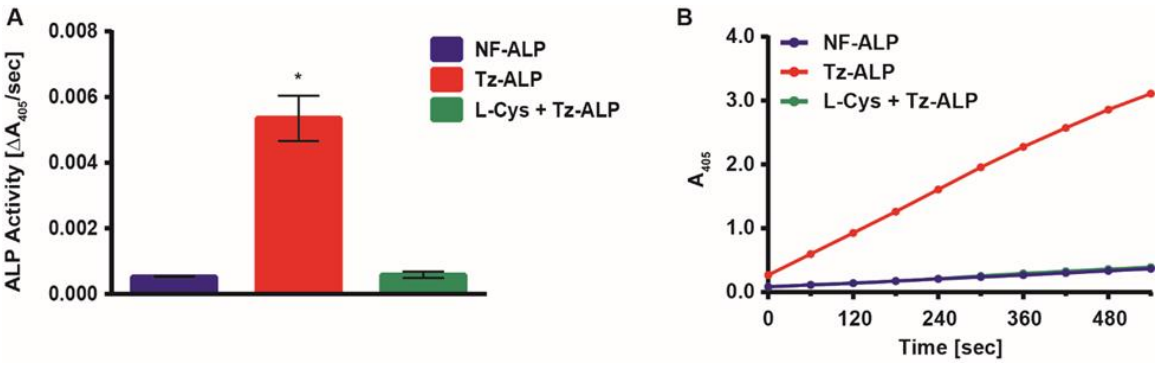

Figure VI-7. Bioactivity of Microparticles Lacking Norbornene Groups. (A) Average ALP activity of Tz-ALP, NF-ALP, and L-Cysteine + Tz-ALP microparticle samples with standard deviations. Data was analyzed by one-way ANOVA followed by post-hoc comparisons (Tukey's method). The symbol * indicates significant differences between Tz-ALP and both NF-ALP and L-Cys + Tz-ALP ($p < 0.05$). (B) Representative curves of absorbance versus time for microparticles functionalized with Tz-ALP, NF-ALP, and L-Cys + Tz-ALP, and then incubated with the ALP substrate p-nitrophenyl phosphate (Note: NF-ALP and L-Cys + Tz-ALP curves overlap). Importantly, no statistical difference ($p > 0.05$) was observed between NF-ALP and L-Cys + Tz-ALP samples, whereas the Tz-ALP only treatment resulted in significantly increased bioactivity ($p < 0.05$). These results indicate that the presence of unreacted norbornenes in the microparticles is essential for the tetrazine click-mediated conjugation of Tz-ALP, as expected. Reprinted with permission from "Sequential thiol-ene and tetrazine click reactions for the polymerization and functionalization of hydrogel microparticles" by F. Jivan, R. Yegappan, H. Pearce, J. K. Carrow, M. McShane, A. K. Gaharwar, and D. L. Alge. *Biomacromolecules*, 2016, 17, 3516 – 23. Copyright 2016 American Chemical Society.[133]

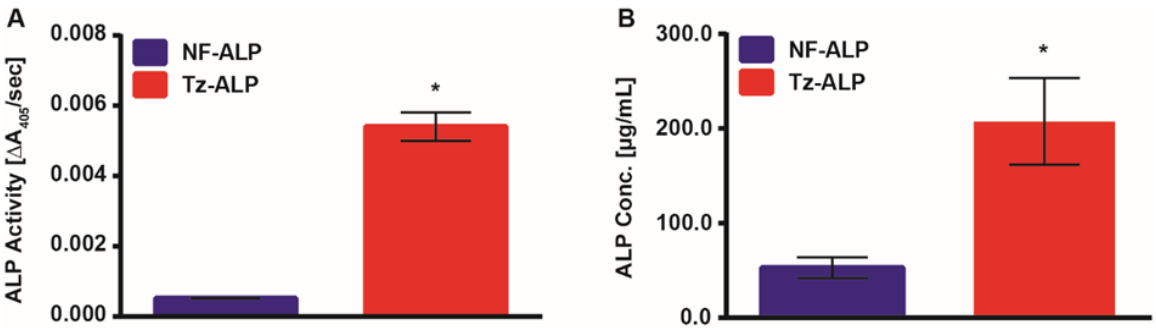

Figure VI-8. Bioactivity and Quantification of ALP Conjugation. (A) Average ALP activity of Tz-ALP and NF-ALP microparticles with standard deviations. (B) Concentration of Tz-ALP and NF-ALP protein conjugated to microparticles. Data was analyzed by non-parametric t-test. The symbol * indicates significant differences between the Tz-ALP and NF-ALP groups (n = 3; $p < 0.05$). Tetrazine click-mediated ALP conjugation resulted in significantly increased bioactivity that correlated with significantly increased protein concentration. Reprinted with permission from "Sequential thiol-ene and tetrazine click reactions for the polymerization and functionalization of hydrogel microparticles" by F. Jivan, R. Yegappan, H. Pearce, J. K. Carrow, M. McShane, A. K. Gaharwar, and D. L. Alge. *Biomacromolecules*, 2016, 17, 3516 – 23. Copyright 2016 American Chemical Society.[133]

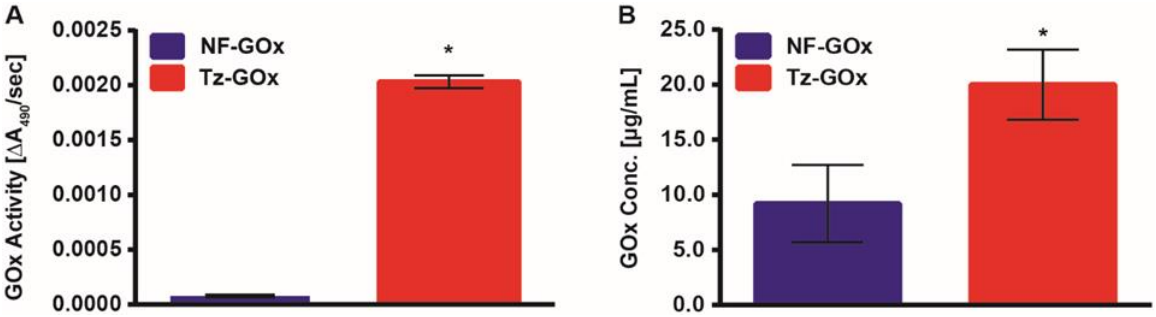

Figure VI-9. Bioactivity and Quantification of GOx Conjugation. (A) Average GOx activity of Tz-GOx and NF-GOx microparticles with standard deviations. (B) Concentration of Tz-GOx and NF-GOx protein conjugated to microparticles. Data was analyzed by non-parametric t-test. The symbol * indicates significant differences between Tz-GOx and NF-GOx concentrations (n = 3; $p < 0.05$). Tetrazine click-mediated GOx conjugation resulted in significantly increased bioactivity that correlated with significantly increased protein concentration. Reprinted with permission from "Sequential thiol-ene and tetrazine click reactions for the polymerization and functionalization of hydrogel microparticles" by F. Jivan, R. Yegappan, H. Pearce, J. K. Carrow, M. McShane, A. K. Gaharwar, and D. L. Alge. *Biomacromolecules*, 2016, 17, 3516 – 23. Copyright 2016 American Chemical Society.[133]

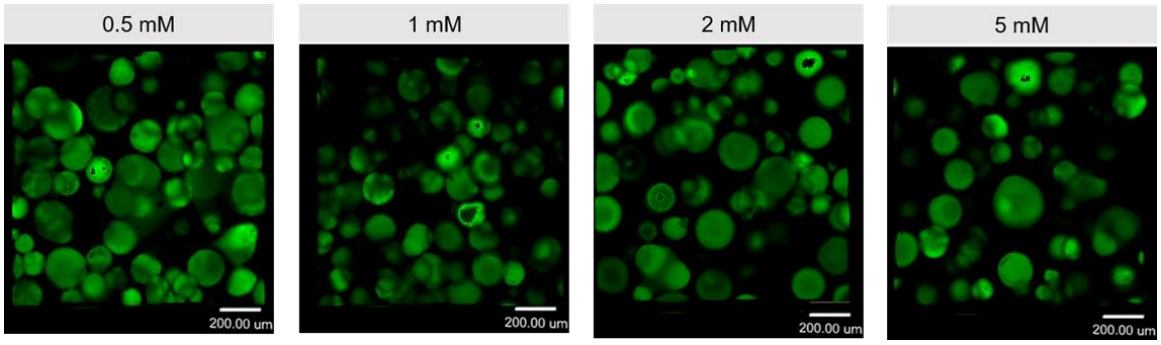

Figure VI-10. MAP Hydrogel Porosity. Representative images (z-stack = 100 μm) of fluorescently labelled MAP hydrogels crosslinked with varying concentrations of PEG-di-Tz.

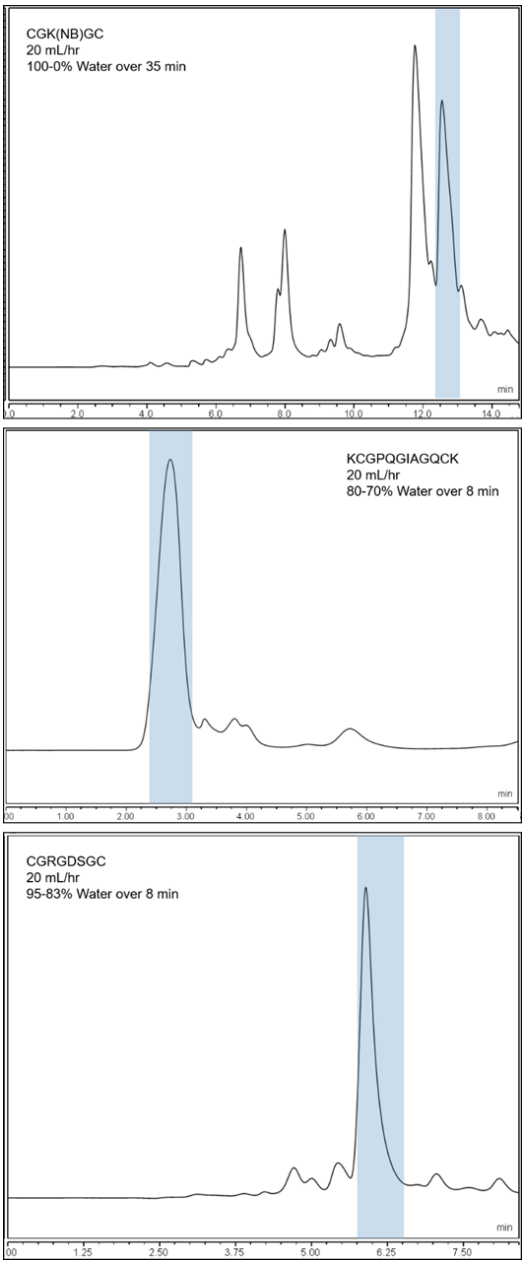

Figure VI-11. Crude HPLC Spectra for Peptide Sequences. HPLC spectra of synthesized peptides used to make BCP precursors. The instrument method (acetonitrile and water mobile phase) and collected fraction are shown for each sequence. Reprinted from "Orthogonal click reactions enable the synthesis of ECM-mimetic PEG hydrogels without multi-arm precursors" by F. Jivan, N. Fabela, Z. Davis, and D. L. Alge. *Journal of Materials Chemistry B*, 2018, 6, 4929-36. with permission from The Royal Society of Chemistry.[208]

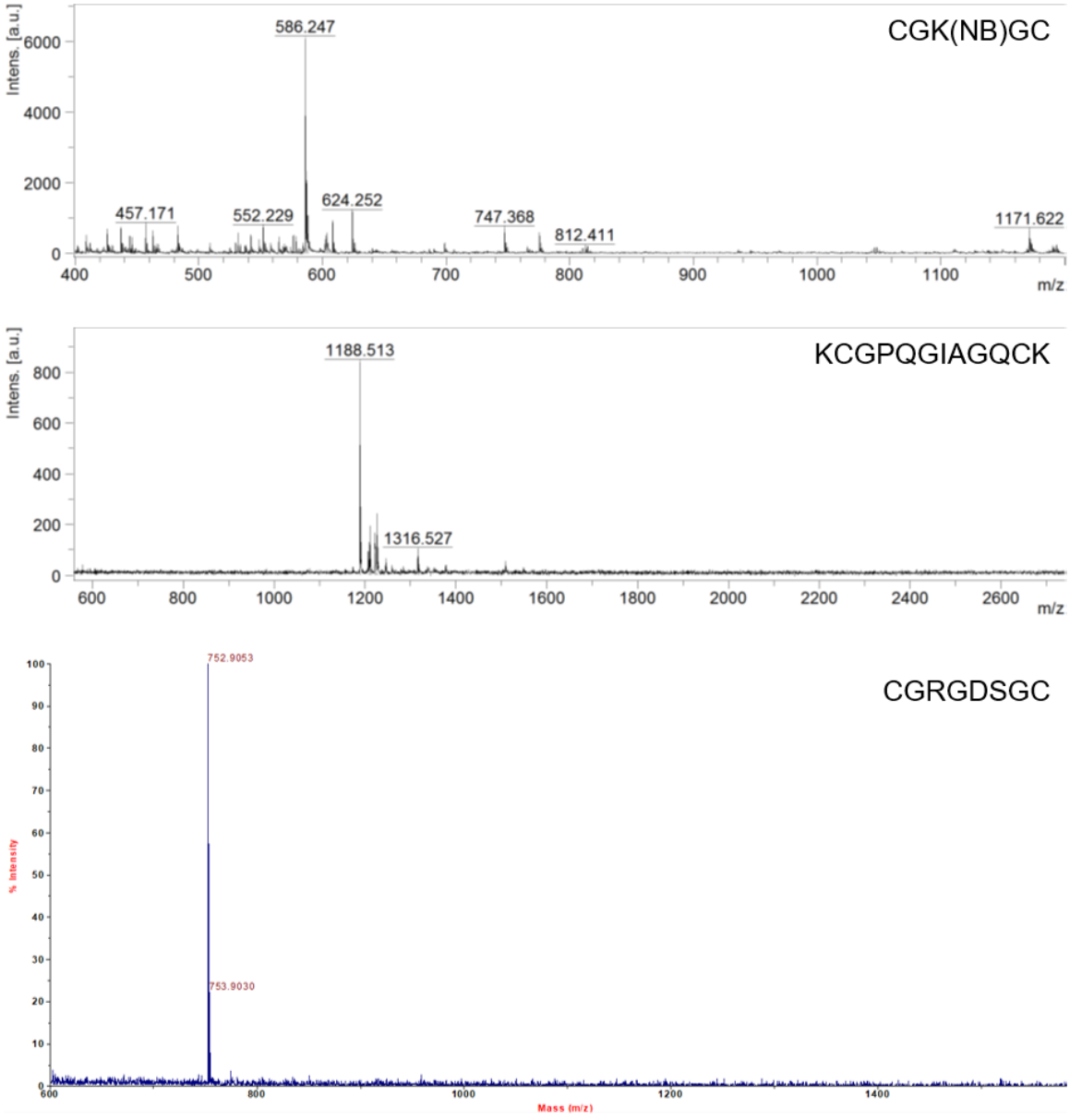

Figure VI-12. MALDI Spectra for Peptide Sequences. MALDI spectra for the selected HPLC fraction collected for each of the synthesized peptide sequences. Reprinted from "Orthogonal click reactions enable the synthesis of ECM-mimetic PEG hydrogels without multi-arm precursors" by F. Jivan, N. Fabela, Z. Davis, and D. L. Alge. *Journal of Materials Chemistry B,* 2018, 6, 4929-36. with permission from The Royal Society of Chemistry.[208]

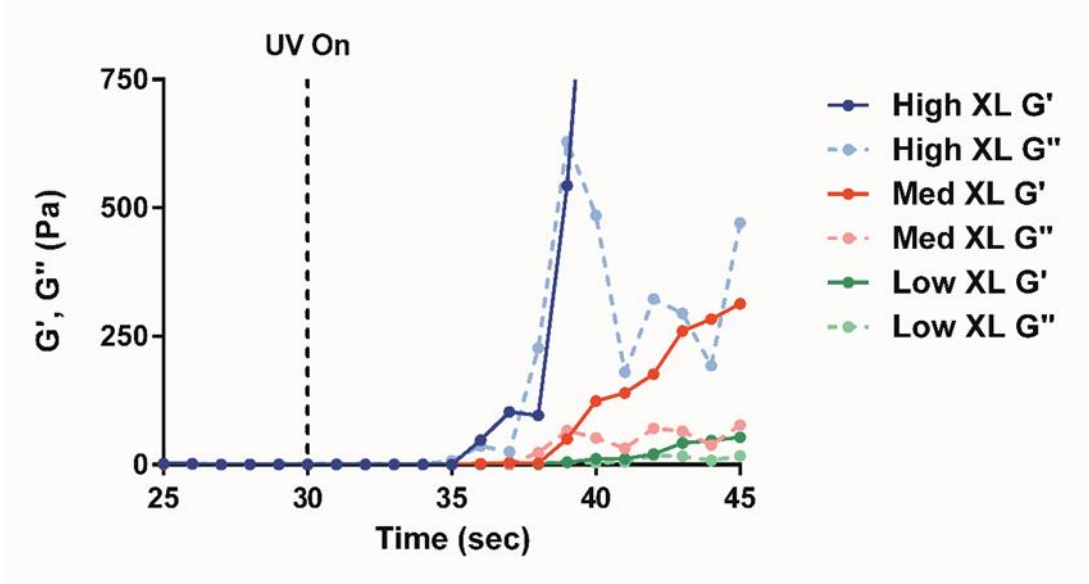

Figure VI-13. *In Situ* Rheology Showing Gelation Point. Zoomed in area of representative storage (G') and loss (G") modulus curves from *in situ* rheology of various BCP crosslinking densities. The dashed line shows when UV initiation begins and the gel point is when G' is maintained higher than G" (after approximately 10 seconds). Reprinted from "Orthogonal click reactions enable the synthesis of ECM-mimetic PEG hydrogels without multi-arm precursors" by F. Jivan, N. Fabela, Z. Davis, and D. L. Alge. *Journal of Materials Chemistry B,* 2018, 6, 4929-36. with permission from The Royal Society of Chemistry.[208]